UNIVERSITY OF CALIFORNIA
Santa Barbara

WATERSHED MANAGEMENT TO ADDRESS SEDIMENTATION OF ECUADOR'S RIO CHONE ESTUARY

A Group Project submitted in partial satisfaction of the requirements for the degree of
Master of Environmental Science and Management
for the
Bren School of Environmental Science & Management

By:
FRANCESCA DE LEON
STEVEN JOHNSON
JAKE MARCON
NATALIE PHARES

Faculty Advisor:
STEVEN GAINES

March 2015

ACKNOWLEDGEMENTS

We would like to thank everyone who has assisted and supported us throughout the duration of this project. Many people were instrumental in the planning and execution of our technical work, which has not only aided in the production of this report but in the enrichment of our experience. In addition, the financial support we received, allowing us to carry out international work, can be attributed to a small group of individuals to whom we are indebted to. We would especially like to extend our gratitude to the following people:

Faculty advisor:
Dr. Steven Gaines (Bren School of Environmental Science & Management)

External committee members:
Dr. Derek Booth (Bren) and William Brandt (Bren)

Client:
Global Student Embassy, specifically Lucas O'Shun and Ramiro Medina

Special thanks to:
Dr. Stuart Hamilton, Salisbury University
Dr. Tom Dunne, Bren School of Environmental Science & Management
Ben Best, National Center for Ecological Analysis and Synthesis
Tim Cohen, AECOM
Lynn Scarlett, The Nature Conservancy
Ross Sheldon, R. Sheldon Productions
Mayra Vera, Ministerio de Ambiente, Ecuador

Additional thanks to: Marcos Douglas Calle Marán & his students at the Universidad Católica de Bahía de Caráquez: Martin Castelo, Rosa Emilia Cevallos, Camila Chávez, Elisa Pazmiño Garcia, and Karla Falconi Vélez

We would like to thank the faculty and staff at the Bren School of Environmental Science & Management at the University of California, Santa Barbara for all of their support and assistance.

Finally, we would like to express our deepest gratitude to all of our friends and family who supported and encouraged us throughout this process.

WATERSHED MANAGEMENT TO ADDRESS SEDIMENTATION OF THE RIO CHONE ESTUARY, ECUADOR

As authors of this Group Project report, we are proud to archive this report on the Bren School's website such that the results of our research are available for all to read. Our signatures on the document signify our joint responsibility to fulfill the archiving standards set by the Bren School of Environmental Science & Management.

FRANCESCA DE LEON

STEVEN JOHNSON

JACOB MARCON

NATALIE PHARES

The mission of the Bren School of Environmental Science & Management is to produce professionals with unrivaled training in environmental science and management who will devote their unique skills to the diagnosis, assessment, mitigation, prevention, and remedy of the environmental problems of today and the future. A guiding principal of the School is that the analysis of environmental problems requires quantitative training in more than one discipline and an awareness of the physical, biological, social, political, and economic consequences that arise from scientific or technological decisions.

The Group Project is required of all students in the Master of Environmental Science and Management (MESM) Program. The project is a year-long activity in which small groups of students conduct focused, interdisciplinary research on the scientific, management, and policy dimensions of a specific environmental issue. This Group Project Final Report is authored by MESM students and has been reviewed and approved by:

STEVEN GAINES

March 20th, 2015

Table of Contents

List of Tables

List of Figures

List of Abbreviations and Terms

BMP: Best Management Practice
CBA: Cost Benefit Analysis
EPA: United States Environmental Protection Agency
ESA: European Space Agency
FAO: Food and Agriculture Organization of the United Nations
GIS: Geographic Information Systems
GSE: Global Student Embassy
HWSD: Harmonized World Soil Dataset
IERAC: Ecuadorian Institute for Agrarian Reform and Colonization
IIASA: International Institute for Applied Systems Analysis
INOCAR: Instituto Oceanografico de la Armada (Ecuador's Navy)
InVEST: Integrated Valuation of Environmental Services and Tradeoffs
LULC: Land Use/Land Cover
MERIS: Medium Resolution Imaging Spectrometer Instrument
NatCap: Stanford's Natural Capital Project
PMRC: Coastal Resources Management Program (Spanish acronym)
PROBONA: Programme for Native Andean Forests
RCE: Rio Chone estuary
RCW: Rio Chone watershed
ROI: Region of Interest
RUSLE: Revised Universal Soil Loss Equation
USGS: United States Geological Survey
USLE: Universal Soil Loss Equation
UN: United Nations

Abstract

The Rio Chone estuary, located on the Pacific Coast of Ecuador, is subject to high sedimentation rates due to unsustainable agricultural practices and deforestation within its watershed. This report seeks to address sedimentation of the water body from a watershed perspective. The estuary's biodiversity and value to human use is threatened, as some regions have seen accretion of up to seven meters of sediment over the assessed period of 21 years. We analyzed bathymetric data to ascertain the current rate of sedimentation. We then created a sediment budget for the watershed to identify which erosional processes were the largest contributors of sediment, and ran a sediment generation model to quantify the volume of sediment produced from surface water erosion. Finally, we modeled different land use scenarios to explore how changes in land use could affect erosion rates. Our work showed that sheetwash erosion is the dominant geomorphic process generating sediment in the watershed. We conclude that strategic implementation of soil conservation strategies on cultivated parcels and reforestation of fallowed degraded lands has the potential to mitigate high sheetwash erosion rates, and have a significant damping effect on future sedimentation of the Rio Chone estuary.

Executive Summary

Ecuador's Rio Chone estuary was once a vibrant ecosystem supporting large stocks of fish, shellfish, and sea birds, while harboring expansive mangrove forests. The mangrove forests provided a range of essential ecosystem services including sediment stabilization, shoreline protection, nutrient uptake, and nursery grounds for numerous marine species (Hamilton and Collins, 2013). This important ecosystem has been largely impacted by shrimp aquaculture. As of 1999, mangroves existed in only 20% of the areas they once inhabited (Twilley et al., 1999). Aquaculture provides great value to the regional economy, but has caused the estuary to lose much of its previous resilience.

Our team was initially asked to study prioritization of mangrove reforestation efforts to help rebuild some of this critical ecosystem. Despite the glaring need for this research, our preliminary results identified estuarine sedimentation as a more pressing issue that should be addressed before mangrove restoration is considered. Mangrove habitat selection is largely driven by the extent of tidal flows, with different species specializing in different tidal regions. Our initial research suggested that mangrove recruitment through natural succession is often very rapid when natural hydrologic regimes are present. However, anthropogenic disturbance of the estuary system and the surrounding watershed has caused major changes to the hydrology and geomorphology of the estuary. Essentially, mangrove restoration efforts cannot be considered sustainable until the natural hydrologic regime is returned. Therefore, we turned the focus of our research to sedimentation of the Rio Chone estuary from a watershed perspective.

Project Objectives

Our project objectives included answering the following questions:

1. What level of sedimentation has occurred within the Rio Chone estuary?
2. What are the major sources of sediment within the Rio Chone watershed?
3. Which abatement practices have the potential to reduce sedimentation most effectively?

Sedimentation

Our results show that areas of the Rio Chone estuary lost up to seven meters of depth between 1990 and 2011 (Figure A). Such heavy sedimentation significantly alters the hydrology of the estuary, reducing its capacity to dilute effluent delivered by inflows, and likely changing its salinity, temperature, and water quality (Wilber & Clarke, 2011).

Sediment Sources

To identify the largest contributors of sediment to the estuary we constructed a sediment budget. Our sediment budget estimated the probable magnitudes of sediment production from streambanks, unpaved roads, and surface water erosion from sheetwash and rilling processes.

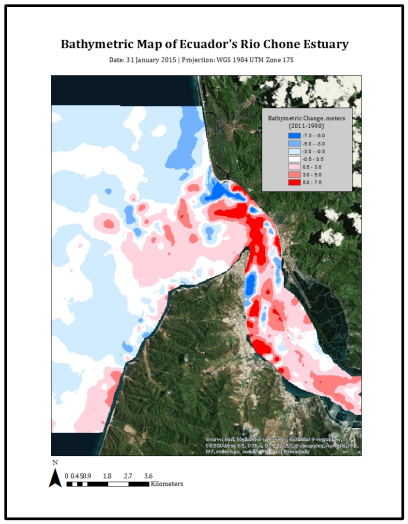

Figure A. Bathymetric change of the Rio Chone estuary (1990-2001)

Given the data available we selected the InVEST Sediment Retention Model to simulate sheetwash erosion. This model calculates the average annual soil loss from a land parcel, pairing the Revised Universal Soil Loss Equation with geographic information system technologies. We ran the model for an average climatic year to provide intuition to the typical magnitude of sheetwash erosion within the watershed (Figure B). In addition, we ran the model for a simulated El Nino year because local sources indicated that sediment delivery in El Nino years is significantly higher than in years of average climate.

Model projections suggest that the greatest sediment sources are areas that have been cleared of native vegetation for farming activities. In addition, increased erosion risk was highly correlated with steep hillslope gradient and high average annual precipitation.

Management Strategies

Several management strategies could potentially reduce erosion risk within the Rio Chone watershed. We analyzed the effects of two strategies with the greatest likelihoods of dramatically reducing erosion – reforestation of converted native lands and

implementation of soil conservation techniques in agricultural operations. Although the strategies employ very different tactics and monetary costs, our model analyses suggest that they would provide similar gains in erosion control.

Beneficial soil conservation techniques include reduced downslope tilling, increased use of water retention trenches, marginal hedgerows, and mulching. Our analyses show that mulching on agricultural fields, in particular, could dramatically reduce erosion throughout the watershed. In addition, the use of erosion control techniques on cultivated properties could not only benefit the estuary through reduced sediment delivery, they add value to long-term farm productivity by limiting the loss of valuable topsoil. Therefore, it may be in the best economic interest of farmers to take actions that will also have indirect benefits for the downstream estuary.

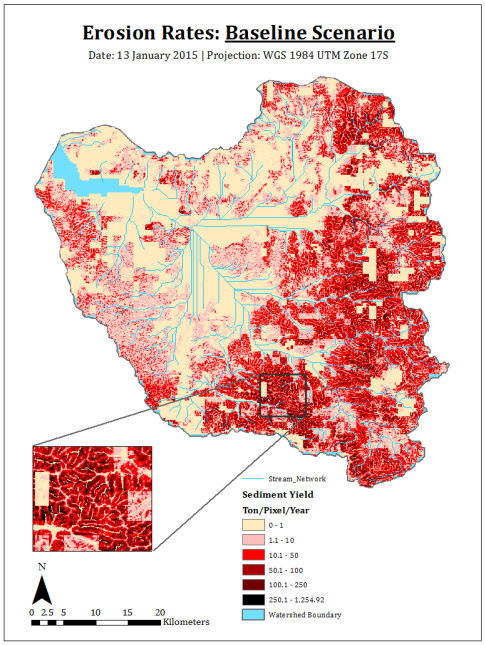

Figure B. Erosion rates in the Rio Chone watershed under the baseline land use regime during a non-El Nino rain vear

Finally, we analyzed hypothetical scenarios involving different levels of reforestation, which showed reforestation can provide significant reductions in potential erosion. Reforestation can be undertaken passively, by allowing natural succession to reclaim the land, or actively, by planting species that would not have regenerated as quickly if left to passive successional processes.

Conclusion

The sedimentation problem in the Rio Chone estuary likely arises from land use practices that are, and have been carried out in the greater watershed. Therefore, solving the estuarine problem requires reducing the magnitude of sediment eroded from the land. Many stakeholder groups would benefit directly or indirectly from reductions of the sedimentation problem, but the incentives of land managers must specifically be taken into account when attempting to address the issue. Fortunately for soil conservation, farmers would directly benefit from reducing the amount of topsoil eroded from their lands through sustained productivity. By contrast, although reforestation could also solve the sedimentation problem, this solution incurs significant opportunity costs on land managers and current farmers, and would likely be a more time intensive solution as erosion reductions from reforestation take years to decades. Our research shows that selective implementation of reforestation and soil conservation techniques has the potential to address sediment loading from the Rio Chone watershed and reduce future sedimentation of the estuary. These are key steps that must be implemented before efforts to replant mangroves in the estuary could be successful.

1.0 Introduction

Following deforestation and mangrove removal, sediment loading and accretion has increased dramatically in the Rio Chone estuary over the last few decades. The contextual significance of our project is discussed herein, followed by our project objectives and the mechanism(s) used to address each task.

1.1 Project Significance

The Rio Chone estuary lies along Ecuador's central coast at the outlet of a 2,700km^2 watershed (Figure 1.1). The low rolling hills surrounding the estuary support dry tropical forests that are littered with subsistence scale agriculture. In the past, the estuary's waters were home to large swaths of mangrove forests, which served as nursery grounds for many of the local fisheries (Twilley et al., 1999). Mangroves perform a range of essential ecosystem services for people, including sediment stabilization, shoreline protection, carbon sequestration, and filtration of water borne nutrients (Hamilton and Collins, 2013). Many of these historical characteristics of the estuary, however, have been lost. By 1999, roughly 80% of the estuary's mangrove forests were removed to create shrimp ponds that now dominate the shoreline (Twilley et al., 1999). This aquaculture provides great value to some regional stakeholders, but these benefits have come at the expense of the ecosystem services and biodiversity it used to support.

Our team was initially enlisted to study the potential for mangrove reforestation to regain some of these prior benefits. Mangrove loss is a global issue, and often incurs dramatic environmental consequences. We spent the initial two months of our study in the summer of 2014 assessing the potential for mangrove restoration in the Rio Chone estuary. Although mangrove reforestation would provide many potential benefits, our initial analyses showed that a focus on mangrove replanting would likely be unsuccessful. Anthropogenic disturbance within and around the Rio Chone waterways has caused major changes to the hydrologic and geomorphic regimes of the landscape. If attempting to return the estuary to its native state is the goal, controlling sediment delivery to the river network feeding the Rio Chone must be addressed first. Returning hydrologic regimes to their historical state is a necessary precursor for successful mangrove reforestation; although hardy, mangroves are sensitive to changes in water depth and salinity, both parameters that have been altered in the estuary over the last few decades correlated with increased human disturbance in the watershed. Fortunately, mangrove recovery is often rapid and can occur passively when the proper physical characteristics are restored.

Our results show that areas of the estuary lost up to seven meters of depth during our study period, 1990 to 2011. Heavy sedimentation threatens the natural hydrology of the estuary, reducing the volume of water available to dilute the effluent being delivered by creeks and rivers, and reducing the capacity of the estuary to act as a mixing reservoir. If sedimentation is allowed to continue, effects on water quality could be widespread, and native fisheries could suffer even further. The yields and productivity of the aquaculture shrimp industry will continue to decrease as many shrimp farmers rely on clean estuarine waters to flush out their ponds daily.

While the removal of soil from the Earth's surface is a natural process, the increase in pace displayed in the Rio Chone watershed is attributed to two distinct drivers. Firstly, land use intensification and modification in the upper watershed have greatly increased the amount of sediment being delivered to the estuary from the land surface. The estuary's watershed has a long history of deforestation, and the removal of vegetative cover subsequently increases the magnitude of erosion. While the initial forest removal was for logging, a majority of the land was subsequently cleared to make way for agricultural activities. Unfortunately, these small-scale operations utilize slash-and-burn methods between crop cycles instead of employing soil conservation techniques, leading to significant soil losses throughout the year. Secondly, the massive deforestation of estuarine and riverine mangroves caused the destabilization and redistribution of sediments that had long been bolstered by the matrix of mangrove root structures. Sediment that was previously encapsulated by mangrove roots has now been released into the waterways, contributing significantly to sediment redistribution and built up.

Many stakeholders have identified the potential effects of continued sedimentation within the estuary and recognize the need to address the issue. Our research focuses on identifying regions of major sediment generation within the terrestrial environment to offer a strategic plan for restoration. We explore the potential effects that changing land use could have on reducing erosion rates in the watershed, assuming that reforestation of degraded lands and employment of soil conservation techniques on cultivated properties could ensue. As such, this project provides a preliminary characterization of problem areas within the watershed and suggests remediation strategies to reduce the sediment contribution from terrestrial sources.

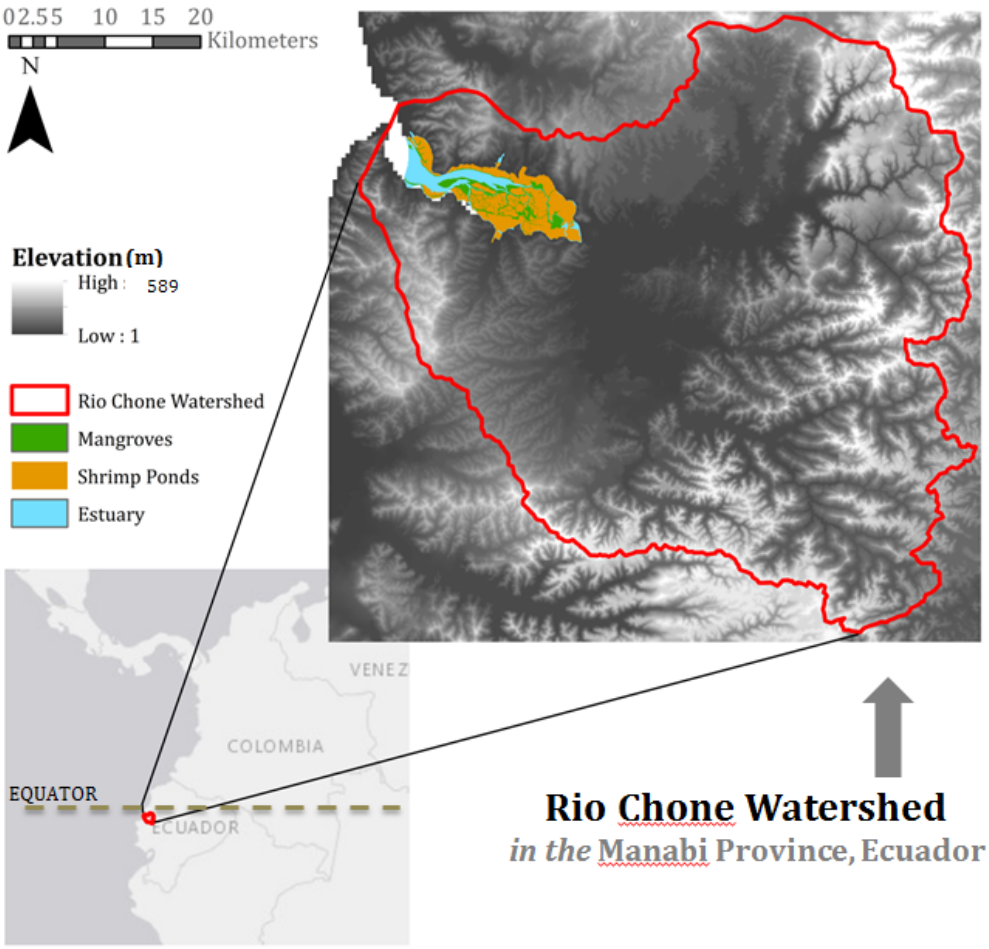

Figure 1.1 Location and elevation of Ecuador's Rio Chone watershed

1.2 Project Objectives

The aim of this project was to provide Global Student Embassy, the Ecuadorian Ministry of the Environment, and local communities with an assessment of the sedimentation issue within the Rio Chone estuary from a watershed perspective. To address this issue our research attempts to answer the following questions:

1. What are the main sources of sediment in the Rio Chone watershed?
2. What management methods will be successful in reducing the amount of sediment being delivered to the estuary?

With these questions in mind, our project's objectives include the following:

1. Calculate the volume of sediment deposited and retained in the estuary
2. Identify the major sources of sediment production
3. Assess the effect that altering land use could have on reducing erosion rates

To meet our project objectives, we used bathymetric maps to visualize the change in depth in the estuary and calculate an accretion rate. Next, we accounted for the major sources of sediment production from the watershed through the construction of a sediment budget. This allowed us to identify which erosional processes were contributing the greatest volume of sediment to the stream network. Finally, we used a model that paired geographic information system (GIS) technologies with the Revised Universal Soil Loss Equation to estimate the volume of sediment produced from sheetwash and rilling processes and to test the potential impact that land use alterations could have on erosion rates.

2.0 Background

A survey of available literature was performed to characterize our study site in terms of its pertinent history, physical characteristics, and the social, economic, and political drivers behind the severe land degradation experienced in the watershed. Then, the fundamentals and drivers of erosion and estuarine sedimentation are discussed, including an overview of current erosion reduction methods in practice.

2.1 History of the Rio Chone estuary

The Rio Chone estuary has a rich and varied history, having been populated by humans since indigenous people first arrived in South America between 40,000 and 12,000 years ago. These indigenous cultures were generally able to avoid interference from the Incas when they invaded Ecuador in the 1400s, but were decimated by diseases and dominance by the Spanish in the 16th Century. Those who remained went through Ecuador's colonial era in the service of *haciendas*, or large private estates. After surviving centuries of revolutions, changes in power, and periods of economic downturn, the people of the Rio Chone estuary welcomed the introduction of shrimp aquaculture in the 1970s. In recent years, however, the local view of shrimp aquaculture has shifted, prompting interest in restoring some of the degraded environment that aquaculture and agriculture have created (Ades et al., 2013).

2.1.1 Agroforestry

A recent archaeological breakthrough resulting from ancient botanical and faunal evidence suggests that the area surrounding Rio Chone estuary has been inhabited by farmers who practiced agroforestry since 2000 BC (Stahl & Pearsall, 2012). Agroforestry is the ancient practice of creating deliberate space between cultivated woody species of trees, and is understood to have positive ecological benefits (Nair, 1989). Evidence shows that agroforestry helped create a healthy, sustainable environment for indigenous Ecuadorians that lasted for nearly four millennia (Stahl & Pearsall, 2012). In essence, until recently the Rio Chone watershed had been used for growing food crops in a successful, sustainable manner for centuries.

2.1.2 Rise and Decline of Agriculture

Much of the land surrounding the Rio Chone estuary was cleared of native vegetation and converted to agriculture during the first half of the 20th century (Coello et al, 1993). Bahía de Caraquéz, located at the mouth of the estuary, was a fast growing port in Ecuador as the area benefited from export of the rubber, balsa wood, tagua, bananas, cocoa, coffee, and cotton being produced on the cultivated hillslopes (Coello et al., 1993). Ready access to the port increased the clearing of native vegetation in the area to expand the production of cash crops.

Recession hit the estuary during the late 1950s due to reduced foreign demand for the area's resources and the creation of a larger port at the nearby city of Manta. Local farmers were prompted to shift their practices to subsistence farming by growing two primary crop types, maize and cotton. By the 1960s, most of the original dry tropical forest in the watershed was gone (Coello et al., 1993).

2.1.3 The Emergence of Shrimp Farming

The 1970s ushered in the age of shrimp farming to the Rio Chone estuary. Commencing in the salt flats, shrimp farming eventually expanded to areas once populated by mangroves as aquaculture gained popularity. The rise in shrimp cultivation saw a corresponding drop in estuarine fisheries and water quality. Consequently, native small-scale fishermen were forced into other areas of the local economy or left the Rio Chone area all together (Coello et al., 1993).

2.2 Watershed Characterization

While erosion is a natural process, its rate is greatly affected by how people interact with the landscape. To provide the context for evaluating the scope of the problem and the potential solutions, we begin with an overview of the watershed's physical characteristics.

2.2.1 Location and Size of the Study Site

Ecuador's Manabi province is a low-lying coastal region, a seven-hour drive from the country's capital Quito. Its largest watershed is the Rio Chone, housing the town of Chone and the coastal towns Bahia de Caraquez and San Vicente. The main native ecosystems in close proximity to the estuary include dry tropical forest, mangroves, La Segua marsh, estuary, and beaches. The estuary is 36 kilometers long and ranges in width from 3 kilometers to 15 meters, narrowest at its headwaters in Simbocal (Coello et al., 1993). The 4,560 hectares of land framing the waterway are a mixture of fallowed lands, cultivated plots, and dry tropical vegetation. The estuary and Bahia de Caraquez are located at approximately 1°35' of south latitude and 80°25' of longitude west (Figure 2.1) (Arriaga et al., 1999).

Two large river systems feed into the estuary, the Rio Chone river and the Carrizal river (Figure 2.1) with additional discharges from 21 micro-basins (12 on the north margin, 8 on the south). The micro-basins and estuary comprise 17% of the total area of the Rio Chone basin, while the watersheds of the Carrizal and Rio Chone river drains 2,597 km^2 (Arriaga et al., 1999). The drainage basin discharges an approximate annual medium flow of 38 m^3 s^{-1} to the estuary (Arriaga et al., 1999). A network of low-lying coastal hills surrounds the estuary with a maximum elevation between 400 and 630 meters (Coello et al., 1993). Having a dry tropical climate, multiannual data from the meteorological station of Bahia de Caraquez reports an average annual temperature of 24.8°C, humidity (dry months) of 82%, with an average annual rainfall of 494.5 mm. Maximum precipitation occurs during Ecuador's rainy season between January and April (Arriaga et al., 1999).

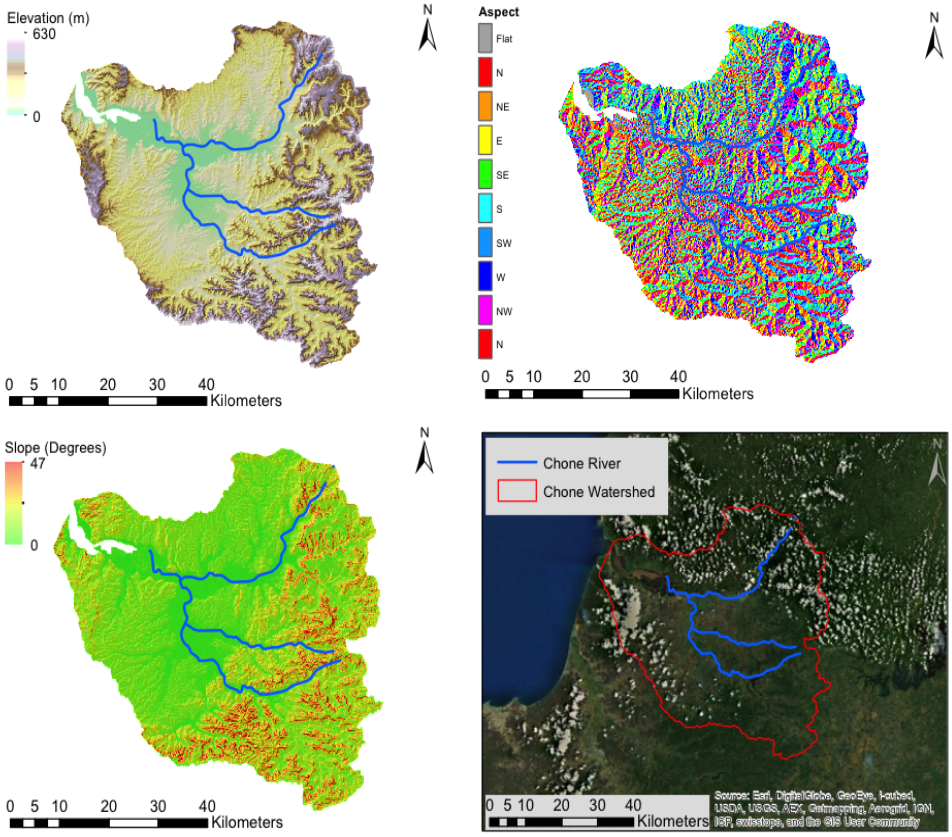

Figure 2.1 Elevation, aspect ratio, slope, and location of the Rio Chone watershed. Map created by William Brandt, University of California, Santa Barbara

2.2.2 Oceanography and Coastal Processes

Coastal currents near the mouth of the Rio Chone estuary run in a northwest direction at an average speed of 0.7 knots. Dominant coastal processes include coastal transport, erosion,

and accretion, the latter a product of erosion of the cliffs located south of Bahia and drainage from the Rio Chone and Carrizal rivers (Arriaga et al., 1999).

2.2.3 Geology and Geomorphology

The geologic materials in the Rio Chone estuary's vicinity originated in the Jurassic period, with additional formations from the Superior Eoceno, Oligoceno, and the Inferior Mioceno. The valleys were formed over long periods of time from riverine erosional processes, and the micro-basins were dilled with sands, gravels, and silts in alignment with the quaternary formations. The greater Rio Chone watershed is pocked with dramatic reliefs of hard rocks deposited in thick strata. The weathering of this material over time has produced hills with abrupt ragged to domed tops. Of these, abrupt reliefs and rolling slopes exist over planes of fractures and geologic slides with interfluvials in "V" form (Arriaga et al., 1999).

2.2.4 Capacity of the estuary

As material enters the estuary, both as sand from the coast with incoming tides and from river input, the estuary loses its capacity to hold water (UNESCO, 1994). Average discharges of freshwater from the Carrizal and Rio Chone rivers are 32 and 76 $m^3\ s^{-1}$ respectively, with the lowest flows occurring during the dry season between July and December.

Our study attempts to prove that the capacity of the Rio Chone estuary to hold water has been decreased due to sedimentation. Impacts caused by the drainage of domestic wastewater and shrimp pond effluent, the La Esperanza Dam in the Carrizal River, and received soil drained off of the terrestrial watershed are exacerbated by reduced capacity as dilution of estuarine-water contents is impeded (Arriaga et al., 1999). The cumulative volume of shrimp ponds was measured at 40 million cubic meters in 1994, compared to a low-tide volume of the entire estuary of 68 million cubic meters and a high-tide volume of 105 cubic meters. Productivity problems within the shrimp aquaculture industry have been identified as a product of decreased water quality conditions and decreased water-holding capacity (UNESCO, 1994).

2.2.5 Mangroves

Arriaga et al. (1999) observed four species of mangrove native to the Rio Chone estuary, including *Rhizophora mangle* (red mangrove), *Avicennia germinans* (black mangrove), *Laguncularia racemosa* (white mangrove), and *Pelliciera rhizophorae* (piñuelo mangrove). Each species has different growth characteristics and tends to inhabit distinct areas within their habitats. Species presence is often dictated by the elevation gradient of the shore. Rhizophora typically grows on the shorelines, in the harshest environments, ranging from +0.06 to +0.49 m above mean sea level (Lewis, 2005). It is able to prosper in these areas of low competition due to prop roots that grow downward from its branches. *Avicennia* grows at the next level of the elevation gradient from +0.12 to +0.76 m, and *Laguncularia* typically

inhabits the highest bank elevations from +0.21 to +0.76 m (Lewis, 2005). The Rio Chone estuary had lost 80% of its mangrove forest by 1999, with stands shrinking from 3,973 Ha to 392 Ha between 1969 and 1995 (Figure 2.2) (Arriaga et al., 1999).

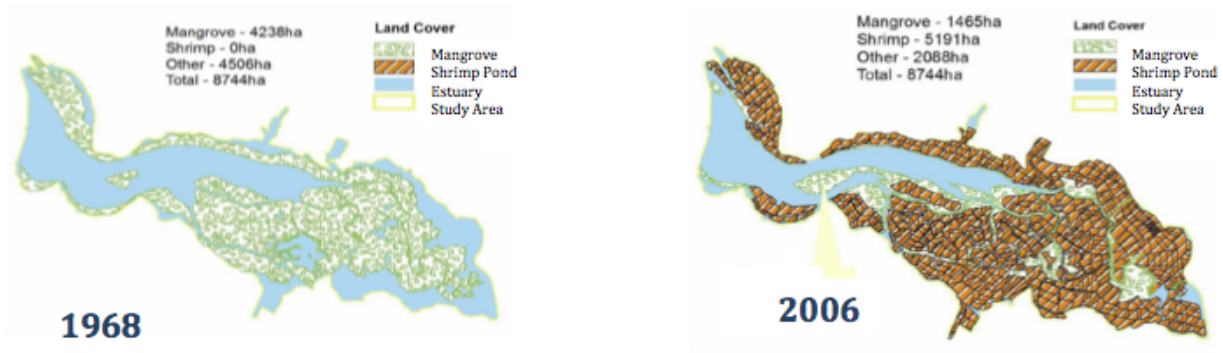

Figure 2.2 Conversion of mangrove extent to shrimp ponds from 1968 to 2006 in the Rio Chone estuary. Image modified, original from Hamilton & Collins, 2013

Pelliciera rhizophorae (piñuelo mangrove) was listed in 2010 as "vulnerable" in the IUCN Red List of Threatened Plants, having been extirpated and out-competed in much of its original habitat (Ellison et al., 2010). Its limited present distribution is due to a combination of factors, but primarily the influence of increased soil salinity. *Pelliciera* thrives in sites with high precipitation and abundant runoff, which jointly act to reduce soil salinities. The species is characteristically sensitive to soil salinity, intolerant of salinity levels exceeding 37 parts per thousand (Jimenez, 1984). However, sedimentation of the Rio Chone estuary counteracts the dilutive effects of high precipitation and runoff, causing increases in salt concentrations as water-holding capacity is reduced. For comparison, *Avicennia germinans* has been found in maximum soil salinities of 100 parts per thousand (ppt), *Laguncularia racemosa* has been found in soil salinities up to 80 ppt, and *Rhizophora mangle* in soil salinities of 60 ppt. Along with the sensitivity to soil salinities, it has been suggested that Pelliciera has been reduced due to competition by *Rhizophora* species in many of its preferred channel fringe habitats (Jimenez, 1984).

2.3 Land Use in the Rio Chone watershed

The hills surrounding Bahia de Caraquez contained 2,760 hectares of dry tropical forest in 1999, with an additional 1,800 hectares on San Vicente's northern shoreline (Arriaga et al., 1999). As noted, removal of vegetation from the low-lying hills surrounding the Rio Chone estuary has increased erosion rates and sediment transport into the receiving waterways. Ecuador has one of the highest rates of deforestation on the continent. A global land cover/land use raster collected from the European Space Agency indicates that 68% of the watershed's area was cropland in 2009. The remaining 32% was characterized as native vegetation, sparse vegetation, or water bodies (Arino et al., 2011).

The economic development of the Rio Chone basin is largely correlated with cultivation of the terrestrial lands, and conversion of dry tropical forest to agricultural plots has been underway since the 1950s. In 1999, agriculture was still considered a significant source of employment for Ecuadorians in the Manabi province, covering 3,280 hectares of land with grasses and short-cycle crops. Forest clearing in the region is accomplished using slash-and-burn strategies. Principal large-scale crops include cotton, corn, coffee, citrus fruits, banana, peanuts, and soybean to meet the needs of edible oil producing companies. Small-scale subsistence farmers often cultivate vegetables, pumpkin, melon, cucumber, and watermelon (Arriaga et al., 1999).

Urbanized areas in the watershed include the cities of Bahia de Caraquez, Chone, San Vicente, and San Antonio. Much of the watershed's population inhabits the coastal zones north and south of the estuary's ocean outlet. The 2010 census tallied populations of 20,921 and 52,810 for Bahía and Chone respectively (Figure 2.3) (NEC, 2011).

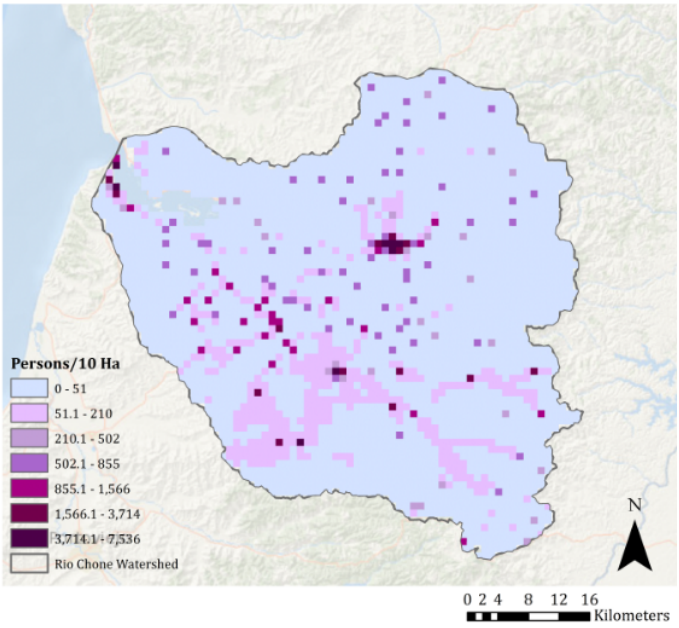

Figure 2.3 Population in the Rio Chone watershed, shown in number of persons per 10 hectares

2.4 Stakeholders and Socioeconomics

The watershed boasts several economic sectors, including aquaculture, agriculture, and tourism, in addition to its service and business industries. Commercial fishing of crab and shellfish was once common, but has been greatly diminished in the vicinity of the estuary due to the loss of mangrove habitat, as crab and shellfish use mangrove roots as nursery grounds. Most of the current small boat fishing fleet within the estuary work on a purely artisanal level and seek white fish, shrimp, and shellfish (Arriaga et al., 1999). Here, we discuss the socioeconomics of our study area as the economic sectors mentioned are shareholders intimately linked to the estuary's wellbeing.

2.4.1 Aquaculture

The main forms of aquaculture in the watershed are chame and shrimp cultivation. The chame fish (*Dormitator latifrons)* is farmed in the waters of La Segua, a marsh located upstream of the Chone-Carrizal confluence. Shrimp cultivation provides the lion's share of the Rio Chone's aquaculture economy with annual shrimp cultivation amounting to close to 11 million pounds in 1999, making up 10% of Ecuador's total shrimp production. Just 10% of shrimp ponds in the Rio Chone estuary have been created on private property, with 90% on lands being leased from the state for 10 year increments (Arriaga et al., 1999).

2.4.2 Agriculture

Agricultural practices in the Chone and Carrizal river basins exploded in the 1950s. Although in decline in recent years, the sale of produce is still a significant source of income for the indigenous people (Arriaga et al., 1999). The cutting and burning of native vegetation to grow cotton and corn was at one time commonplace. As previously mentioned, this was a primary driver of the expansive deforestation experienced in the Rio Chone watershed (Coello et al., 1993).

Coffee, citrus fruits and bananas are the predominant industrial-scale crops. Subsistence farming makes up the remaining farming activities, growing crop-types including pumpkin, melon, cucumber, and watermelon (Arriaga et al., 1999). See section 2.3 for a more detailed discussion of the crops grown in the Rio Chone watershed.

2.4.3 Tourism

The beaches of the Rio Chone estuary are the chief draw of the watershed for tourists (Arriaga et al., 1999). Inhabitants of the Ecuadorian interior, especially Quito, seek Bahía de Caráquez's white sand beaches and multiple hotels to escape the confines of the more heavily urbanized areas. The tame waters of the estuary provide a family-friendly beach that generates revenue for beach-side restaurants, souvenir stands, and kayak rental agencies. *International Living* has ranked Ecuador as the number one place to retire multiple years running and Bahía has benefitted tremendously from real estate tourism (Tamariz & Rinaldi, 2012).

The estuary's biodiversity also remains a draw for nature enthusiasts. Local boat operators and tour guides take advantage of the estuary's remaining mangrove forests around Isla de Corazón and the frigate birds that nest there. On land, tropical dry forests entice tourists looking to spot anteaters, sloths, and iguanas. Another draw is La Segua, a partially protected wetland located just east of the estuary that is home to more than 164 different bird species (Adès et al., 2013).

2.5 Fundamentals of Erosion

Every year, 75 billion tons of soils are eroded from the Earth's surface. Most of this soil is lost from lands cultivated for agriculture, with soil loss rates from cropland ranging from 13 to 40 tons/hectare/year. The rate at which soil is formed, however, is extremely slow in comparison, resulting in a soil loss rate that is 13-40 times faster than the rate of soil renewal. This loss of soil decreases productivity and can rapidly render land unusable for agriculture. The resulting productivity lull often drives further conversion of native lands for agriculture when the previously farmed parcel is left fallow. Through this process, erosion is a leading cause of deforestation around the world (Kounang & Pimentel, 1998). Here, we discuss erosional processes, the effects of erosion on downstream water bodies and agricultural productivity, and the impacts of erosion on our particular study area.

2.5.1 How Erosion Happens

Agricultural land is especially susceptible to erosion because tilled or bare land is exposed to the two main causes of erosion, rain and wind. First, raindrops hit exposed soil and dislodge soil particles from the ground, launching them into the air. The soil particle is then more easily carried away by water into streams and rivers. This process is more efficient as the slope of hillsides increases, with over half of dislodged soil particles ending up in downstream water bodies on average. The second cause of erosion is wind. Wind energy dislodges soil particles and carries the particles away from their original production location. Wind and rain act together to remove a thin sheet of soil from the land surface, which is known as sheet erosion. Sheet erosion is the leading form of land erosion worldwide (Kounang & Pimentel, 1998).

Land cover plays an important role in reducing soil erosion. Plant biomass, either living or dead, acts as a protective layer against wind and rain energy by dissipating their intensity above the soil surface. Tree coverage is also effective in reducing erosion as the branches and leaves intercept and diminish the energy of rain and wind. Cropland is highly susceptible to erosion because repeated tilling leaves segments of the soil exposed to erosive processes, and land is often left bare between plantings (Kounang & Pimentel, 1998).

Although agricultural production is responsible for approximately three-fourths of soil erosion worldwide, erosion also occurs naturally. For example, the fast movement of water along stream banks is a powerful force often removing significant levels of soil as it flows. Even on flat land with a two percent slope, stream banks can erode easily. Flooding from heavy rainfall events further exacerbates this process (Kounang & Pimentel, 1998).

In addition, soil structures influence the rate of erosion. Soils with medium to fine texture, low organic matter content, and weak structural development are most susceptible to erosion. These soils have a low infiltration rate, which results in higher levels of surface runoff, providing transport for loose soil particles. Lastly, landslides and earthquakes cause

soil erosion, but their overall contribution to erosion on a global scale is low since these events are rare (Kounang & Pimentel, 1998).

2.5.2 Effects of Erosion Downstream

Erosion poses a significant threat to downstream water bodies through the eventual deposition of detached soil particles and/or increase in turbidity from the suspended materials (Kounang & Pimentel, 1998). Over time, streams and rivers carry sediment downstream where they build up in sediment sinks, often lakes and estuaries. This lag time between erosion from the land surface to deposition in a large water body can be considered a "sedimentation debt". The concept of a "sedimentation debt" signifies that once detachment occurs, it is only a matter of time until the particles are transported to a water body. In some situations, the "sedimentation debt" can be quite long, which means that the costs of land use practices continue long after the land alteration has occurred. The lag time varies by system, depending on drainage area, runoff amount, length and slope of topography, intermediate depositional sinks, and particle size (Woznicki & Nejadhashemi, 2013). Small particles are more mobile than large, and therefore delivered more quickly to large water bodies; the larger the particle, the longer the potential lag time.

The buildup of eroded sediment has significant consequences for these water bodies in terms of water quality. Soil particles often carry fertilizers and pesticide chemicals from upstream agricultural practices, which harm aquatic ecosystems, reducing water quality, and contaminating water and sediments. The buildup of sediment also leads to the siltation of reservoirs and dams, leading to reduced water storage, increased cost of dam maintenance, and shortened lifetime of reservoirs (Kounang & Pimentel, 1998). The effects of erosion on downstream water quality and habitat are discussed further in section 2.6.

2.5.3 Effects of Soil Loss on Agricultural Productivity

Soil erosion has adverse economic effects resulting predominately from the loss of agricultural productivity on degraded land. Most of the 75 billion tons of soil lost around the globe each year stems from the way cultivated lands are managed (Lal, 2001). Currently, approximately 80% of the world's agricultural lands suffer from moderate to severe erosion. The loss of topsoil negatively affects crop yields as erosion decreases soil quality, reducing soil water holding capacities, soil organic content, and soil nutrients. Erosion increases the amount of water runoff, hindering the soil's ability to absorb the volume of water necessary to sustain agricultural production. Furthermore, soil organic matter, a vital element in the creation of rich, dense soils and strong soil structure, is typically found in the surface layers of soil. This is the first material-type to be transported downgradient. Lastly, important soil nutrients like nitrogen, phosphorous, and potassium are easily eroded by wind and water. Typically, eroded soil contains three times more nutrients than the soils left behind (Pimentel et al., 1995). As a result, much of this soil, water, and nutrient loss contributes to declined agricultural productivity. It is estimated that soil erosion on agricultural lands contributes to a 32% loss of production worldwide each year (Lal, 2001).

To compensate for the depleted soils, farmers often invest in fertilizers to replenish the lost nutrients. Not only is this costly for the farmer, it is costly to the environment. Overcompensation of nutrient loss by fertilizer application increases the amount of nitrogen, phosphorous, and various other chemicals reaching water bodies downstream as soil continues to be eroded after fertilizers have been applied. Increased nutrient concentrations in water bodies can cause eutrophication, degrading water quality. For those farmers who cannot access or afford products to augment their soil, losses are combated by fallowing the degraded plot and moving to new parcels, clearing additional native vegetation for this task (Pimentel et al., 1995). This further deforestation leads to continued erosion on the newly cultivated land, perpetuating a cycle of continuous soil depletion.

2.5.4 Erosion in Ecuador

Excessive erosion in Ecuador is occurring due to the removal of native vegetation and the subsequent land use practices occurring on the cleared land. Potential drivers of land degradation include a lack of governmental oversight on government-owned lands and poor support for land conservation, among other things. In Ecuador, farmers generally utilize annual cropping strategies rather than a permanent crop cover, which would protect the soil to a greater degree. In a study of Ecuador's Rio Chimbo watershed, sites under annual cropping showed the greatest soil loss relative to areas with more continuous ground cover. When soil becomes so degraded it can no longer provide enough nutrients for agriculture, it is abandoned and the process is repeated on a new plot of land. In some cases it takes years for degraded soil to become re-stabilized to a point where it could again support vegetation. In addition, heavy grazing from sheep, goats, and cattle exacerbates soil erosion on cleared land. Grazing animals eat remaining vegetation and dislodge soil grains when walking on top of the bare earth (Henry et al., 2013).

Ecuador’s current agricultural methods leave significant room for scientifically-based improvements. From the mid-1960s to the mid-1980s, two-thirds of the increase in agricultural production in Ecuador came from expansion of the area of land in cultivation; only the remaining third came from improved productivity. Unlike methods that increase yield and productivity, the expansion of agricultural land sprawl leads to further deforestation and erosion. The Ministry of Agriculture and Livestock estimates that 84% of the land in the Northeastern part of the country should never be cleared for farming or grazing because of its limited fertility potential according to soil type, high probability of erosion according to soil type and hillslope gradient, and poor drainage promoting surface runoff (Whitaker & Southgate, 1992). However, much of this land is in cultivation.

2.6 Estuarine Sedimentation

Increased sediment loading into waterways degrades water quality and increases turbidity in the water column. In addition, sedimentation of a waterway can alter its hydrology and concentrate constituents as water holding capacity decreases.

The Rio Chone estuary has been drastically affected by intensified sediment loading as a result of dry deforestation, mangrove deforestation, and shrimp farming practices. The estuary's inter-estuarine sediment transport regime is discussed herein, to provide context for the following discussion of the effects of sedimentation on the estuary's hydrology, biogeochemistry, biology, and socioeconomics.

2.6.1 Inter-Estuarine Sediment Transport

An estuary's morphology is principally determined by its residual sediment transport pattern, though residual transport patterns in turn partially depend on morphology. Due to this feedback loop it is important to first define what processes affect the residual sediment transport pattern within an estuary. Transport is dependent on the dissimilarity in magnitude and duration of ebb (outgoing) and flood (incoming) tidal currents (Dronkers, 1986). This dissimilarity in tidal magnitude, or tidal asymmetry, is caused by the interaction of the tidal wave with the relatively shallow bathymetry of an estuary, as propagation of the tidal wave is affected nonlinearly by friction and continuity (Blanton et al., 2002). Essentially, within estuaries the velocity of tidal inflow is often different from the velocity of tidal outflow.

Two major processes contribute to the movement of sediment within estuaries: transport of suspended load, and movement along the bottom. These processes affect particle sizes differently because larger particles with higher settlement speeds are more often transported along the bottom, and smaller particles with lower settlement speeds are more often transported through advection. However, the relative partitioning of particles sizes into these categories is heavily dependent on flow velocities (Dronkers, 1986).

The Rio Chone estuary (1-3m tidal range) falls within the mesotidal range (2-4m tidal range), and follows the mesotidal categorical expectation that it would have larger ebb-tidal deltas than flood tidal deltas (Hayes, 1980). The domination of the ebb tide processes on residual sediment transport is indicated by greater deposition of sediment outside the mouth of the estuary relative to the deposition of sediment inside of the estuary's mouth. This difference is caused by the duration of slack water preceding ebb and flood tides, which particularly influences the settlement of fine particles, as their settlement speed is slow, as well as the difference between maximum tidal current velocities during ebb and flood tides, which largely influences the deposition of course grain sediments (Dronkers, 1986).

The bathymetry of an estuary is therefore dynamically driven by asymmetric tidal transport of sediment. The transport residuals define where sediment will build up and

what proportion will be moved throughout the estuary. Additionally, wave energy and storm surges can induce abrupt changes in estuarine bathymetry (Dronkers, 1986). Net sedimentation of an estuary is only able to occur if the sediment input rate from the watershed is greater than the transport rate out of the estuary (Wolanski et al., 2001).

2.6.2 Hydrologic and Biogeochemical Effects

Estuaries are unique ecosystems. Salinity, temperature, pH, dissolved oxygen, redox potential, and particle composition can vary dramatically as the freshwater outlet meets marine, creating vertical and horizontal gradients. Salinity varies spatially (both laterally and vertically) and is the controlling factor for the partitioning of contaminants between sediments and overlying or interstitial water. Faunal distributions in estuaries are controlled first by salinity, and second by factors such as substrate, temperature, dissolved oxygen, and anthropogenic pollution (Wilber & Clarke, 2011).

Increased sedimentation in the Rio Chone estuary has caused significant decreases in water depth in certain areas. These depth changes are a likely driver of significant changes in salinity, temperature, and other water quality factors, as decreased water-holding capacity reduces dilution capacity (Wilber & Clarke, 2011). A study of reservoirs in Kansas performed by the United States Geological Survey (USGS) (2013) showed that water pollutants and certain sediment-derived constituents increased in concentration and/or their propensity to bioaccumulate as sedimentation occurred. Phosphorous, for example, increased in concentration resulting in eutrophication, while several trace elements and organochlorine compounds exceeded threshold-effect levels (the concentration at which toxic biological effects occur) set by the U.S. Environmental Protection Agency (EPA) subsequent to sedimentation (USGS, 2013).

The Rio Chone estuary suffers from low dissolved oxygen, partially due to its turbid waters. Turbidity reduces the ability of light to penetrate the estuary's water, causing a reduced rate of photosynthesis by aquatic plants and phytoplankton, and hindering oxygen creation by plant-matter. Low oxygen levels can be extremely detrimental to fish and aquatic life (Chapman & Wang, 2001).

Suspended particles can also increase the impact and extent of pollution, acting as sinks for water quality constituents. Hydrocarbons, heavy metals, polychlorinated biphenyls, and pesticides can bind to suspended particles depending on their physiochemical properties (molecular weight, density, solubility, volatility, octanol-water partitioning, flammability and flash point, chemical incompatibility, etc.). Particulates can also deliver nutrients through similar processes. Contaminated particles are available to be ingested by filter feeders, leading to the transfer of contaminants to higher trophic levels. Contaminants can then become concentrated in higher trophic level species through biomagnification (Berry et al., 2003).

2.6.3 Biological Effects

Sedimentation of water bodies has three major effects on fishes: 1) direct physiological effects of suspended sediment, such as suffocation, 2) effects from decreased water clarity, and, 3) effects due to sediment deposition that increases burial of eggs and larvae. The first effect is a direct impact on the organism from abrasion, the clogging of filtration mechanisms affecting respiration and ingestion, and in extreme cases, smothering and burial resulting in mortality (Wilber & Clarke, 2011). In a study investigating the effect of sedimentation in the ACE (Ashepoo, Combahee, and Edisto) Basin in South Carolina, several estuarine fishes were found to be highly sensitive to elevated turbidity. Effects included hindered immune functioning, and tissue and cellular structural impairment of the organisms (Wenner et al., [unpublished date]). Second, sedimentation can disrupt feeding efficiency and fish behavior. Changes in water clarity can disturb food web dynamics through decreased predator feeding success and enhanced prey survival. This can lead to a decrease in species diversity if food web disturbances affect species dissimilarly. The third effect, sediment deposition, has been reported to influence the migration and spawning behaviors of fish. This can include decreased disease resistance and alterations to hatching success, growth, and egg development. Many mobile estuarine species move away from areas with elevated suspended sediments, which may compound the aforementioned problems of decreased species biodiversity (Wilber & Clarke, 2011).

2.6.4 Social and Economic Effects

The increased rate of sedimentation in the estuary has already had negative impacts and threatens the success of the shrimp industry. The presence of mangroves and the habitat provided by the estuary were originally important contributors to the success of the shrimp industry, because the estuary provided ample nursery habitat for post larval shrimp (Twilley, 1999). Therefore, maintaining the health of the estuary is necessary for the shrimp aquaculture industry to function. Shrimp ponds exchange 10% of their volume with the estuary daily and are flushed with the change of the tide (Hamilton, 2013). They depend on the estuary's waters to provide high quality water that will enhance growth of the crustaceans. Ponds in the upper reaches of the estuary are no longer accessed by the estuary's tides, forcing their operators to implement hydraulic pumps to accomplish the task tidal inundation once performed. If sedimentation continues, shrimp ponds along the estuary will likely have to convert to more intensive flushing mechanisms.

Additionally, in 1826 the estuary functioned as a full service port, with channels deep enough to allow large boats to access coastal regions within the estuary (Alejandro, Santos, Pers. Comm.). Though it was once a dominant port in Ecuador, the estuary is now too shallow to function as such. Waters are no longer navigable by any craft other than small boats during high-tide (Alejandro, Santos, Pers. Comm.).

Estuaries are one of the most productive marine ecosystems in the world. The Rio Chone estuary has had its capacity to provide critical habitat for the life and development (e.g., rearing, feeding, migration routes, and nursery grounds) of many aquatic species reduced.

Subsistence fisheries in the estuary have suffered due to this degradation, and many stakeholders stand to be negatively impacted by further degradation of the estuary.

2.7 Effects of Ecuadorian Policy on Land Degradation

Ecuador's history of land degradation is closely linked to the laws (or lack thereof) describing how the natural environment is to be managed. For example, Ecuador practices *patrimonio forestal* (forest patrimony), which grants the government ownership over all forested lands. Unfortunately, the Ecuadorian government has openly acknowledged that they have limited resources to oversee their expansive holdings. As a result, they have resorted to leasing lands on a short-term basis to private parties who rarely have incentives to conserve the land's resources. To compound the problem, land tenure is officially won by destroying native vegetation in order to colonize the desired parcel of land, resulting in increased deforestation. In addition to these deleterious tenures, unlawful trespassers on the land see the forest's resources as free and take what they please. For farmers cultivating cleared lands, incentives to farm sustainably and utilize soil conservation techniques are low when they have no long-term claim on the land (Southgate & Whitaker, 1992).

In addition to poor tenurial arrangements, the Ecuadorian government has interfered with the market forces that would normally encourage forest conservation. Resource subsidization, enforced low prices for domestic resources, inflated currencies, and the implementation of tariffs on foreign goods by the Ecuadorian government have reduced economic incentives to conserve the land's resources. Artificially low prices for agricultural inputs, such as fertilizer, and government forcing of standard petroleum prices have resulted in inefficiencies as well as excess pollution in rural areas (Southgate & Whitaker, 1992). While Ecuadorian policy makers have become aware of these environmentally detrimental market influences and have begun to address the issue, multiple institutional policies have remained in place and continue to promote unsustainable practices among smaller farmers and land managers (Follis & Nair, 1994).

2.8 Addressing Current and Future Erosion Risk

Soil erosion is a leading cause of land degradation worldwide (Descheemaeker et al., 2006). Implementing the duel methods of reforestation and soil conservation in agriculture are two main recourses to reduce the amount of sediment entering the Rio Chone estuary from its surrounding watershed.

2.8.1 Reforestation of Degraded Lands

Reforestation is the natural or intentional return of forest cover to areas where it existed before intentional removal (US Forest Service, 2015). Forested lands have far lower soil loss than agricultural lands and grassland (El Kateb et al., 2013). This is due to the increase in protective structures provided by the leaf canopy and the forest's soil stabilizing root

systems (El Kateb et al., 2013). Because of the erosion protection benefits provided by reforestation, our project explores the use of reforestation/re-vegetation as a possible long-term solution for stabilizing soil in the Rio Chone watershed.

Bare hillslopes are particularly vulnerable to surface water erosion. However, increasing vegetative cover can counteract this erosional process (Dlamini, 2011). Zuazo and Pleguezelo (2008) found that sediment loss and runoff decrease exponentially as vegetative cover increases. This negative correlation comes into effect after vegetative cover increases past the threshold level of 15% coverage (Bochet et al. 2006). However, the question remains: what percent vegetative cover is optimal to prevent soil erosion?

Zhou et al. (2008) assessed data rich restoration scenarios in China's Upper Min River watershed, comprised of hillslopes averaging 26 degrees. They concluded that reforesting high-risk erosion areas to 40-60% vegetative cover will capture most of the erosion reduction benefits (Zhou et al., 2008). Descheemaeker et al. (2006) experimented on hillslopes with multiple gradations in Tigray, Ethiopia. They concluded that runoff exponentially increases as percent vegetation decreases and also found what they call a "vegetative threshold percentage." They argue that the benefit to stopping erosion from vegetative cover maxes out at around 65% (Desheemaeker et al., 2006). This 65% value reaches beyond the upper bounds of the Zhou et al. (2008) findings and becomes a logical conservative goal for a restoration project seeking to prevent the loss of topsoil from surface water erosion (Zhou et al., 2008).

Though Descheemaeker et al. (2006) report that rainfall and storm duration are not the critical erosive variables when compared to total vegetation cover, precipitation rate does intensify erosion (Bochet et al., 2006). Rainfall intensities of less than 25 millimeters per hour generally cause no erosion for vegetative cover over 55%, while intensities four times as extreme (100 mm/h) can cause erosion even when vegetative cover exceeds 90% (Bochet et al., 2006). In effect, the percentage of cover needed to reduce erosion is dependent on the erosivity of the rainfall event. The Rio Chone watershed experiences short periods of intense rainfall during its rainy season, making rate-of-rainfall a consideration when selecting an ideal land cover percentage. If the watershed were protected by the Descheemaeker threshold of 65% plant cover, as long as rain intensity were not to increase above 25 millimeters per hour, erosion reductions should be significant.

Though the Rio Chone watershed only experiences an average of 500 mm of rainfall per year, intense rain years, such as those experienced during El Nino cycles, exceeds this threshold. Taking into account the magnified intensity and increased volume of precipitation periodically experienced, and the effects of climate change on the region (see section 2.9), the 65% vegetation cover value should be considered ideal. However, greater percentages of cover will provide greater fortification for hillslopes from sheetwash erosion.

Reforestation as a means to prevent soil erosion should be seen as a long-term process and solution to erosion. Newly planted seedlings must first go through a three to five-year

establishment period, during which weed management is crucial to the reforestation effort's success. A stand's eventual success at countering erosion will be attributed to the ability of the new trees' vegetative structure to provide ground cover with its foliage, soil surface stability with its roots, and soil protection with a layer of duff. Reforestation sites must be cared for until maturity is reached (Le et al., 2012). Efforts to reforest areas of the Rio Chone watershed are likely to help prevent soil erosion within eight to ten years of planting, with maximum erosional benefits reached after approximately 30 years (Marden, 2012; Huang et al., 2010). Still, it is important to consider that long-term success of reforested land has been a great challenge for some sites in developing countries (Le et al., 2012).

2.8.2 Soil Conservation Techniques

Because the use of reforestation to manage soil loss can take years to become fully-realized, more immediate erosion control methods were researched. Soil conservation strategies have the potential to reduce erosion rapidly once implemented by farmers and land managers.

2.8.2.1 Agrotechnical Methods

Agrotechnical infrastructure, such as pre-planned channeling for runoff and placement of branches or logs as erosion barriers, can reduce hillslope erosion (Sapountizis et al., 2007). Tang et al. (2014) recommend marginal hedgerows and retention trenches to capture sediment on hillslopes being used for agriculture. These work to increase the infiltration of water into soils and minimize runoff. Tang et al. (2014) also recommend limiting the practice of downslope tilling on farmland, which is the strongest anthropogenic force leading to topsoil displacement in agricultural areas (Tang et. al, 2014).

2.8.2.2 Mulching

Mulch is any material, organic or inorganic, that is placed around plant life that helps to retain soil moisture, soil temperature, and reduce erosion (Niemiera, 2009). Mulches are an economically efficient means to promote plant growth, reduce erosion, and enhance chances of survival in tropical dry areas (Guadalupe Barajas-Guzmán & Barradas, 2013). Reductions in erosion are provided by the physical protection from particle dislodgment by rain and wind. Therefore, when mulching annual crops, it is critical to provide coverage when the crop is initially emerging (Erenstein, 2003). This is because the agricultural crop itself does not yet provide protection from erosive processes, and because land preparation activities, which could harm mulch coverage, have likely been completed. Mulch would likely need to be reapplied after a field is tilled, so retention of mulch between crop cycles is most efficient in reduced and no-till systems.

Organic mulch from vegetative sources can be produced off-site, or can be internally sourced by utilizing the non-market biomass produced by the previous crop cycle. Live

mulch, or cover crops, can be used by incorporating low lying plants between rows, though a height difference should be present between the target crop and the cover crop to limit light competition. Water and nutrient competition must also be considered, but the use of legumes can aid the growth of target crops through nitrogen fixation (Ngwira et al., 2011). Mulching has a significant effect on soil fertility by reducing the loss of topsoil to erosion, conserving water by reducing run-off and evaporative losses, and adding to the pool of soil organic matter (Erenstein, 2003).

The landowner or manager has the final say on which, if any, soil conservation techniques are practiced. As such, implementation is most successful when private returns are likely to increase. In practice, mulching can create up-front costs to the farmer due to adapted seeding equipment that make the process of sowing more time consuming. Security of land tenure is an additional pre-requisite for incentivizing farmers to invest the time and maintenance costs mulching requires (Erenstein, 2003). Considering this, government incentives and public bolstering might be necessary in order to make the beneficial soil conservation techniques of mulching a reality.

2.9 Climate Change

Anthropogenic forcing of global climate change is widely accepted within the scientific community. While our research does not focus heavily on climate change, it is imperative that we contextualize our work with a discussion of the dynamic localized manifestations of global climate change in the Rio Chone estuary. Kitoh et al. (2011) show that mean annual precipitation is expected to increase within the watershed in the future. Rainfall intensity measured as maximum five day precipitation is also expected to increase (Kitoh et al., 2011). Global climate change will increase the intensity of seasonality in precipitation, meaning that dry seasons will become drier, while wet seasons become wetter (Kitoh et al., 2011).

An extreme El Nino event struck the Rio Chone watershed in 1997/98 causing massive flooding and sediment delivery to the estuary. Though some uncertainty exists in the climate projections, Cai et al. (2014) assert that the frequency of these extreme El Nino events will increase due to global climate change. Power et al. (2013) also report robust projections of increased intensity of El Nino oscillations with climate change, increasing precipitation in the eastern equatorial Pacific, including Ecuador. These projections further underline the necessity of erosion management in the watershed (Power et al., 2013).

Nearing et al. (2004) discuss the potential effects of climate change on erosional processes, providing a conceptual starting point for the Rio Chone watershed. As precipitation and the frequency of high intensity precipitation events increase, rainfall erosivity will increase within the watershed. Rainfall erosivity is a fundamental factor affecting erosion and this change will act to increase the potential for erosion within the Rio Chone watershed (Nearing et al., 2004).

Climate change will produce more complex feedbacks on the native vegetative communities within the watershed. Increases in annual precipitation could increase the canopy cover in native areas, thus decreasing erosion rates, however, increased seasonality may leave native areas badly denuded after unusually extended dry periods, thus increasing erosion. Regardless, managed agricultural lands are the largest source for erosion within the watershed, and we do not expect climate change to heavily affect the canopy cover of agricultural lands (Nearing et al., 2004).

The increase in erosivity projected by climate change models is worrying due to the current high levels of erosion in the watershed. The climatic changes that the Rio Chone watershed can expect will make management of erosion all the more necessary, because the already high magnitude of losses can be expected to increase.

2.9.1 Sea Level Rise

Church et al. (2013) predict that Ecuador will experience sea level change at a magnitude consistent with the global average, about half a meter by 2100 (about 0.6 cm/year). Given the current rate of sedimentation (about 4 cm/year), it is clear that global sea level rise will not offset the sedimentation issue within the Rio Chone estuary (Church et al, 2013).

3.0 Methods

Tasked with understanding the causes of estuarine sedimentation, potential management options, and the implications of erosion on the local environment and economy, a number of studies were pursued. Field reconnaissance was initially performed to prioritize action items in the Rio Chone estuary. First, bathymetric maps were gathered from Ecuador's Navy, the Instituto Oceanografico de la Armada (INOCAR), with the aim to analyze the changing bathymetry of the estuary. Second, a sediment budget was composed to estimate the likely contributions of sediment from the different erosional processes at play within the terrestrial watershed. Finally, a soil loss model was used to estimate the amount of sediment produced from sheetwash and to test the effect that changing land use within the watershed could have on erosion rates.

3.1 Bathymetric Map

To quantify sedimentation in the Rio Chone estuary, we compared depth measurements from bathymetric maps created in 1990 and 2011. Bathymetric measurements were gathered by INOCAR with coastline data based on cartographic measurements taken by the Institute of Geography. Measurements of both maps were taken during low tide using a tri-point Geographic Information System (GIS) tool. The maps provide depth measurements in meters at a spatial scale of 1:25,000. Depth measurements were taken every 0.2 to 0.5 kilometers extending approximately 7 kilometers off the coast and 12 kilometers up the estuary. Our analysis looked at the data collected for the estuary and seven kilometers off

the coast, as our primary concern is change that can be attributed to estuarine sedimentation. The total study area encompassed 107.88 square kilometers.

We employed a variety of methods to generate a visible representation of the depth decrease in the estuary. Our final goal was the creation of a single map representing the change in bathymetry from 1990 to 2011. An interpolation of the various depth measurements in each map constructed prediction surfaces for both years, and when compared, created a single smooth surfaced bathymetric difference map. This analysis was done using ArcGIS 10.2. From this, we were able to calculate the volume of sediment deposited and retained in the estuary over the 21 period timeframe and estimate a crude accretion rate.

3.1.1 Georeferencing

Pictures of each map were digitized into ESRI's ArcGIS. The maps had coordinates given in latitude and longitude, with a vertical line for every two latitudinal and longitudinal minutes. Each quadrant of our region of interest was imported into GIS and georeferenced. Georeferencing, a tool in GIS, allowed us to associate our map images with their true spatial locations. Being cognizant of the different projections used in the creation of the two maps was crucial; the 1990 map was in the PSAD 1956 South American projection, while the 2011 map was in the WGS 1984 UTM Zone 17S projection. As a result, georeferencing had to be performed on two different maps based on the longitude and latitude coordinates, referencing four points for each of the map's quadrants.

3.1.2 Creating a Shapefile of Depth Measurements

Once georeferenced, the 1990 map was reprojected to match with the current WGS 1984 UTM Zone 17S projection of the 2011 map. A shapefile was created with a series of points denoting the depth (Z), and the longitudinal and latitudinal coordinates (X and Y) associated with each depth measurement. The "create" feature tool was employed to mark the depth point, automatically inputting its coordinates into the shapefile's attribute table. Its associated depth was then entered into our attribute table manually. X and Y coordinates were identified for every z location, or depth measurement, for each map. The kriging method was used to display the depth differences on a smoothed surface, interpolating expected depths based on the other surrounding depth measurements.

3.1.3 Kriging

To generate a smooth surface from a shapefile of scattered points, there are three basic interpolation methods: Inverse Distance Weighted (IDW), Spline Interpolation, and Kriging (ArcGIS Resource Center, 2012). Both IDW and Spline interpolation, known as deterministic interpolation methods, are based on the surrounding measured values or specific mathematical values that determine the smoothness of the surrounding surface (ArcGIS Resource Center, 2012). In these methods, points that are far away have less of an

influence than points that are close. Kriging, on the other hand, is a geostatistical method based upon statistical models. Kriging forms weights from surrounding measured values to predict unmeasured locations, rather than relying solely on the measured values closest to the unmeasured locations (ArcGIS Resource Center, 2012). This is necessary as kriging relies on autocorrelation, or the tendency for two types of variables to be related (ArcGIS Resource Center, 2012). The notion of autocorrelation hinges on the idea that things closer together tend to be more similar than things that are farther apart. Therefore, the rate at which the correlation decreases depends on distance, allowing one to model autocorrelation as a function of distance (ArcGIS Resource Center, 2012). In kriging, the data is expressed in the following mathematical formula:

$$\hat{Z}(s_0) = \sum_{i=1}^{N} \lambda_i Z(s_i)$$

Where,

Z(s$_i$) = the measured value at the *i*th location
λ_i = an unknown weight for the measured value at the *i*th location
s_0 = the prediction location
***N* =** the number of measured values

Kriging was chosen as the interpolation method because depth measurements were not evenly spaced. This methodology allows the measurements in closest proximity to an interpolated point to have the greatest predictive power over the value assigned to the surface. In addition, it takes into account the differences in the depths by assigning weights to the various depth measurements. Depths throughout the estuary ranged between 0 to 10 meters; it was imperative that these differences were taken into account when determining the prediction surface. Kriging can further be broken down into three basic methods: simple kriging, ordinary kriging, and universal kriging. We chose ordinary kriging for our analysis, as ordinary kriging does not assume that the mean is constant over the entire domain as is assumed in simple kriging. Rather, it assumes that the mean is in the local neighborhood of each estimation point (Lefohn et al., 2005). Kriging with a trend, or universal kriging, assumes a linear or high order trend in the *X* and *Y* coordinates of the data points (Lefohn et al., 2005).

The kriging process undergoes two steps when creating a prediction surface map. First, it must uncover the dependency rules on which the predicted values will be based on. To accomplish this it creates the variograms and covariance functions to estimate the statistical dependence values. The first step involves the creation of a semivariogram, which depicts the spatial autocorrelation of the measured sample points. The process involves the pairing of one point with all other measured locations (Figure 3.1). In GIS, the Kriging tool provides one with different types of models from which to choose for modeling the empirical semivariogram. Our analysis used spherical modeling with an output cell size of 25 meters and 12 as the number of points to influence the predicted value. The spherical model is most commonly used to show a decrease of spatial surfacing until a threshold distance is reached; autocorrelation then becomes zero. During the second step, the actual

prediction is expounded based on the revealed dependency rule (ArcGIS Resource Center, 2012).

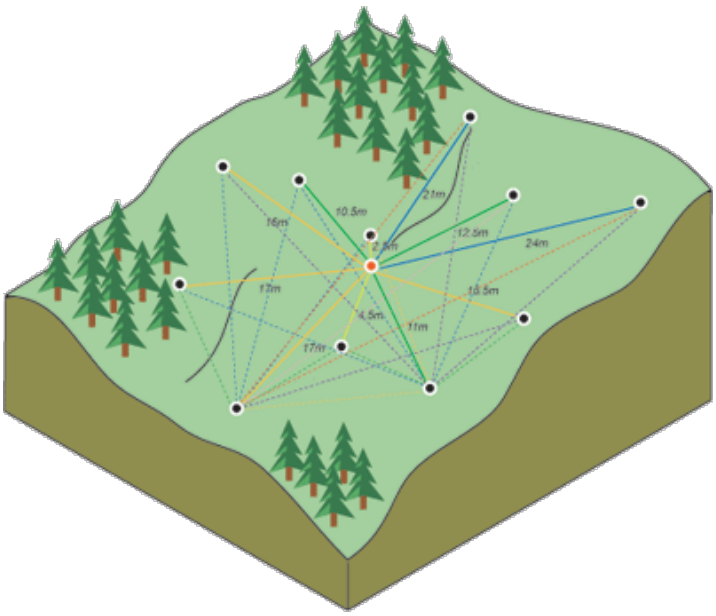

Figure 3.1 Calculating the difference squared between the paired locations. From ArcGIS Resource Center (2012)

3.1.4. Creating a Single Map of Bathymetric Change

The two kriged surfaces were overlaid so depths from the 1990 surface could be subtracted from the 2011 to create a single layer. The standalone map with a color gradient showing bathymetric change was generated with changes ranging from 7.3 meters of depth lost to 7.1 meters of depth gained. The values were multiplied by negative one so the data show bathymetric change as opposed to depth change.

3.1.5 Accretion Rate Estimation

The kriged surfaces allowed the use of a raster subtraction tool to find the total change in sediment per year. The total difference in bathymetry was exported into excel and summed to get a total overall bathymetric change for the study area (Figure 4.1). As only 24 square kilometers of the 34 square kilometer estuary had measurements provided in the original bathymetric maps, we extrapolated the additional 10 square kilometers with the mean depth change of the measured.

To find the total volume of sediment deposited and retained in the estuary each year we calculated the mass of sediment. This was based on the area and total height of sediment change, as well as the density of soil to get a volume of sediment. Different soil types have different densities, however since the majority of soil in the Rio Chone Watershed can be characterized as a silty loam we based our calculation on the density of silt. A literature

review revealed a range of soil densities between 1200 kilograms/meter^3 and 1635 kilograms/meter^3, averaging 1466 kilograms/meter^3. This average soil density was multiplied by the area of the estuary and the sediment input over the 21 year study period. Finally, we divided our resulting number by 21 to find an accretion rate in tonnes per year.

3.2 Sediment Budget of the Rio Chone watershed

To assess the sources of sediment in an individual watershed and compare their relative magnitudes, estimating the contribution of material produced by each of the major geomorphic processes occurring in the landscape is required. This allows for prioritization of management actions to reduce erosion. With this in mind, we created a sediment budget for the Rio Chone watershed.

A sediment budget accounts for all the sources of sediment generated from the land surface that will exit the drainage basin of study (Dunne & Reid, 1996). The creation of a descriptive sediment budget provides a useful analysis to help predict the amount of sediment produced and delivered to an endpoint from erodible streambanks, surface water erosion (sheetwash and rilling), unpaved roads and their associated cutslopes, and treethrow (Ramos-Scharrón & MacDonald, 2007). Dunne & Reid (1996) also include gullies, mass wasting, wind erosion, and animal burrows as possible sources of sediment production.

Field surveys, an analysis of aerial photos or satellite imagery, and models are typically used to determine the erosion rates from these sources (Dunne & Reid, 1996). Most commonly, sheetwash erosion is quantified through a sediment model. For our analysis, we used the InVEST model based on the Revised Universal Soil Loss Equation to accomplish this.

Sediment generated from animal burrows, treethrow, gullies, and wind erosion, was excluded from the budget. Soil loss from animal burrows, treethrow, and wind erosion was determined negligible in comparison to estimated contributions from unpaved roads, streambanks, and sheetwash after a careful inspection of aerial imagery was performed with the aide of a professional hydrologist. Regarding gullying, ground-truthing and analysis of aerial imagery indicated that gullying is not a major geomorphic process in our study area, and as such was not quantified either. Sediment generated from mass wasting events (landslides) was considered negligible as well and therefore excluded from the sediment budget, for reasons discussed in section 3.2.3. Sediment generated from erodible streambanks, unpaved roads, and sheetwash was quantified and tallied as the sediment budget end-product.

3.2.1 Erodible Streambanks

Streambanks are likely to contribute a significant amount of sediment to the estuary. We used ArcGIS to quantify the length of all tributaries in the watershed.

Ramos-Scharrón & MacDonald (2007a) calculated an erosion rate of 10 kilograms of sediment per square meter of streambank per year by finding a mean site erosion rate of approximately 7 millimeters/year. They surmised this value by averaging between sites that had erosion rates between 1 millimeter/year and 15 millimeter/year. Lawler (1993) supports these findings with his review of river bank erosion rates (Lawler, 2993). We used a value of 7 millimeter/year, or 9 kilograms/meter^2*year.

This converts to approximately 100 megagrams of streambank sediment per hectare per year after multiplying the erosion rate by the estimated dry bulk density of sediment of 1.4 megagram/meter^3. This value was multiplied by the total length of streams in the watershed. The resulting formula is:

$$[10\ kg/m^2]\times 2\times \textit{channel length with erodible banks}\times \textit{bank height}\times \textit{years}$$

This calculation results in an estimation of the total sediment load due to streambanks in kilograms per year (Ramos-Scharrón & MacDonald, 2007a). The length of stream banks is multiplied by two to account for the dual banks of a stream channel.

The role of riparian vegetation is known to be a strong stabilizing force for streambeds and is a source of uncertainty in our evaluation of the sediment delivery rates of streambanks (Pollen, 2007). We estimated a stream bank height of one meter based on visual analysis and photo documentation of various stream banks in the Rio Chone watershed.

3.2.2 Road Surface and Cutbank Erosion

Unpaved roads, which make up most of the transportation infrastructure in the watershed, also have the potential to be a major source of sediment. The road surface is typically responsible for roughly 91% of sediment creation on unpaved roads while road cutslopes provide the remainder (Ramos-Scharron & MacDonald, 2007a). Ramos-Scharron (2010) found erosion rates on roads to be 15-50 times higher than natural erosion rates nearby.

The most critical determinant of erosion rates from unpaved roads is the amount of usage a road gets (Reid & Dunne, 1984). Reid and Dunne (1984) defined “light use” as no logging trucks but light vehicles and “moderate use” as one to four logging trucks driving the road per day. Based on observed traffic patterns around the watershed, we estimated that the roads could be classified into light to medium usage.

Reid and Dunne (1984) report rates of 36 tonnes/kilometers/year for moderate use and 3.4 tonnes/kilometer/year for light use roads. Similar rates were found in research on building sites in Maryland and road cuts in Georgia (Wolman & Schick, 1967; Diseker & Richardson, 1962). We approximated erosion from unpaved roads in the Rio Chone estuary to be 10-20 tonnes/kilometer*year.

Cutbanks have a surprisingly small influence on sediment creation (Reid & Dunne, 1984). Erosion rates from cutbanks are expected to be less than 2 tonnes/kilometer*year (Reid & Dunne, 1984). Photographic and satellite imagery showed few stretches of road that use

constant cutbanks within the watershed, so we considered their effect to be negligible within the estuary's sediment budget.

We estimated the length of roads in the Rio Chone estuary by evaluating the entire watershed by satellite imagery. Areas of the watershed were classified as one of three potential categories of road density: urban, minimal, and undeveloped (Figure 3.2). We estimated that areas of "urban" road density had approximately 7,300 meters of road per 300,000 meters^2 and that areas of "minimal" roads had a road density of approximately 3,000 meters of road per 300,000 meters^2.

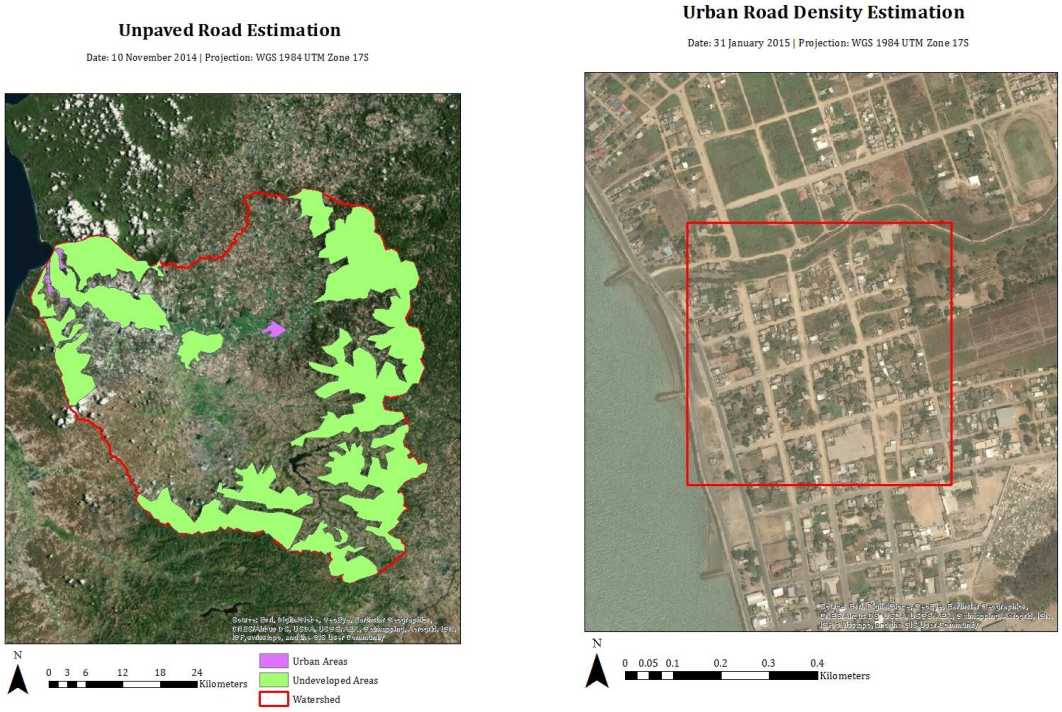

(a) **(b)**

Figure 3.2 (a) Rio Chone watershed sectioned off for "urban" areas (purple fill) and "undeveloped" areas (green fill). The remaining, uncolored areas (a majority of the watershed) were deemed as "minimal" road density designated area and were found to have an average of 3000 meters of road per 300,000 meters^2 block. **(b)** Urban road density was estimated by finding an average of 7,300 meters of road for a 300,000 meters^2 block of "urban" road designated area.

Our analysis classified 3 million square meters of the watershed as "urban" and 947 million square meters as "minimal", to total a length of 10.4 million meters of unpaved road in the Rio Chone watershed.

3.2.3 Landslides

The most critical aspect of whether landslides participate in the total sediment budget of the watershed is whether the eroding material gets transported directly into the delivery

network (Claessens et al., 2007). If stream networks provide transport of the displaced material, it will contribute to the sedimentation of the estuary and should therefore be included in a sediment budget.

After careful evaluation of the amount and placement of landslide scarps within the Rio Chone watershed using satellite imagery, we determined that landslides likely provide a negligible amount of sediment to the estuary. The landslides that were identified did not intersect stream channels. Also, the gently sloping topography of the watershed is not prone to mass wasting.

It is important to note that landslide occurrence has a direct correlation with rainfall. Increased soil porosity elevates the amount of water a given volume of soil can hold, conferring an increased likelihood of slope failure. Greater porosity paired with high precipitation rates exaggerates the likeliness of a landslide to occur (Dai & Lee, 2001). While much of the interior portions and upper slopes of our watershed is geologically characterized as silty loam, the hills surrounding the estuary feature soil classes of a courser grain. The high magnitude of precipitation in the Rio Chone watershed during the 1997/1998 El Nino event triggered landslides near cleared steep residential areas around Bahía de Caráquez and caused multiple fatalities (Berg, 1999). These tragic events were highly publicized, but do not change the fact that landslides play a minimal role in the overall volume of sediment generated in the watershed.

3.3 InVEST Sediment Retention Model

We used a sediment production model to quantify the amount of sediment produced from sheetwash and rilling processes. First, the principles of environmental modeling are discussed, followed by an explanation of the InVEST Sediment Retention Model and our chosen model scenarios. See Appendix 8.2 and Appendix 8.3 for further information on our use of the InVEST product.

3.3.1 Fundamentals of Environmental Modeling

Environmental modeling is used to make a feature or process in the natural world easier to understand, define, visualize, quantify or simulate. While models can be used to explore any number of potential relationships between items or systems, they will fall into two general categories. Models of theory attempt to build conceptual comprehension and are based on processes and physical relationships. Models of data are empirical, using observations and statistics. The type of model employed is dependent on the physical processes the user is trying to simulate, the equations or algorithms that are working internally to describe relationships between the model inputs, and the inputs themselves. Empirical models attempt to characterize the response of an environment to observed data. Typically, an empirical model will require a less detailed set of input data than the physical or conceptually-based model. As such, the empirical model is a good starting point when attempting to ascertain the sources of sediment generation in a landscape.

Conversely, a conceptual model will try to establish and estimate the interaction strengths between different environmental factors, but does not attempt to quantify the amount of soil generated from an erosional event. Conceptual soil loss models often break a catchment up into a series of internal storages and seek to understand how water and soil moves between these theoretical compartments. Lastly, physically-based models work upon a set of pre-established fundamental equations that describe the streamflow and sediment generated in a catchment basin. As such, this model type requires detailed datasets and should be implemented when the study area is well studied and documented (Merritt et al., 2013).

There are a number of different soil loss and sediment transport models available, many using the same basic principles as their counterparts. Determining which type(s) of erosional processes are to be explored is key when choosing which model to use. Ranging in data needs, complexity, and capability, a model should also be chosen according to the outputs desired and questions needing to be addressed. Soil erosion models explore the avenues by which soil may be moved, and will use either water, wind, or both as the means by which grains of soil are detached and transported. Information on where and how much soil may be lost or transported from a particular landscape is often needed on both temporal and spatial scales in accordance with how much precipitation and/or wind is experienced (Merritt et al., 2013).

3.3.2 Choosing the InVEST Sediment Retention Model

An empirical model was chosen to identify the amount and location of sediment produced from sheetwash based on the data available to us. We explored a suite of land use scenarios to help understand the role that land use/land cover (LULC) plays in sediment production. This analysis provided an assessment of the erosion reduction potential of dissimilar land use patterns within the catchment basin.

We used the Natural Capital Project's InVEST Sediment Retention Model to perform our soil erosion analysis. The terrestrial Sediment Retention Model quantifies soil retention, and values the avoided cost of water treatment or dredging. Specifically, the InVEST model uses information on geomorphology, climate, vegetative coverage, and land use/land cover to estimate the amount of sediment retained on a land parcel. This is then inverted to predict the amount of soil transported away from the parcel under the environmental conditions being analyzed (InVEST, 2014). Our analysis made use of the data inputs described in Appendix 8.2.

3.3.3 Model Summary

InVEST calculates the average annual soil loss from a raster grid pixel, or land parcel. Like many of the models available today, InVEST marries the Revised Universal Soil Loss Equation (RUSLE) with a GIS component at a grid cell scale, integrating LULC patterns with environmental properties, such as soil composition and slope gradient. When evaluating at the pixel-scale, the actual resolution of the analysis is dependent upon the coarseness of each input layer. Performing analyses at pixel-scale allows for the heterogeneity of an

environment to be expressed at the level of coarsest resolution, as opposed to aggregating at the sub-basin or basin scale. The RUSLE equation is expressed as the following:

$$\boldsymbol{A = RKLSCP}$$

Where,

R = rainfall erosivity
K= soil erodibility
LS= slope length-gradient factor
C= crop management factor
P= support management factor

The Universal Soil Loss Equation was first published in 1964 in the United States Department of Agriculture (USDA) Agricultural Handbook 282, after which improvements were made to the empirical model by Wischmeier and Smith (Wischmeier and Smith, 1965). The revised version, RUSLE, was published in 1978 in USDA Agricultural Handbook 537, where each of the factors in the equation were revised to become more accurate (Cooper, 2011).

To calculate the potential soil loss, the model uses input rasters for rainfall erosivity, soil erodibility, and LULC. Each pixel of the study area is assigned an explicit integer value for rainfall and soil erodibility, and a classification number for LULC, which maps *C* and *P* factors according to values assigned in an LULC parameter table. The *LS* factor is calculated byway of a digital elevation model (DEM) of the study area, which computes the interaction between topography and flow accumulation (see Appendix 8.2 for a complete discussion on RUSLE's variables). In essence, the USLE-*LS* component relies not only on the percentage and length of the slope, but also on the flow expected to occur over the land surface (Ozcan et al., 2007). The InVEST model accomplishes this task by using the following equation, adopted from Desmet and Govers (1996) for two-dimensional surfaces (InVEST, 2014):

$$\boldsymbol{LS = S * ((A + D^2) - A^{(m+1)})/(D^{(m+2)} * x^m * 22.13^m)}$$

Where,

S = the slope factor calculated for the raster grid cell as a function of slope degree according to the following:

$$S = 10.8 * sin(\theta) + 0.03, \qquad where\ slope\ is\ < 9\%$$

$$S = 10.8 * sin(\theta) + 0.03, \qquad where\ slope\ is\ \geq\ 9\%$$

A = the contributing area (m^2) at the inlet of the grid cell that is calculated from the D-infinity flow accumulation algorithm
D = the grid cell linear dimensions (m)
x = a factor that adjusts flow length across a cell it is equal to
m = the length exponent factor, according to (McCool et al., 1989) in the table below:

Table 3.1 Determination of the length exponent factor (m) according to McCool et al. (1989)

m	slope (%)
0.2	slope ≤ 1%
0.3	1% ≤ slope < 3.5%
0.4	3.5% ≤ slope < 5%
0.5	5% ≤ slope < 9%
$\frac{\beta}{1+\beta}$; $\beta = \frac{\sin(\theta)/0.896}{3\sin(\theta)^{0}.8+0.56}$	slope ≥ 9%

To calculate upstream retention capacity, the model assumes that a cell with zero retention capacity receiving flow from an upstream cell will transport sediment to the closest cell(s) downstream. The model only considers vegetative cover and ignores channel geometry when analyzing whether a particle will settle. The upstream retention parameter functions as a cell retention efficiency factor, defined by the LULC value assigned in the parameter input table. The InVEST model negotiates retention capacity according to the following mass balance equation (InVEST, 2014):

$$S_i = \left(\sum_{j \in \{i_{neighbors}\}} S_j \right) (1 - E_i) + USLE_i$$

Where,

$\boldsymbol{S}$ = the total volume of sediment retained, according to the sum of the sediment retained on the individual pixel in accordance with the C and P factors, and the sediment transported out due to infiltration capacity according to routing filtration (InVEST, 2014).

3.3.4 Model Assumptions, Simplifications, and Limitations

InVEST's Sediment Retention Model makes a number of assumptions and simplifications due to operating under considerable limitations. The accuracy of the retention value is limited by the quality of information and constraints upon the model's capabilities. In addition, calibration of the model was limited due to lack of available information for the Rio Chone watershed. While streamgage data is publicly accessible, information on total suspended solids is not.

During the calculation of potential soil loss, the InVEST model makes the following assumptions:

- The environment is in steady state

- All sediment entering a delivery channel will be carried out of the basin during the same year it entered (no carry-over)

The InVEST model's capabilities to make accurate and meaningful estimates of sediment loading are limited by the following factors:

- The model is parameterized by several different equations which each describe a stochastic process, its applicability to regions that do not share similar characteristics to the ones each equation was created to represent may be limited. The InVEST model interface does not allow for manipulation of internal equations

The RUSLE is in itself an erosion model, which considers sediment produced by splash, sheet, and rill erosion from agricultural plots. It has been used prolifically because of its relative simplicity and robustness, however the RUSLE is constrained by the following limitations (Ozcan et al., 2007):

- The USLE/RUSLE equation only considers sediment produced by the erosional processes of rill and sheet erosion; it ignores soil losses by gully, wind or tillage erosion, earthflow losses (e.g., mass failure events), and stream-bank erosion
- Depositional processes are not considered
- The USLE/RUSLE equation was created for selected cropping and management systems on agricultural parcels with low to no slope gradients (Ozcan et al., 2007)
- The relationship between rainfall intensity and kinetic energy propounded in the USLE/RUSLE model might not hold true in mountainous land parcels because it was designed for use in the American Great Plains
- The equation only considers the individual effect of each variable, ignoring the potential for cumulative effects over space and time (InVEST, 2014)

3.3.5 Model Scenarios

To test the impacts of current and potential land use regimes on sediment loading in the Rio Chone watershed, the InVEST model was run using different land use scenarios. This was accomplished by manipulating values in the Biophysical Table input (shown below for each scenario), specifically the *C* factors, *P* factors, and sediment retention efficiency values when appropriate. Values in the erosivity raster were changed for the *"Baseline land use during El Nino"* scenario. Of note, all scenarios save the aforementioned assumed average precipitation rates.

1. **Baseline land use:** The most recent land use regime in the Rio Chone estuary was represented by the European Space Agency's (ESA) GlobCover 2009 LULC raster. As such, model results using the validated 2009 LULC were considered baseline sediment loads.

Land Use Code	Description	C factor	P Factor	Sediment Retention Efficiency
14	Rainfed croplands	0.36	0.45	0.25
20	Mosaic cropland (50-70%) / vegetation (grassland/shrubland/forest) (20-50%)	0.26	0.38	0.4
30	Mosaic vegetation (grassland/shrubland/forest) (50-70%) / cropland (20-50%)	0.13	0.28	0.6
40	Closed to open (>15%) broadleaved evergreen or semi-deciduous forest (>5m)	0.003	0.2	0.6
50	Closed (>40%) broadleaved deciduous forest (>5m)	0.004	0.2	0.6
110	Mosaic forest or shrubland (50-70%) / grassland (20-50%)	0.035	0.2	0.5
130	Closed to open (>15%) (broadleaved or needleleaved, evergreen or deciduous) shrubland (<5m)	0.06	0.2	0.5
140	Closed to open (>15%) herbaceous vegetation (grassland, savannas or lichens/mosses)	0.01	0.2	0.4
150	Sparse (<15%) vegetation	0.85	0.85	0.05
170	Closed (>40%) broadleaved forest or shrubland permanently flooded - Saline or brackish water	0.003	0.2	0.6
210	Water bodies	0	0.5	0.8
0	No data	0	0	1

2. **Baseline land use during El Nino:** The erosivity layer was manipulated to simulate an extreme El Nino event. The precipitation input to the erosivity calculation (which agreed with findings from Farrow (2009) shown in Figure 3.3 below) was increased by 386% for every pixel based on the following information, which suggested that during the 1997 and 1998 El Nino years, precipitation anomalies of 386% were experienced in the vicinity of the city of Chone:

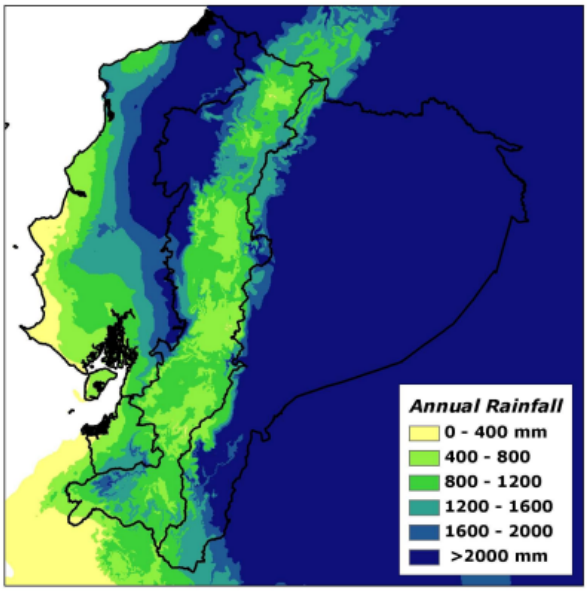

Figure 3.3 Average annual rainfall (millimeters) in the Rio Chone watershed fall between 400-1200 millimeters/year during a non-El Nino year. From Farrow (2009)

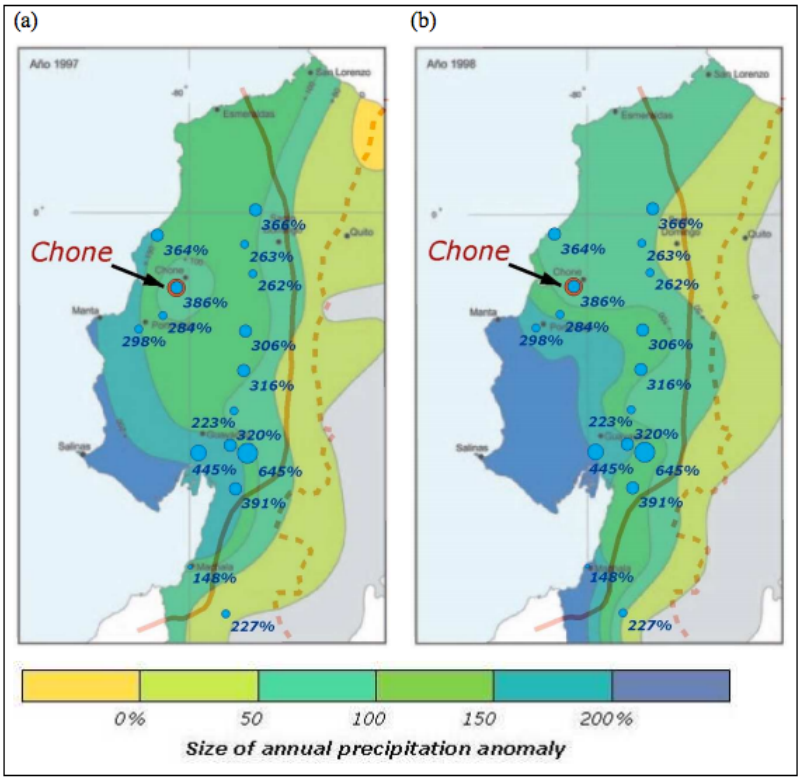

Figure 3.4 Precipitation anomalies in the (a) 1997 and (b) 1998 El Nino years for Ecuador's Pacific coastline. From Farrow (2009)

3. **100% Native Vegetation (Pre-Disturbance):** To get an estimate of sediment loading prior to deforestation, all pixels classified as rainfed cropland or mosaic cropland with at least 50% crop coverage were re-classified to share the average *C* factor, *P* factor, and sediment retention efficiencies of all native vegetation coverage.

Land Use Code	Description	C factor	P Factor	Sediment Retention Efficiency
14	Rainfed croplands	0.035	0.21	0.54
20	Mosaic cropland (50-70%) / vegetation (grassland/shrubland/forest) (20-50%)	0.035	0.21	0.54
30	Mosaic vegetation (grassland/shrubland/forest) (50-70%) / cropland (20-50%)	0.13	0.28	0.6
40	Closed to open (>15%) broadleaved evergreen or semi-deciduous forest (>5m)	0.003	0.2	0.6
50	Closed (>40%) broadleaved deciduous forest (>5m)	0.004	0.2	0.6
110	Mosaic forest or shrubland (50-70%) / grassland (20-50%)	0.035	0.2	0.5
130	Closed to open (>15%) (broadleaved or needleleaved, evergreen or deciduous) shrubland (<5m)	0.06	0.2	0.5
140	Closed to open (>15%) herbaceous vegetation (grassland, savannas or lichens/mosses)	0.01	0.2	0.4
150	Sparse (<15%) vegetation	0.85	0.85	0.05
170	Closed (>40%) broadleaved forest or shrubland permanently flooded - Saline or brackish water	0.003	0.2	0.6
210	Water bodies	0	0.5	0.8
0	No data	0	0	1

4. **10%-90% Reforestation:** To assess the impact different levels of reforestation could have on reducing erosion rates, 10%-90% of the pixels classified as rainfed or mosaic cropland with at least 50% crop coverage were randomly pulled out and reassigned to share the average *C* factor, *P* factor, and sediment retention efficiencies of the average of all native vegetation coverage.

Land Use Code	Description	C factor	P Factor	Sediment Retention Efficiency
14	Rainfed croplands	0.36	0.45	0.25
20	Mosaic cropland (50-70%) / vegetation (grassland/shrubland/forest) (20-50%)	0.26	0.38	0.4
30	Mosaic vegetation (grassland/shrubland/forest) (50-70%) / cropland (20-50%)	0.13	0.28	0.6
40	Closed to open (>15%) broadleaved evergreen or semi-deciduous forest (>5m)	0.003	0.2	0.6
50	Closed (>40%) broadleaved deciduous forest (>5m)	0.004	0.2	0.6
110	Mosaic forest or shrubland (50-70%) / grassland (20-50%)	0.035	0.2	0.5
130	Closed to open (>15%) (broadleaved or needleleaved, evergreen or deciduous) shrubland (<5m)	0.06	0.2	0.5
140	Closed to open (>15%) herbaceous vegetation (grassland, savannas or lichens/mosses)	0.01	0.2	0.4
150	Sparse (<15%) vegetation	0.85	0.85	0.05
170	Closed (>40%) broadleaved forest or shrubland permanently flooded - Saline or brackish water	0.003	0.2	0.6
210	Water bodies	0	0.5	0.8
0	No data	0	0	1
1	% reforested (10, 20, 30, 40, 50, 60, 70, 80, 90)	0.035	0.21	0.54

5. **100% Implementation of Agricultural Soil Conservation Strategies**: To assess the impact that soil conservation strategies could have on reducing erosion rates, all pixels classified as rainfed or mosaic cropland with at least 50% crop coverage were assigned new *P* factor values representing the following soil conservation methods:

a. Mulching

Land Use Code	Description	C factor	P Factor	Sediment Retention Efficiency
14	Rainfed croplands	0.36	0.01	0.4
20	Mosaic cropland (50-70%) / vegetation (grassland/shrubland/forest) (20-50%)	0.26	0.01	0.4
30	Mosaic vegetation (grassland/shrubland/forest) (50-70%) / cropland (20-50%)	0.13	0.28	0.6
40	Closed to open (>15%) broadleaved evergreen or semi-deciduous forest (>5m)	0.003	0.2	0.6
50	Closed (>40%) broadleaved deciduous forest (>5m)	0.004	0.2	0.6
110	Mosaic forest or shrubland (50-70%) / grassland (20-50%)	0.035	0.2	0.5
130	Closed to open (>15%) (broadleaved or needleleaved, evergreen or deciduous) shrubland (<5m)	0.06	0.2	0.5
140	Closed to open (>15%) herbaceous vegetation (grassland, savannas or lichens/mosses)	0.01	0.2	0.4
150	Sparse (<15%) vegetation	0.85	0.85	0.05
170	Closed (>40%) broadleaved forest or shrubland permanently flooded - Saline or brackish water	0.003	0.2	0.6
210	Water bodies	0	0.5	0.8

b. Buffer Strip-Cropping

Land Use Code	Description	C factor	P Factor	Sediment Retention Efficiency
14	Rainfed croplands	0.36	0.25	0.4
20	Mosaic cropland (50-70%) / vegetation (grassland/shrubland/forest) (20-50%)	0.26	0.25	0.4
30	Mosaic vegetation (grassland/shrubland/forest) (50-70%) / cropland (20-50%)	0.13	0.28	0.6
40	Closed to open (>15%) broadleaved evergreen or semi-deciduous forest (>5m)	0.003	0.2	0.6
50	Closed (>40%) broadleaved deciduous forest (>5m)	0.004	0.2	0.6
110	Mosaic forest or shrubland (50-70%) / grassland (20-50%)	0.035	0.2	0.5
130	Closed to open (>15%) (broadleaved or needleleaved, evergreen or deciduous) shrubland (<5m)	0.06	0.2	0.5
140	Closed to open (>15%) herbaceous vegetation (grassland, savannas or lichens/mosses)	0.01	0.2	0.4
150	Sparse (<15%) vegetation	0.85	0.85	0.05
170	Closed (>40%) broadleaved forest or shrubland permanently flooded - Saline or brackish water	0.003	0.2	0.6
210	Water bodies	0	0.5	0.8

6. **Worst-Case Scenario:** To assess the impact that converting all of the undisturbed land to agricultural plots would have on erosion, all pixels classified as being covered with at least 70% native vegetation were re-classified to share the same *P* factor, *C* factor and sediment retention efficiency as the average of the rainfed and mosaic croplands:

Land Use Code	Description	C factor	P Factor	Sediment Retention Efficiency
14	Rainfed croplands	0.36	0.45	0.25
20	Mosaic cropland (50-70%) / vegetation (grassland/shrubland/forest) (20-50%)	0.36	0.45	0.25
30	Mosaic vegetation (grassland/shrubland/forest) (50-70%) / cropland (20-50%)	0.36	0.45	0.25
40	Closed to open (>15%) broadleaved evergreen or semi-deciduous forest (>5m)	0.36	0.45	0.25
50	Closed (>40%) broadleaved deciduous forest (>5m)	0.36	0.45	0.25
110	Mosaic forest or shrubland (50-70%) / grassland (20-50%)	0.36	0.45	0.25
130	Closed to open (>15%) (broadleaved or needleleaved, evergreen or deciduous) shrubland (<5m)	0.36	0.45	0.25
140	Closed to open (>15%) herbaceous vegetation (grassland, savannas or lichens/mosses)	0.36	0.45	0.25
150	Sparse (<15%) vegetation	0.85	0.85	0.05
170	Closed (>40%) broadleaved forest or shrubland permanently flooded - Saline or brackish water	0.36	0.45	0.25
210	Water bodies	0	0.5	0.8

3.3.6 Sediment Delivery Ratio

When a grain of soil is detached and becomes vulnerable to transport, the proximity of the detached grain to a delivery channel will play a large part in its likelihood of becoming re-deposited or carried downstream. In addition, a landscape's ability to deliver dislodged soil particles to stream channels or watershed outlets is dependent upon the upstream drainage area from the soil grain's origin, as well as the slope and slope-length of the landscape. InVEST uses a routing algorithm and applies a sediment retention factor to each pixel to determine the mass of sediment transported downgradient from each pixel. The sediment delivery ratio, or the ratio of sediment delivered to the stream or watershed outlet relative to the total erosion from the contributing areas is indicative of the landscape's ability to deliver soil eroded by rain events. Because InVEST pairs the RUSLE with GIS technology, it allows for automated estimation of the equation's *S* factor (slope) and *L* factor (length) based on the DEM. Slope is derived directly from the DEM. The *L* factor for rill and interrill erosion is calculated through estimation of the upslope contributing area per unit contour width by computing flow direction and accumulation. This is the sum of the grid cells from which water flows into the cell of interest, based on the chosen parameter value for "Threshold Flow Accumulation" (Appendix, 8.2.3). Longer slopes have a higher probability of redeposition. Deposition typically occurs on slopes 120-150 meters or longer (Fernandez et al., 2003).

It should be noted that, although the InVEST model considers the environment's morphologic capability for delivering sediment to a delivery channel, it does not consider travel time. A sediment delivery distributed (SEDD) model would need to be employed to do this. It would discretize watersheds into morphological units of like aspect, length and steepness to calculate flow distance and velocity, or travel time to a defined endpoint (e.g., the Rio Chone estuary) (Fernandez et al., 2003).

4.0 Results

Bathymetric maps were used to prove that sedimentation of the estuary is occurring, and to allow a crude rate of accretion to be calculated. A sediment budget was then constructed to analyze which geomorphic processes were contributing the most to estuarine sedimentation. Next, a sediment production model was employed to estimate the amount of sediment generated from sheetwash, a component of our sediment budget. These results provide insight into the relative scales of sediment addition to the estuary and allow for preferential management of the largest sources. Lastly, the sediment production model was used to test how changing land use in the watershed could impact erosion rates.

4.1 Bathymetric Map

The results of our bathymetric map analysis show a notable change in depth from 1990 to 2011 (Figure 4.1). Red demarks the areas of the estuary that have seen an increase in bathymetric elevation from 1990 to 2011, while blue demarks the areas that have seen a decrease. The maximum decrease in bathymetric elevation seen is 7.3 meters, while the maximum increase in bathymetric elevation 7.5 meters. The map indicates that a greater portion of the estuary has seen an increase in bathymetric elevation over time.

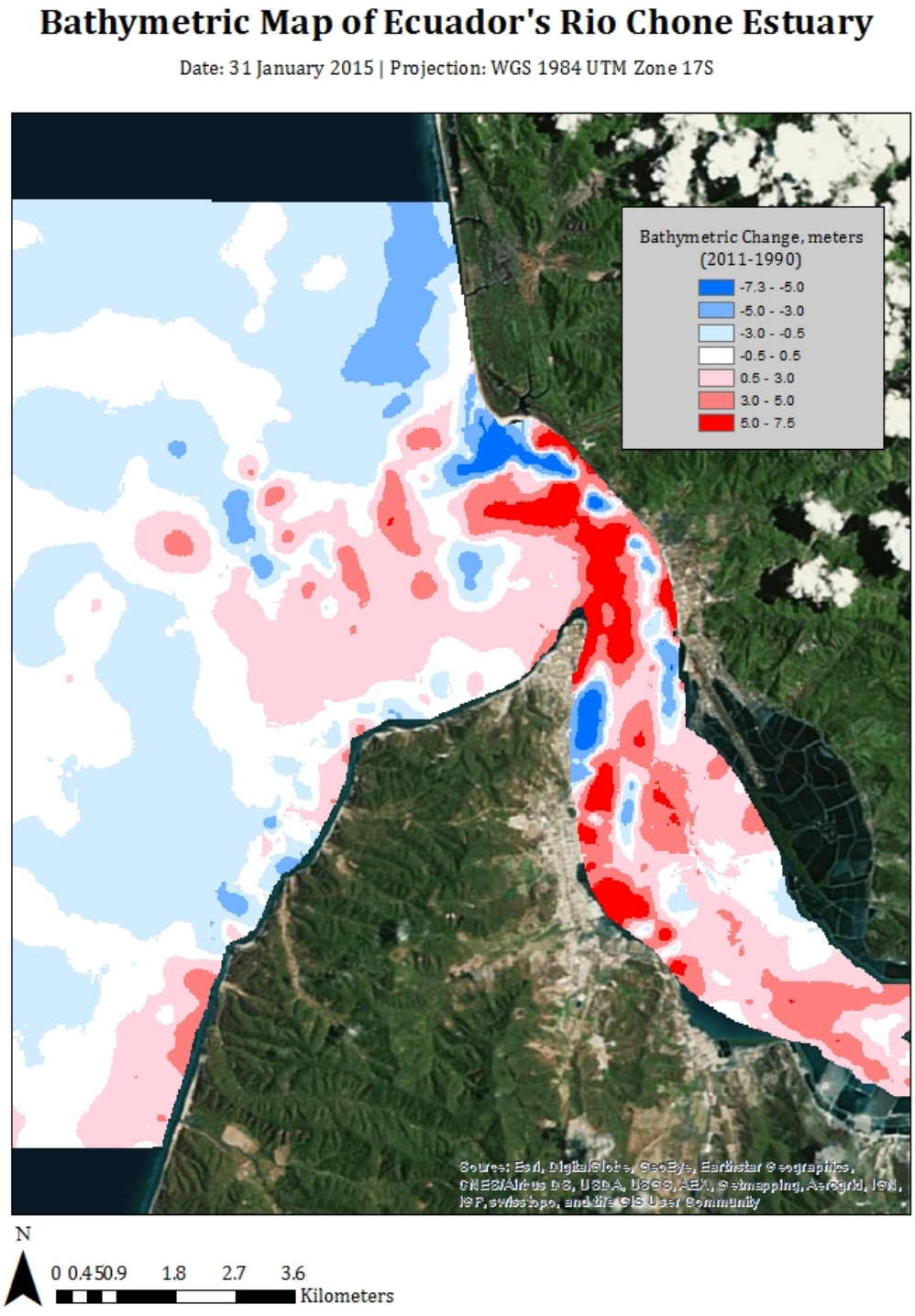

Figure 4.1 Bathymetric map of Ecuador's Rio Chone estuary. Bathymetric change represented in meters was calculated through a subtraction of 1990 bathymetric data from 2011 bathymetric data. Blue demarks areas with a decrease in bathymetric elevation, red demarks areas with an increase in bathymetric elevation.

4.1.1 Total Sediment Input per Year

We estimated the area of the estuary in ArcGIS to be 34 million square meters (excluding shrimp ponds). Our bathymetric analysis resulted in a calculated total addition of 50 million tonnes of sediment over the 21 year period. This provides an average addition of approximately 2.4 million tonnes per year.

Table 4.1 Estimation of the total change of sediment in the estuary per year given our study area, estimation of soil density, and bathymetric change over a 21 year period (1990-2011)

Area (m^2)	*Soil Density (kg/m^3)*	*Total Sediment (tonnes)*	*Sediment (tonnes/year)*
34,000,000	1,466	50,000,000	2,400,000

4.2 Sediment Budget

The relative contribution of sediment sources within the Rio Chone watershed is estimated by our sediment budget.

4.2.1 Sediment Budget Calculations

Starting with a streambank erosion rate of 7 millimeters/year, we converted erosion rates to a weight in kilograms per year using an estimated dry bulk density for the sediment in the watershed (1.4 megagrams/meter^3*yr).

$$[7mm/yr] \times [1.4Mg/m^3] = 9.8\ kg/m^2*yr \sim 10\ kg/m^2*yr$$

This estimated erosion rate of 10 kilograms/meter^2*year was used to find the total amount of sediment derived from our stream network.

$$[10\ kg/m^2*yr] \times [2]\ \textit{sides of bank} \times \textit{channel length} \times \textit{bank height}\ [\sim 1\ m] \times \textit{years}\ [1\ yr]$$

We used ArcGIS to estimate channel length (Section 3.4.4) to find a total of 1,075,000 meters (~1,000 kilometers) of stream length.

$$[10\ kg/m^2*yr] \times [2] \times [1{,}000{,}000\ m] \times [1\ m] \times [1\ yr] = 20 \times 10^6\ kg$$

This produced an estimate of 20 million kilograms (20,000 tonnes) of sediment per year from erodible streambanks.

We estimated a total of 80 kilometers of roads within the Rio Chone watershed's "urban" space and 10,328 kilometers of roads within its "minimal" road space. This provided an approximation of 10,400 kilometers of unpaved road within the watershed.

We combined this approximation with our estimate of "light/moderately" used unpaved roads (10,000-20,000 kilogram of sediment per kilometer of road per year),

$$[10{,}400 \text{ km}]\ \textit{road} \times [10{,}000 \text{ to } 20{,}000 \text{ kg/km*yr}] = 104 \times 10^6 \text{ to } 208 \times 10^6 \text{ kg/yr}$$
$$\sim 100 \times 10^6 \text{ to } 200 \times 10^6 \text{ kg/yr}$$

estimating 100 – 200 million kilograms (100,000 – 200,000 tonnes), of sediment eroded from unpaved roads each year.

4.3 InVEST Sediment Retention Model

Results from the InVEST Sediment Retention Model were used to: 1) estimate the volume and location of sediment produced from sheetwash and rilling processes, and 2) assess the relative impacts that different land use scenarios could have on erosion rates at the catchment basin level. Because most of the data inputs were collected from open access sources in varying resolutions, the findings from the model are estimates of the magnitude of sediment transport only. This should be kept in mind when using these numbers for further research or to inform decision-makers. InVEST's model uses several different equations, each with parameters that describe a stochastic process. A parameter is a coefficient within an equation that describes the bulk behavior of a system. The InVEST model does not allow for manipulations of such parameters, so the inherent uncertainty of the processes being modeled in any scenario aside from the one upon which these equations were built demands consideration. The InVEST team recommends large-scale decisions not be based upon single model runs and instead suggests model results be used as an indicator of how land use changes may affect relative magnitudes of sediment production.

4.3.1 Sediment Production for each Land Use Scenario

For our analysis, we utilized the rasterized output showcasing the amount of sediment exported from each pixel (30x30m resolution, or 900m^2) in tonnes/pixel/year, and the total volume of sediment reaching the stream network in the watershed per year in tonnes/watershed/year after accounting for the sediment delivery ratio. The former highlights the locations of greatest soil loss within the Rio Chone watershed, while the latter allows for comparison of the efficiency of each land use scenario in combating erosion.

The following table summarizes the amount of sediment transported from the terrestrial environment into the stream channel for each land use scenario, as a mass (tonnes) per year for the entire watershed. Additionally, the sediment export rasters were used to visualize where erosion was occurring within the watershed. This worked to enrich our understanding of what types of environmental conditions promote soil loss. The product could be used as a means to inform reforestation or soil conservation efforts and inform land managers where these efforts should be prioritized.

Table 4.2 Summary of results from the InVEST Sediment Retention Model for each land use scenario

Scenario:	**Approximate Total Sediment Export (Million Tonnes/Watershed/Year):**
100% Native Vegetation (Pre-Disturbance)	5
Baseline (0% Reforestation/Soil Conservation) Average Rain	50
Baseline (0% Reforestation/Soil Conservation) for an El Nino Year	180
100% Deforestation (Worst-Case)	90
100% Soil Conservation (Buffer Strip-Cropping)	30
100% Soil Conservation (Mulching)	3

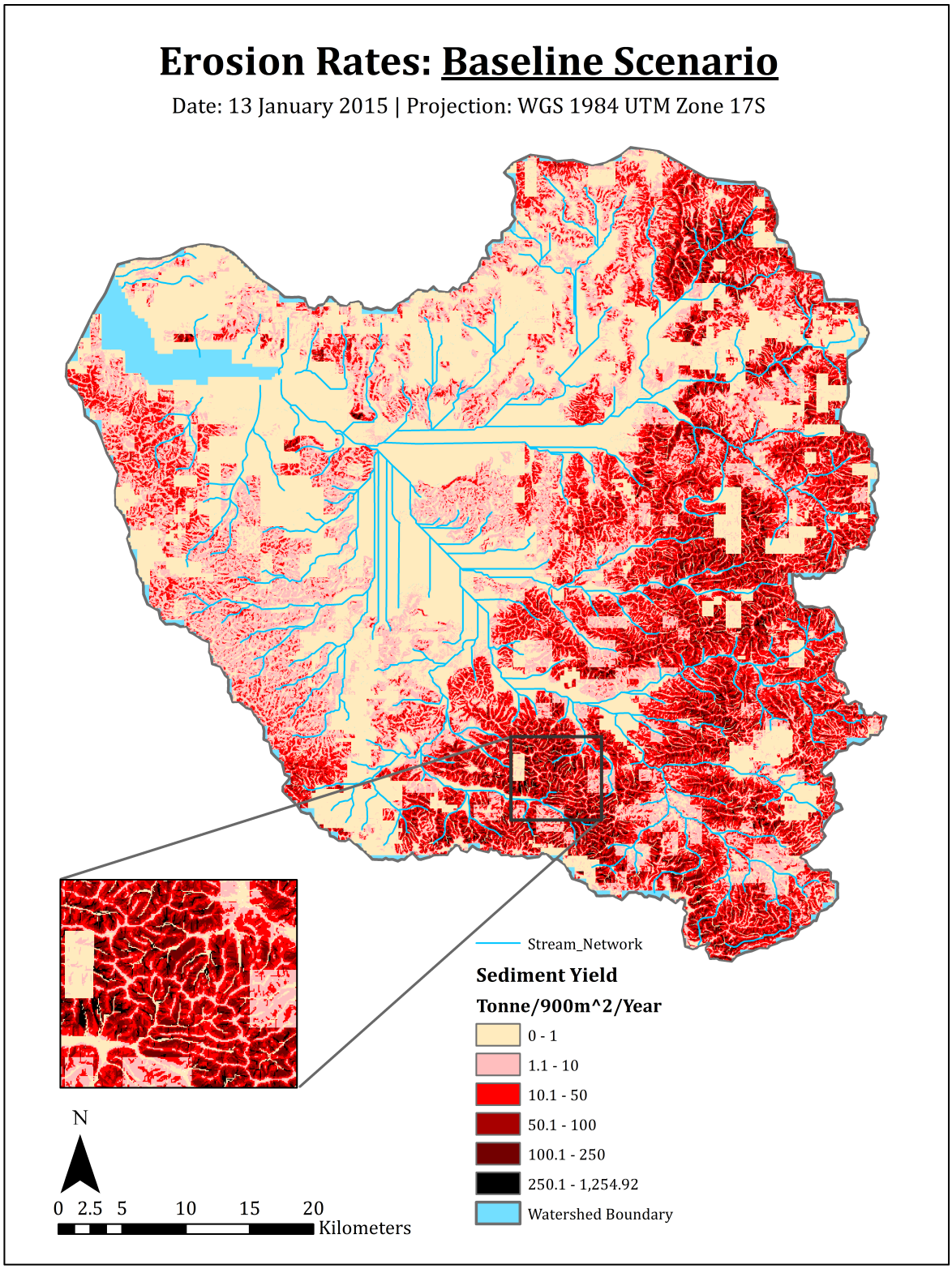

Figure 4.2 InVEST Sediment Retention model results showing erosion rates under the baseline land use/land cover regime as of 2009 (ESA's LULC input raster) during an average rain year

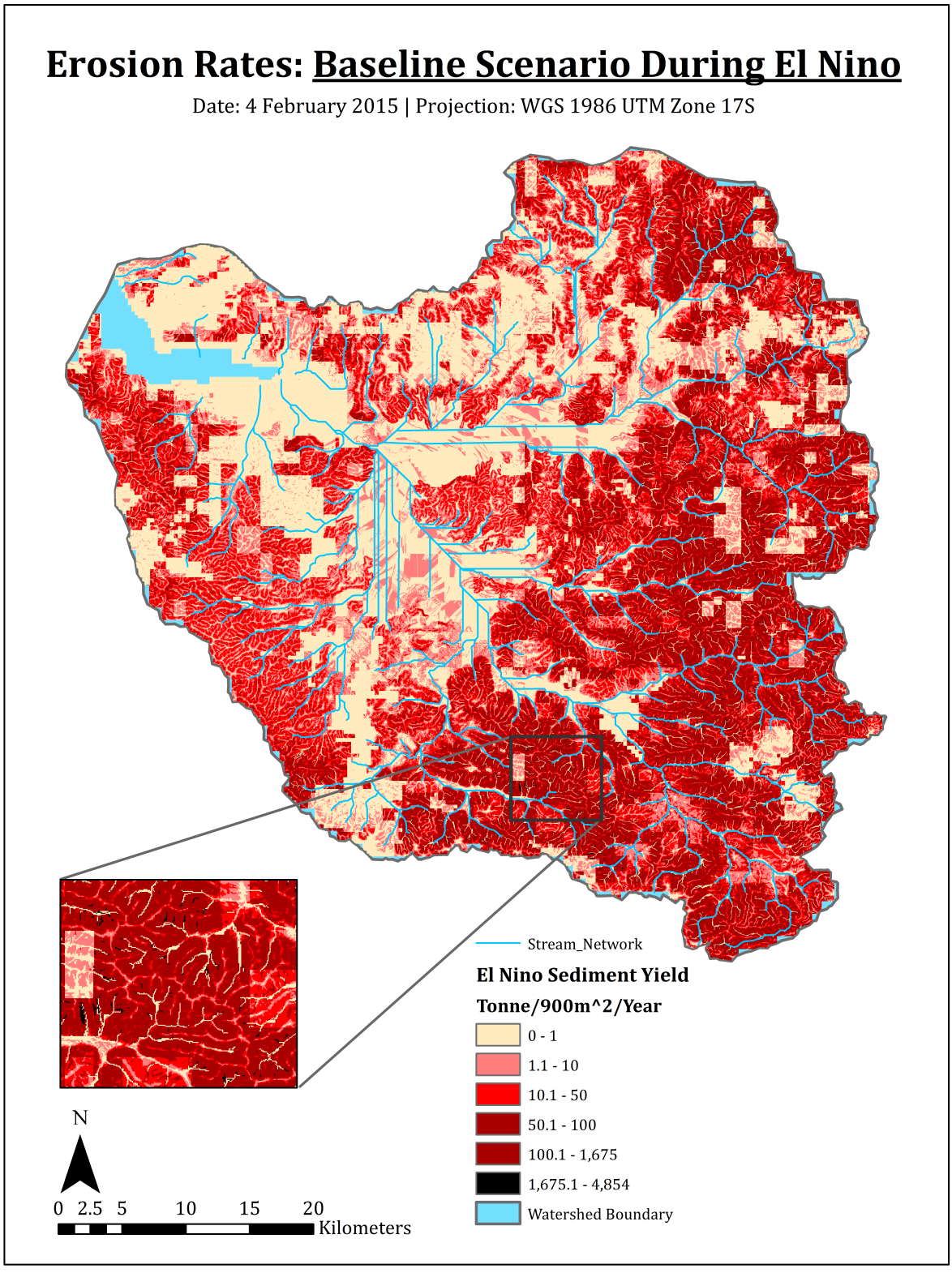

Figure 4.3 InVEST Sediment Retention model results showing erosion rates under the baseline land use/land cover regime as of 2009 (ESA's LULC input raster) during an El Nino rain year

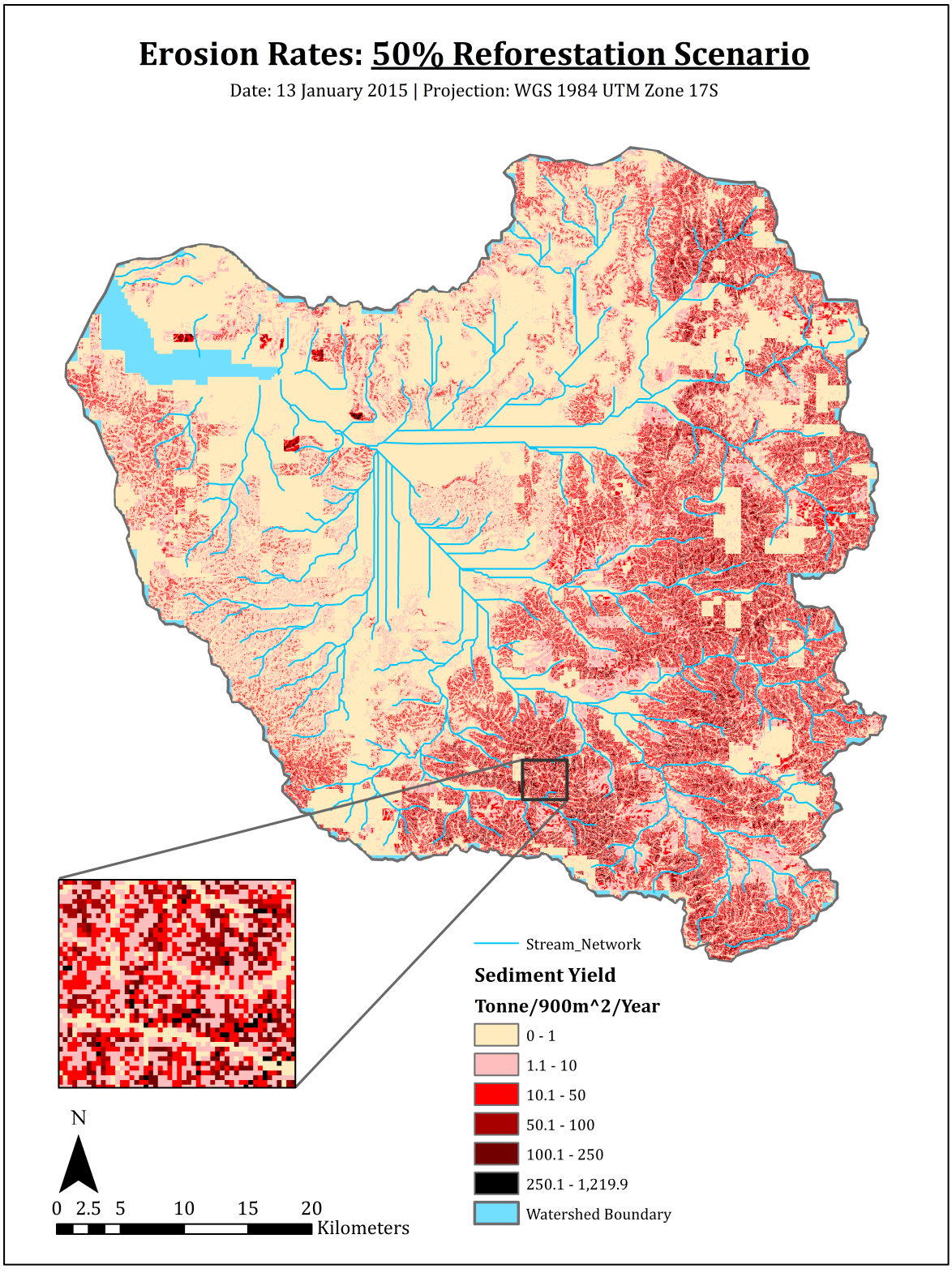

Figure 4.4 InVEST Sediment Retention model results showing erosion rates when 50% of the crop lands with at least 70% crop cover in the study area are reforested with native vegetation during an average rain year

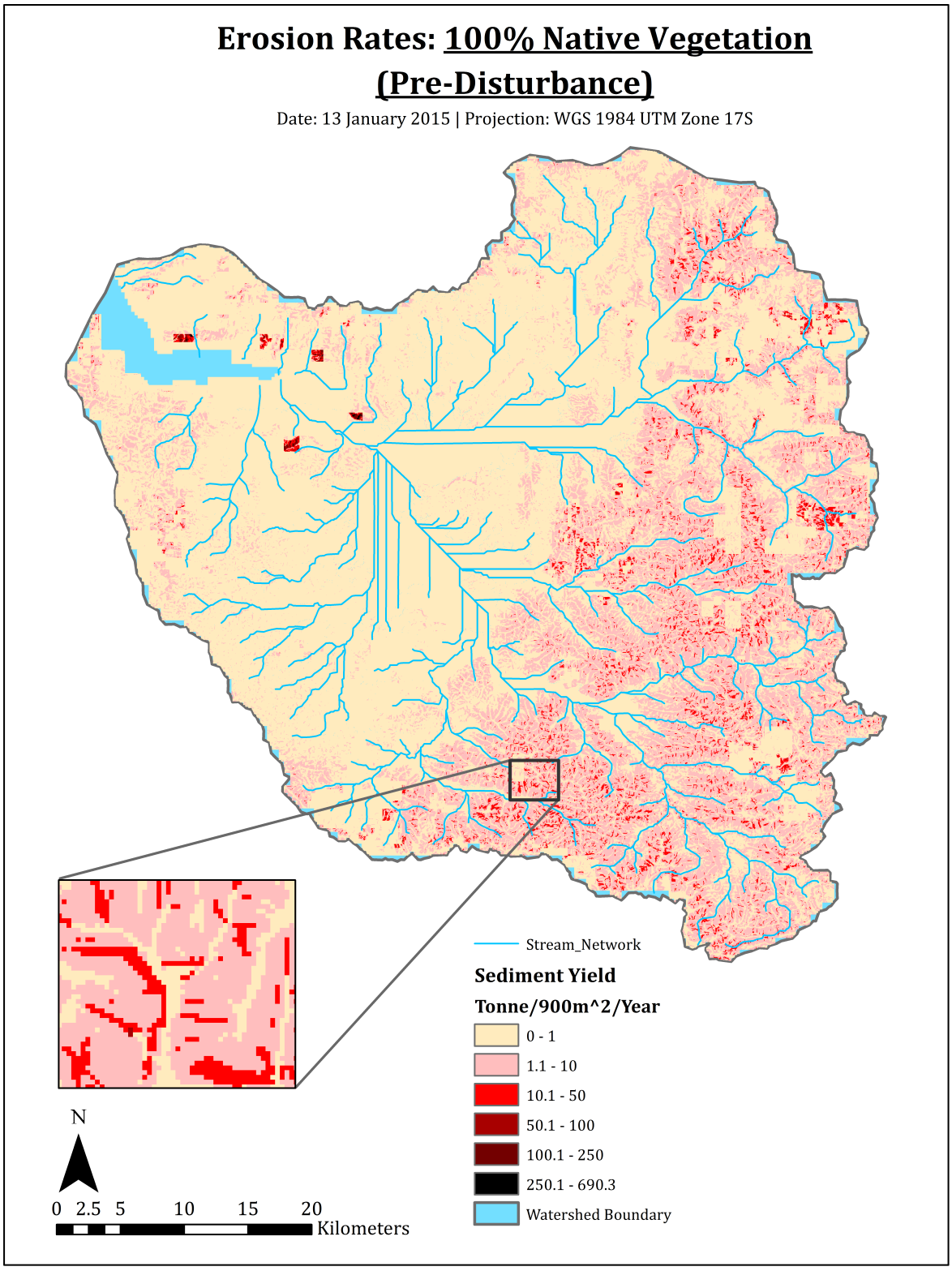

Figure 4.5 InVEST Sediment Retention model results showing erosion rates when 100% of the crop lands with at least 70% crop cover in the study area are covered with native vegetation during an average rain year

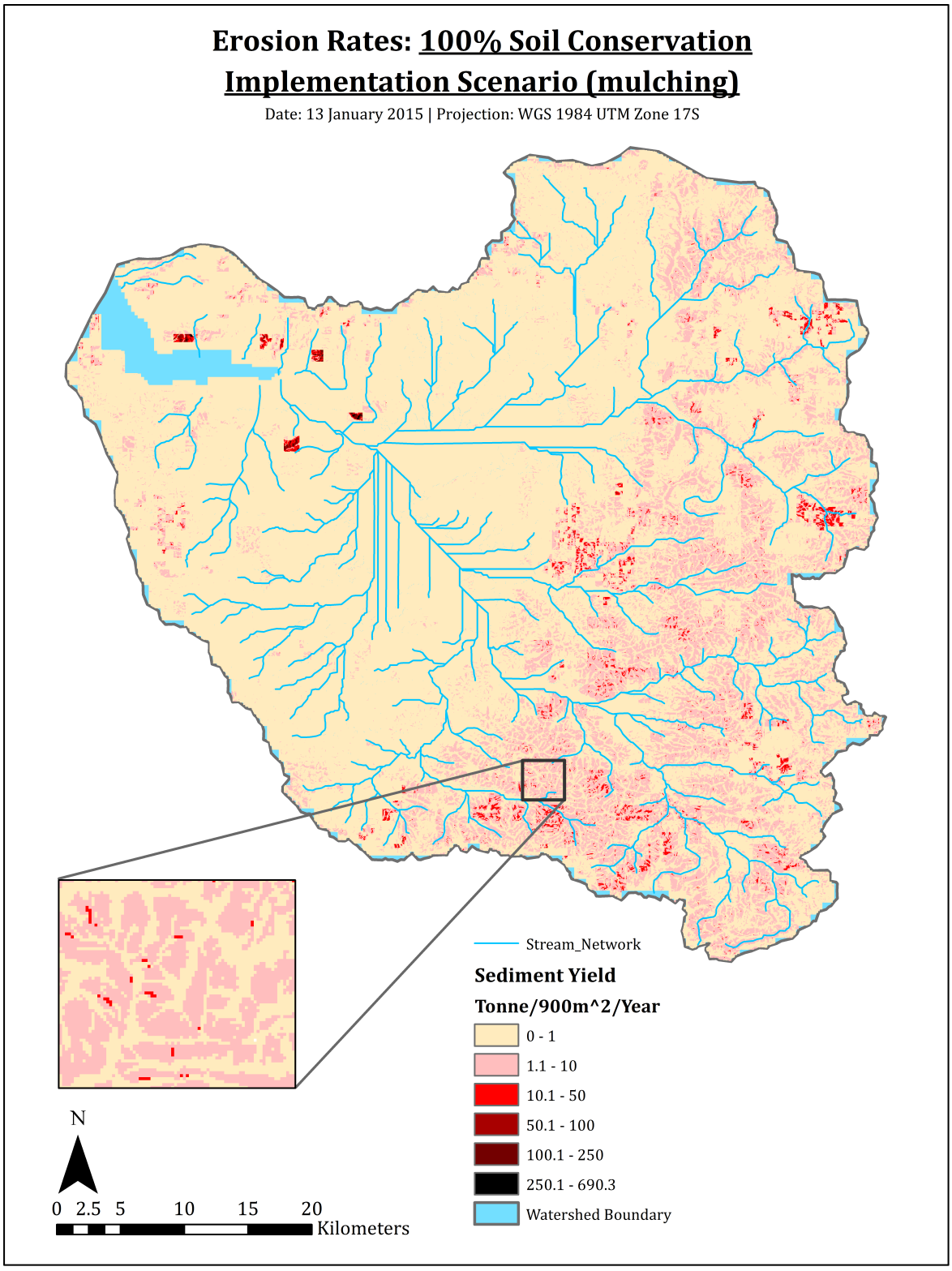

Figure 4.6 InVEST Sediment Retention model results showing erosion rates when 100% of the crop lands with at least 70% crop cover in the study area have the soil conservation technique mulching employed during an average rain year

4.3.2 Impact of Varying Levels of Reforestation on Erosion Rate

To study the effect that varying levels of reforestation would have on reducing soil erosion, LULC rasters depicting the reforestation of 10%, 20%, 30%, 40%, 50%, 60%, 70%, 80% and 90% of the rainfed cropland and mosaic cropland (≥70%) pixels were run through the InVEST model. As pixels were randomly selected for each percentage raster, "reforestation" did not occur on pixels of highest priority first. As such, the following linear relationship was observed:

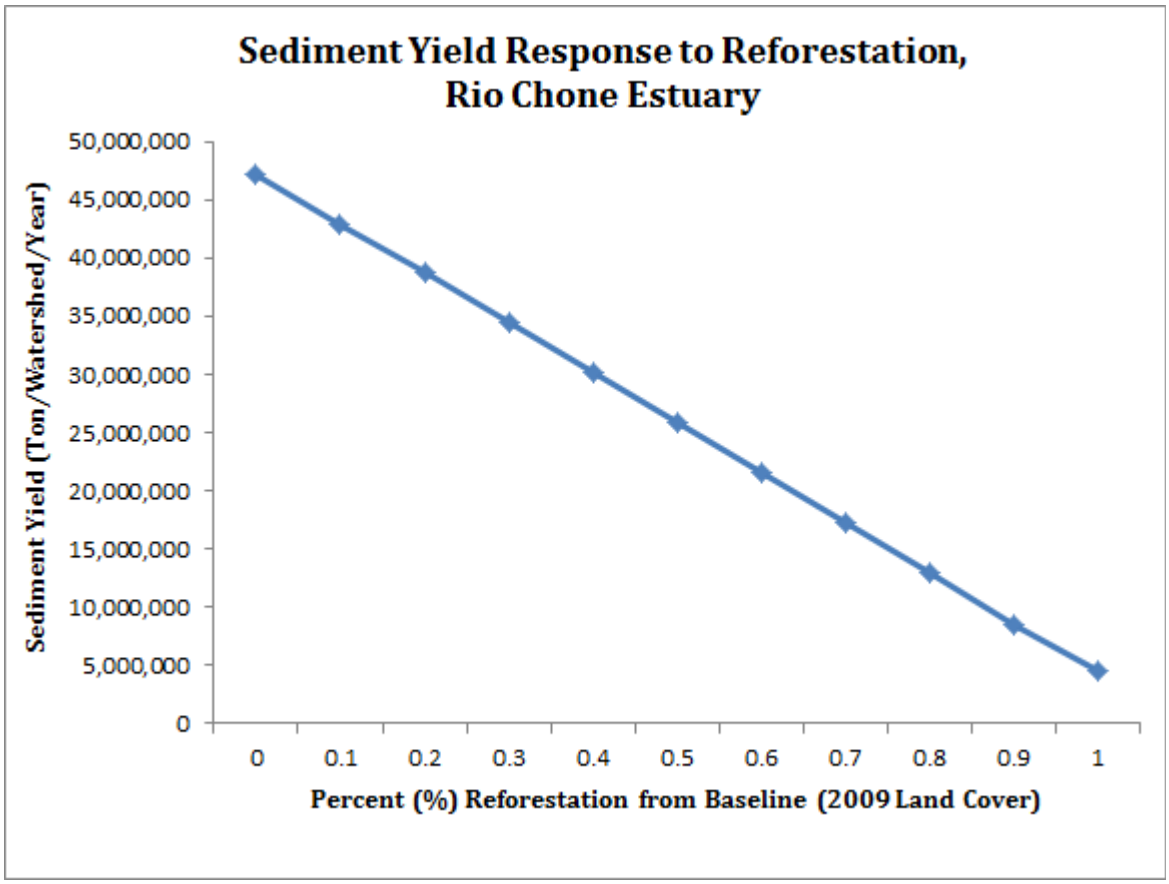

Figure 4.7 The response in sediment yield to reforesting different percentages of crop cover with native vegetation. Units are in metric tons (tonnes)

4.4 Total Sediment Estimate

We estimate that approximately 50 million tonnes of sediment wash into the Rio Chone estuary due to streambank erosion, erosion from unpaved roads, and erosion from sheetwash and rilling during a non-El Nino year (Table 4.3). Sediment generated from sheetwash erosion accounts for the majority of this volume.

Table 4.3 Total sediment estimate from sediment budget

Erosional Process	***Approximate Total Sediment Production*** *(Million Tonnes/Watershed/Year)*
Streambank Erosion	0.02
Unpaved Roads	0.2-0.4
Sheetwash and Rilling	**50**
Total Sediment Estimate	50

5.0 Discussion

We assessed the potential impacts of land use modifications on soil loss in Ecuador's Rio Chone estuary through the production of a sediment budget and a soil loss model. The environmental, social, and economic impacts of each management option will help determine which strategy, or combination of strategies, may be most beneficial for the majority of stakeholders in the region. The watershed is home to diverse flora and fauna, farmers, shrimp cultivators, and other diverse shareholders. The estuary's health is essential for all parties involved and the management of soil erosion is a collective undertaking for the entire region.

5.1 Implications of Bathymetric Maps

The bathymetric maps of the Rio Chone estuary showed the change in bathymetry from 1990 to 2011. The comparison map shows an overwhelming increase in bathymetric elevation in the middle of the estuary, whereas decreases in bathymetric elevation are mainly outside of the estuary. Although agricultural practices are cited as the primary cause of estuarine sedimentation, it is important to note that changes in current and water flow over time also influence the movement and input of sediment into the estuary (Mead & Moores, 2005). Tides and wave action both affect sediment transport within an estuary (Mead & Moores, 2005). Tides in the Rio Chone estuary typically range from one to three meters. Though this is a relatively low range, tides provide a source of energy for sediment movement within the estuary (Mead & Moores, 2005). Waves, especially during large storm events, can lift sediment from the seabed and move large quantities of sediment through an estuary's inlet with the incoming tide (Mead & Moores, 2005). However, increases in sediment at the mouth of an estuary can also be caused by the flow of sediment from within the estuary towards the ocean, which is common in mesotidal estuaries like the Rio Chone estuary. In addition to the suspension load periodically flushed out with the tides, scouring along the outlet corridor of the estuary as shown in the bathymetric change map (Figure 4.1) indicates some bedload material is being transported out of the estuary. Despite these processes, an accretion rate of roughly 2.4 million tonnes/year was still observed. We limited our analysis to bathymetric change that can likely be attributed to sedimentation of the estuary, because modeling complex ocean processes is outside the scope of this project. While changes to tides and currents contribute to changes in sediment distribution within the estuary, we observed a net positive change in bathymetric elevation over the past 21 years.

5.2 Implications of Sediment Budget and Model Results

The total amount of sediment generated from unpaved roads and streambanks was small relative to the modeled amount of sediment generated from sheetwash and rilling. Therefore, controlling erosion from sheetwash and rilling has the potential to significantly affect the overall volume of sediment delivered to the Rio Chone estuary from the stream network.

Although model outputs should be considered rough estimates alone, they provide a clear conclusion: re-vegetating lands or implementing aggressive soil conservation techniques has the potential to significantly reduce soil erosion from sheetwash. In addition, results suggest that reforestation and soil conservation strategies could provide reductions in soil loss of relatively the same magnitude (Table 4.1). The model results imply flexibility in the management of the watershed due to the identification of two plausible management techniques that can be implemented according to preference. As farmers are often forced to fallow lands after agricultural productivity declines following soil loss, land managers may consider reforesting fallowed lands and employing soil conservation techniques on currently cultivated properties. While we looked at mulching and strip-crop buffering alone, a myriad of soil conservation strategies exist and should be considered. These include strategies that bulwark the dislodging of soil grains in the first place, such as mulching, to techniques that reduce sediment delivery to stream networks, such as vegetative riparian buffers.

The results of the model estimate an approximate sediment yield from the watershed of 50 million tonnes per year. In comparison, our calculation of sediment deposition and retainment within the estuary from bathymetric maps was an estimated 2.4 million tonnes per year. We found extensive sand bars on the stream network throughout the watershed that may account for this discrepancy since our model did not institute the time lag implied by sand bar formation. Also, a significant proportion of the sediment delivered to the estuary each year may flow out to sea. These processes have acted to reduce yearly sedimentation of the estuary, but not at a high enough magnitude to mitigate the sedimentation phenomenon currently underway. Any future changes to these processes have the potential to affect the magnitude of sedimentation in the estuary.

The discrepancy in accretion rate estimates and sediment production volume per the sediment budget may suggest that the InVEST model should be calibrated using total suspended solids data to ensure overestimation is not occurring. However, even when a sensitivity analysis was performed on model parameters to test the possible range of values, it did not change the bottom line: sediment produced from surface water erosion on cleared lands, namely the volume of sediment generated from sheetwash and rilling, was larger than the sediment produced by all other geomorphic processes assessed by several orders of magnitude.

5.3 Sustainability Strategies: Reforestation and Soil Conservation

When addressing the sedimentation issue, it is both more feasible and more efficient to stop erosion in the first place versus catching it while in transport. As discussed, reforestation of degraded lands and soil conservation strategies have the potential to greatly reduce erosion from the Rio Chone watershed. We recognize the utility of both options for sediment retention because the lands that are currently cultivated provide value, however limited, to the inhabitants of the watershed, and it would be illogical to reforest actively cultivated lands. We therefore expect that a combined management approach will be most successful within the Rio Chone estuary.

5.3.1 Implementation Timelines

Reforestation for the mitigation of erosion can provide significant reductions within eight to ten years of planting. However, maximum erosion reductions may take up to 30 years to be realized, depending on the species planted (Marden, 2012; Huang et al., 2010). These studies considered active reforestation, which involves the "active" planting of tree species, as opposed to passively allowing successional processes to reestablish forests. Passive reforestation would likely require longer time scales.

Conversely, soil conservation strategies can provide erosion benefits immediately after implementation (Section 2.6.1.2). It is the adoption of the soil conservation strategies in the first place, however, that imposes a time lag on erosional benefits when using sustainable farming techniques. Educational outreach to farmers within the Rio Chone watershed has the potential to be met with varying degrees of success. Successful delivery of conservation techniques necessitates an understanding of the farmer's system and close consideration of their incentives (Moldenhauer & Hudson, 1988). The timeline for realization of erosional reductions as a result of soil conservation strategies is therefore most heavily dependent on the success of outreach to farmers within the watershed. In addition, the potential for delivery time lags to exist should be considered, and is discussed in further detail in the following section.

5.3.1.1 Time Lag of Sediment Delivery

Reducing upstream erosion may not confer immediate reductions in downstream estuarine sedimentation should significant delivery time lags occur. While soil conservation strategies and re-vegetation could be used to quickly halt erosion in the watershed, we realize the importance of considering these potential time lags. Even after erosion is managed, sediment that was generated before management strategies were employed may continue to be delivered to the estuary far into the future, depending on the topography and geomorphic structures of the landscape. To address this potential, we surveyed our study area with a professional geologist with aim to identify potential intermediate sediment sinks along the stream network. Sediment deposition was seen along a small number of river reaches in the form of sand bars, however the frequency of these occurrences was minimal. Obvious floodplains, excellent sinks for sediment along stream

networks, were not observed in the Rio Chone watershed. An important consideration: the dam at La Esperanza and the La Segua marsh may be housing fair amounts of sediment that will continue to be released during peak discharges throughout the next few decades. However, while impossible to estimate the likely volume of sediment stored in these sinks, we conclude that these potential sediment reservoirs are relatively minimal in size and retainment capacity when compared to the landscape as a whole system. In sum, the Rio Chone watershed likely delivers sediment to the estuary fairly quickly once the dislodged soil grains reach the stream channel.

5.3.2 Relative Costs

The costs of reforestation vary depending on numerous factors. Global Student Embassy carries out reforestation projects in the Rio Chone watershed, paying $2.75 per tree including post-planting maintenance. They plant approximately 500 trees per hectare, totaling $1,375 per hectare reforested. Passive reforestation only incurs the opportunity cost of forgoing other economic activity on the land in favor of regenerating forest cover.

Soil conservation strategies that have the highest potential to be successful within the Rio Chone watershed are those with the lowest cost to farmers. Farming techniques such as reduced, minimum, and no-till provide advantages for both plant production and soil conservation, often providing direct benefits to farmers (Moldenhauer and Hudson, 1988). The costs of the potential educational campaigns needed to enhance implementation of soil conservation techniques within the Rio Chone watershed are variable and not predicted by our research. Pannell et al. (2014) emphasize that the economic costs versus rewards for implementing conservation strategies vary from location to location as well as with an individual farm's economic capital. This is due to the discrepancies between local farm sizes, interest rates, access to market resources, farm management skills, and the resulting disparity among costs and benefits (Pannell et al., 2014). A decision to implement a recommended strategy is set firmly in a small farmer's reality where short-term implications are particularly important for their livelihood (Erenstein, 2003).

Because of the up-front costs, the successful implementation and maintenance of soil conservation strategies in the watershed might require subsidizing. External payments provided by the Ecuadorian government, or downstream users of the estuary, could be a necessary incentive to coax farmers into using soil conservation techniques.

5.3.3 Conservation Easements

Continued conversion of lands away from native cover will increase erosion in the watershed, and thus estuarine sedimentation. Through the Ministry of the Environment, the Ecuadorian government instituted a program for the creation of conservation easements called the Socio Bosque Programme (Socio Bosque) in 2008, which has the potential to partially address future deforestation pressures. The program is an incentive-based, voluntary program that enhances environmental and socioeconomic goals through annual per-hectare payments in return for maintaining forest cover (de Koning, 2011).

The program takes an "opt-in" approach to deter negotiations. The term of the agreement is set at 20 years, and participants must agree to be subject to annual monitoring. Though the program becomes more lucrative when large land parcels are put into conservation, small landowners have taken advantage of the program as well (de Koning, 2011). However, the program requires that applicants hold the legal title to the land, which can be prohibitive to some poor inhabitants who lease their land from the government (de Koning, 2011).

The western and southwestern regions of the Rio Chone watershed have been identified by the Ministry of the Environment as high priority regions for the Socio Bosque program (de Koning, 2011). We expect that further expansion of this program in the region will continue as the program matures, and we recognize its immense potential to provide assurances against future exacerbation of the sedimentation issue with the estuary.

5.3.4 Property Rights

Whitaker and Southgate (1992) suggested that Ecuador, Latin America's most densely populated country, has been at particular risk for environmental degradation due to population growth and poor structuring of land ownership rights. Government interference with market forces has incentivized degradation of the natural environment, while land tenure arrangements have compounded the issues. These forces contribute dramatically to destructive human interactions with the environment. Tangible environmental problems within Ecuador are often a product of the lack of incentives for long-term land conservation because of the absence of strong property rights for farmers (Whitaker & Southgate, 1992).

Incentives for land stewardship vary widely with the property rights assigned to inhabitants of the landscape. Long-term management of land, which is ecologically favorable, is more likely to occur if stakeholders have stable property rights that allow them to think in the long term. Moldenhaur and Hudson (1988) report instances of poor Ecuadorian farmers planting on unsustainable hillslope gradients, with the understanding that the soil might be gone relatively quickly, because they have no alternatives and no long-term claim to the land. The length of land tenure offered to farmers can help incentivize long-term sustainable management and is thus an important area of concern for the agricultural side of the erosion problem within the Rio Chone watershed (Moldenhaur & Hudson, 1988). If a farmer expects to grow crops on the same plot far into the future, he is more invested in protecting it. Furthermore, the National Development Bank rarely issues loans to farmers who do not have proper land titles, which also discourages the use of soil conservation practices (Whitaker & Southgate, 1992).

Assignment of property rights is also an important consideration in cases where government owned properties are being managed poorly. This is a common scenario in developing nations where complete enforcement proves problematic. Much of Ecuador's tree-covered land is part of a publicly owned reserve or park (discussed in section 2.7). However, encroachment on public-sector land is common, where trespassers regard the resource as a free good, open for exploitation. The issues resonate with the concepts of G.

Hardin's "tragedy of the commons". Where the Ecuadorian government *has* recognized its inability to manage sprawling lands, it has vested property rights in users of these idle lands; unfortunately, the structure of such rights rarely promotes conservative practices.

The tenure insecurity associated with the Ecuadorian Institute for Agrarian Reform and Colonization's convoluted settlement procedures disincentivizes the owners of land from investing in land improvement techniques, including soil conservation measures (Whitaker and Southgate, 1992). Unfortunately, soil erosion in Ecuador causes land productivity to decline rapidly. Once erosion begins, fertilizer application can counter productivity decreases associated with soil loss for a few years, but crop production quickly becomes economically infeasible.

In summary, when farmers do not have true ownership of land they are less likely to treat it sustainably. Implementing soil conservation techniques takes time and motivation, and will likely be ignored if the farmer cannot rely on using the arable land into the future. Until the Ecuadorian government makes it easy and desirable to acquire long-term property rights to a parcel of land, soil conservation is less likely to occur and the deforestation of the dry tropical forest in the Rio Chone watershed may continue, despite the negative effects soil erosion has on agricultural productivity and the health of riverine ecosystems downstream.

5.3.5 Watershed-Scale Planning

As scientists, it is easy to view the conservation issues within the Rio Chone watershed in terms of interactions between plants, soils, and water. However, as with many contemporary issues, political, social, and economic factors are equally important. The factors leading to high erosion rates within the Rio Chone estuary are inextricably linked to human actions. As such, approaches to address the contemporary impacts to the estuary must be seen as human-centric.

Given the drivers of increased erosion within the watershed, management actions endorsed nominally on behalf of environmental conservation have lower potential to gain support from farmers than management actions for sustained agricultural yields. Successful planning on the watershed scale will require close examination of the incentives of all stakeholders.

Management to control the high erosion rates currently found in the watershed have the potential to benefit a number of stakeholders, in addition to farmers. Shrimp aquaculture and tourism, two of the largest economic sectors in the regional economy, are directly tied to the ecological health of the estuary. Shrimp farms use the estuary as a source of water for their ponds, and are thus negatively affected by the reductions in water quality linked with sedimentation (Section 2.5.3). In addition, decreases in the estuary's water-holding capacity caused by sedimentation impedes natural flushing of shrimp ponds by tidal inundation, adding costs to shrimp farmers as they must install hydraulic pumps to

accomplish this same task. Tourism in the region is linked with the aesthetic quality of the estuary and would therefore also benefit from a reduced sedimentation rate.

It would likely be in the interests of these two sectors to fund projects that would reduce erosion in the watershed. This issue will not simply go away if left unaddressed, and these two economic sectors have the most to lose if nothing is done. However, organizations pushing for such collaboration should be wary of the issues involved in prototypical collective action problems.

6.0 Conclusion

The goal of this work was to objectively define the sources of sediment production in the Rio Chone watershed and to assess the relative impacts of changing land use on the amount of material generated. We feel that we have accomplished this task to the extent possible. Additionally, our analysis of the Rio Chone estuary has proven that from 1990 to 2011 the bathymetry of the estuary was severely built up, corroborating local knowledge that identified an increased rate of sedimentation. Our run of the InVEST Sediment Retention model allowed us to identify land uses, and areas, within the watershed that have high potential for erosion, and to quantify the amount of sediment produced from sheetwash and rilling annually. This analysis was intuitively spot-checked with our analysis of physical erosion characteristics within the watershed (Appendix 8.1).

Our analysis made it abundantly clear that land use within the watershed has the potential to significantly impact downstream sedimentation in the estuary. Unsurprisingly, the land parcels that likely contribute the most sediment to the watershed system are those that have been denuded of native vegetation; the principal driver of deforestation is the clearing of lands to make way for agricultural crop production. We feel that a combination of reforestation and soil conservation measures have the highest potential to reduce the sedimentation issue within the Rio Chone estuary. The concept of a "sedimentation debt" due to a history of erosion adds credence to the idea that this issue must be addressed hastily. Climate change projections also indicate that erosive potential is likely to increase within the watershed in coming decades, as the frequency and intensity of storm events increases, as well as the frequency of extreme El Nino events. As a result, prompt action is needed to head off even larger sedimentation rates in the coming decades.

Though reforestation and adoption of soil conservation techniques have the potential to abate current erosion levels within the watershed, conservation of natural lands can also aid the achievement of this project's objectives. Conservation efforts can circumvent the increased erosion potential that would be produced by further conversion of vegetated lands within the watershed.

We do not think that more specific estimates of the sediment load from the watershed will provide additional insight to the management of the problem, because we have isolated the factors, and locations, that produce large amounts of sediment relative to the rest of the watershed. We believe that the best way forward in the Rio Chone watershed will require

three things. First, the government of Ecuador should consider the role of property rights in land degradation. Instead of leasing out lands short-term to farmers, allowing long land tenure will incentivize the new landowner to farm their plot sustainably. Incentivizing farmers to employ soil conservation strategies may be difficult when they have no long-term claim on the land. Second, an outreach program, which integrates the incentives of landowners and downstream water users together, should be shaped to foster greater adoption of soil conservation techniques. Lastly, subsidizing farmers for the employment of soil conservation strategies may be necessary as overcoming the up-front costs of their implementation would be hard for the typical small-scale subsistence farmer in the Rio Chone watershed. In conjunction, programs to ease the cost of reforestation should be sought out. Continuation and expansion of reforestation efforts on lands with high erosion potential has a high potential to aid in the achievement of reducing estuarine sedimentation.

It should be noted that the various uncertainties of our model results would require land managers to use a combination of our model output maps (Figures 4.2-4.6) and the erosion risk potential map (Appendix 8.1, Figure 8.5) when determining high-priority erosion hotspots. While the land use/land cover raster used in our model represents the relative percentages of land use types accurately, an exact geographical representation of land use locations would allow model output maps to be used in direct planning.

The sedimentation issue within the Rio Chone estuary has the potential to be addressed through management of the erosional processes within the watershed. The future of the estuary depends largely on the adoption of the suggested practices. Conversely, mismanagement has the potential to be devastating for the regional economy. The inhabitants of the watershed have the direct potential to control their own future through the management of their own activities, and the future of the Rio Chone estuary lies in their hands.

7.0 Bibliography

Acción Ecológica. (2014, December 1). Documentos de posicion de Accion Ecologica. Retrieved from http://www.accionecologica.org/servicios-ambientes/documentos-de-posicion-de-a-e

Ades, H., Graham, M., & Humphreys, S. (2013). *Rough Guide to Ecuador and the Galapagos Islands* (5th ed.). Rough Guide Ltd.

Akay, A. E., Erdas, O., Reis, M., & Yuksel, A. (2008). Estimating sediment yield from a forest road network by using a sediment prediction model and GIS techniques. *Building and Environment*, *43*(5), 687–695. http://doi.org/10.1016/j.buildenv.2007.01.047

Amaral, A. J., Berton, I., Cogo, N. P., & Barbosa, F. T. (2008). Reduction of water erosion in three soil management systems in an inceptisol of the Planalto Sul-Catarinense Region, Brazil. *Revista Brasiliero Ciencia de Solo*, (32), 2145–2155.

Arino, O., Bogaert, E. V., Bontemps, S., Defourny, P., Kalogirou, V., & Peres, J. R. (2011). *GLOBCOVER 2009 Products Description and Validation Report*. UCLouvain & ESA Team.

Arriaga, L., Montaño, M., & Vásconez, J. (1999). Integrated management perspectives of the Bahía de Caráquez zone and Chone River estuary, Ecuador. *Ocean & Coastal Management*, *42*(2), 229–241.

Barajas-Guzmán, M. G., & Barradas, V. L. (2013). Costos y beneficios de la aplicación de acolchados en la reforestación de los bosques tropicales caducifolios. *Botanical Sciences*, *91*(3), 363–370.

Bartley, R., Hawdon, A., Post, D. A., & Roth, C. H. (2007). A sediment budget for a grazed semi-arid catchment in the Burdekin basin, Australia. *Geomorphology*, *87*(4), 302–321. http://doi.org/10.1016/j.geomorph.2006.10.001

Belmont, P., Gran, K. B., Schottler, S. P., Wilcock, P. R., Day, S. S., Jennings, C., … Parker, G. (2011). Large Shift in Source of Fine Sediment in the Upper Mississippi River. *Environmental Science & Technology*, *45*(20), 8804–8810. http://doi.org/10.1021/es2019109

Benites, J., & Alexandra, B. (2005). *The importance of soil organic matter: Key to drought-resistant soil and sustained food production.* (No. 80). FAO.

Bennett, H. H. (1925). Some Geographic Aspects of Western Ecuador. *Annals of the Association of American Geographers*, *15*(3), 126–147. http://doi.org/10.1080/00045602509356950

Benzer, N. (2010). Using the geographical information system and remote sensing techniques for soil erosion assessment. *Polish J Envirion Stud*, *19*(5), 881–886.

Berg, P. (1999, February). Dispatches from Ecuador.

Berry, Walter, Rubinstein, Norman, Melzian, Brian, & Hill, Brian. (2003). *The Biological Effects of Suspended and Bedded Sediment (SABS) in Aquatic Systems: A Review*. United States Environmental Protection Agency, Office of Research and Development. Retrieved from http://water.epa.gov/scitech/swguidance/standards/criteria/aqlife/sediment/upload/2004_08_17_criteria_sediment_appendix1.pdf

Birch, J. C., Newton, A. C., Aquino, C. A., Cantarello, E., Echeverría, C., Kitzberger, T., … Garavito, N. T. (2010). Cost-effectiveness of dryland forest restoration evaluated by spatial analysis of ecosystem services. *Proceedings of the National Academy of Sciences*, *107*(50), 21925–21930.

Blanton, J. O., Lin, G., & Elston, S. A. (2002). Tidal current asymmetry in shallow estuaries and tidal creeks. In *Tenth Biennial Conference on the Physics of Estuaries and Coastal Seas* (Vol. 22, pp. 1731–1743).

Bochet, E., Poesen, J., & Rubio, J. L. (2006). Runoff and soil loss under individual plants of a semi-arid Mediterranean shrubland: influence of plant morphology and rainfall intensity. *Earth*

Surface Processes and Landforms, *31*(5), 536–549. http://doi.org/10.1002/esp.1351

Bohling, G. (n.d.). Kriging. Kansas Geological Survey. Retrieved from http://people.ku.edu/~gbohling/cpe940/Kriging.pdf

Bryan, B. A., & Crossman, N. D. (2008). Systematic regional planning for multiple objective natural resource management. *Journal of Environmental Management*, *88*(4), 1175–1189. http://doi.org/10.1016/j.jenvman.2007.06.003

Buttle, J. M. (1994). Hydrological response to reforestation in the Ganaraska River basin, southern Ontario. *The Canadian Geographer/Le Géographe Canadien*, *38*(3), 240–253.

Cai, W., Borlace, S., Lengaigne, M., van Rensch, P., Collins, M., Vecchi, G., … Jin, F.-F. (2014). Increasing frequency of extreme El Nino events due to greenhouse warming. *Nature: Climate Change*, *4*(2), 111–116.

Cebecauer, T., & Hofierka, J. (2008). The consequences of land-cover changes on soil erosion distribution in Slovakia. *Geomorphology*, (98), 187–201.

Center for History and New Media. (n.d.). Zotero Quick Start Guide. Retrieved from http://zotero.org/support/quick_start_guide

Chang, B. D., & Navas, W. (2006). Seasonal variation in growth, condition and gonads of Dormitator latifrons (Richardson) in the Chone River Basin, Ecuador. *Journal of Fish Biology*, *24*(6), 637–648.

Chen, L., Huang, Z., Gong, J., Fu, B., & Huang, Y. (2007). The effect of land cover/vegetation on soil water dynamic in the hilly area of the loess plateau, China. *CATENA*, *70*(2), 200–208. http://doi.org/10.1016/j.catena.2006.08.007

Church, J. A., Clark, P. U., Cazenave, A., Gregory, J. M., Jevrejeva, S., Levermann, A., … Unnikrishnan, A. S. (2013). Sea Level Change. In *Climate Change 2013: The Physical Science Basis. Contribution of Working Group I to the Fifth Assessment Report of the Intergovernmental Panel on Climate Change*. Cambridge, United Kingdom and New York, NY, USA: Cambridge University Press.

Claessens, L., Knapen, A., Kitutu, M. G., Poesen, J., & Deckers, J. A. (2007). Modelling landslide hazard, soil redistribution and sediment yield of landslides on the Ugandan footslopes of Mount Elgon. *Geomorphology*, *90*(1-2), 23–35. http://doi.org/10.1016/j.geomorph.2007.01.007

Coastal Zone, Canada Association, University of Rhode Island's Coastal Resources Center, Canadian International Development Research Center, and the Intergovernmental Oceanographic Commission. (1994). *UNESCO: Workshop on Integrated Coastal Management* (No. Workshop Report No. 104).

Coello, S., Proafio-Lerowr, D., & Robadue Jr, D. (n.d.). Ecuador's Rio Chone Estuary. Retrieved from http://simce.ambiente.gob.ec/sites/default/files/documentos/anny/Special%20Area%20Management%20Planning%20In%20Ecuador%27s%20Rio%20Chone%20Estuary.pdf

Coello, S., Proano-Leroux, D., & Robadue, D. J. (1993). Special Area Management Planning In Ecuador's Rio Chone Estuary. In *The Eight Symposium on Coastal and Ocean Management*. New Orleans, Louisiana.

Consumer Price Index Inflation Calculator. (2015, January 6).

Cooper, K. (2011). *Evaluation of the Relationship Between the RUSLE R-Factor and Mean Annual Precipitation*. Colorado State. Retrieved from http://www.engr.colostate.edu/~pierre/ce_old/Projects/linkfiles/Cooper%20R-factor-Final.pdf

Dai, F. C., & Lee, C. F. (2001). Frequency–volume relation and prediction of rainfall-induced landslides. *Engineering Geology*, *59*(3), 253–266.

De Graaff, J., Aklilu, A., Ouessar, M., Asins-Velis, S., & Kessler, A. (2013). The development of soil and water conservation policies and practices in five selected countries from 1960 to

2010. *Land Use Policy*, *32*, 165–174. http://doi.org/10.1016/j.landusepol.2012.10.018

De Koning, F., Aguinaga, M., Bravo, M., Chiu, M., Lascano, M., Lozada, T., & Suarez, L. (2011). Bridging the gap between forest conservation and poverty alleviation: the Ecuadorian Socio Bosque program. *Environmental Science & Policy*, *14*(5), 531–542.

Descheemaeker, K., Nyssen, J., Poesen, J., Raes, D., Haile, M., Muys, B., & Deckers, S. (2006). Runoff on slopes with restoring vegetation: A case study from the Tigray highlands, Ethiopia. *Journal of Hydrology*, *331*(1-2), 219–241. http://doi.org/10.1016/j.jhydrol.2006.05.015

Desmet, P., & Govers, G. (1996). A GIS procedure for automatically calculating the USLE LS factor on topographically complex landscape units. *Journal of Soil and Water Conservation*, *51*(5), 427–433.

Dewaulle, J. C. (1973). Reultats de six annees d'observations sur l'erosion au Niger. *Bois et Forets des Tropiques*, *150*, 15–37.

Díaz-Raviña, M., Martín, A., Barreiro, A., Lombao, A., Iglesias, L., Díaz-Fierros, F., & Carballas, T. (2012). Mulching and seeding treatments for post-fire soil stabilisation in NW Spain: Short-term effects and effectiveness. *Geoderma*, *191*, 31–39. http://doi.org/10.1016/j.geoderma.2012.01.003

Diseker, E. G., & Richardson, C. F. (1962). Erosion rates and control measures on highway cuts. *Transactions of the American Society of Engineers*, *5*, 153–155.

Dlamini, P., Orchard, C., Jewitt, G., Lorentz, S., Titshall, L., & Chaplot, V. (2011). Controlling factors of sheet erosion under degraded grasslands in the sloping lands of KwaZulu-Natal, South Africa. *Agricultural Water Management*, *98*(11), 1711–1718. http://doi.org/10.1016/j.agwat.2010.07.016

Drake, B. E. (2005). Estimating increased erosion and sediment delivery caused by wildfires. *CE394K GIS in Water Resources, University of Texas*.

Drinnan, R. W., & Clark, M. J. R. (1980). *Fraser River Estuary Study Water Quality* (pp. 1–178). Victoria, British Columbia. Retrieved from http://www.env.gov.bc.ca/wat/wq/fraseriver/freswaterchem.pdf

Dronkers, J. (1986). Tidal Asymmetry and Estuarine Morphology. *Netherlands Journal of Sea Research*, *20*(2/3), 117–131.

Durán Zuazo, V. H., & Rodríguez Pleguezuelo, C. R. (2008). Soil-erosion and runoff prevention by plant covers. A review. *Agronomy for Sustainable Development*, *28*(1), 65–86. http://doi.org/10.1051/agro:2007062

Dyer, K. R. (1989). Sediment processes in estuaries: Future research requirements. *JGRC Journal of Geophysical Research: Oceans*, *94*(C10), 14327–14339.

El Kateb, H., Zhang, H., Zhang, P., & Mosandl, R. (2013). Soil erosion and surface runoff on different vegetation covers and slope gradients: A field experiment in Southern Shaanxi Province, China. *CATENA*, *105*, 1–10. http://doi.org/10.1016/j.catena.2012.12.012

Ellison, A., Farnsworth, E., & Moore, G. (2010). *Red List of Threatened Species* (No. IUNC Version 2013.2). IUCN.

Erenstein, O. (2003). Smallholder conservation farming in the tropics and sub-tropics: a guide to the development and dissemination of mulching with crop residues and cover crops. *Agriculture, Ecosystems & Environment*, *100*(1), 17–37.

European Space Agency. (2010). *Data User Element Directory*.

FAO. (2010). *Global Forest Resources Assessment*.

Farrow, A. (2009). *Spatial analysis of social vulnerability to the El Nino phenomenon in Ecuador: producing an assessment of vulnerability* (pp. 120–130). University of East Anglia. Retrieved from https://ueaeprints.uea.ac.uk/19409/1/ThesisFinalNEW.pdf

Fernández, C., & Vega, J. A. (2014). Efficacy of bark strands and straw mulching after wildfire in NW Spain: Effects on erosion control and vegetation recovery. *Ecological Engineering*, *63*,

50–57. http://doi.org/10.1016/j.ecoleng.2013.12.005
Fernandez, C., Wu, J. Q., McCool, D. K., & Stockle, C. O. (2003). Estimating water erosion and sediment yield with GIS, RUSLE, and SEDD. *Journal of Soil and Water Conservation*, *58*(3), 128–136.
Fischer, J., Hartel, T., & Kuemmerle, T. (2012). Conservation policy in traditional farming landscapes: Conserving traditional farming landscapes. *Conservation Letters*, *5*(3), 167–175. http://doi.org/10.1111/j.1755-263X.2012.00227.x
Fitz-Henry, E. (2012). The Natural Contract: From Lévi-Strauss to the Ecuadorian Constitutional Court. *Oceania*, *82*(3), 264–277.
Follis, M. B., & Nair, P. K. R. (1994). Policy and institutional support for agroforestry: an analysis of two Ecuadorian case studies. *Agroforestry Systems*, *27*(3), 223–240.
Fu, B., Liu, Y., Lü, Y., He, C., Zeng, Y., & Wu, B. (2011). Assessing the soil erosion control service of ecosystems change in the Loess Plateau of China. *Ecological Complexity*, *8*(4), 284–293. http://doi.org/10.1016/j.ecocom.2011.07.003
Fu, B., Newham, L. T. H., & Ramos-Scharrón, C. E. (2010). A review of surface erosion and sediment delivery models for unsealed roads. *Environmental Modelling & Software*, *25*(1), 1–14. http://doi.org/10.1016/j.envsoft.2009.07.013
Gitas, I. Z., Douros, K., Minakou, C., Silleos, G. N., & Karydas, C. G. (2009). Multi-temporal soil erosion risk assessment in N. Chalkidiki using a modified USLE raster model. *EARSel eProceedings*, *8*, 40–52.
Hamilton, S., & Collins, S. (2013). Livelihood responses to mangrove deforestation in the northern provinces of Ecuador. *Bosque*, *34*(2), 143–153.
Hanratty, D. M. (1989). *Ecuador: A Country Study*. Washington: GPO for the Library of Congress. Retrieved from http://countrystudies.us/ecuador/
Harmonized World Soil Database (version 1.1). (2009). FAO/IIASA/ISRIC/ISS-CAS/JRC.
Hayes, M. O. (1980). General morphology and sediment patterns in tidal inlets. *Sedimentary Geology*, *26*(1-3), 139–156.
Henry, A., & Mabit, L. (2013). Land use effects on erosion and carbon storage of the Río Chimbo watershed, Ecuador. *Plant and Soil*, *367*, 1–2.
Hijmans, R. J., Cameron, S. E., Parra, J. L., & Jarvis, A. (2005). Very high resolution interpolated climate surfaces for global land areas. *International Journal of Climatology*, *25*, 1965–1978.
Honorato, R., Barrales, L., Pena, I., & Barrera, F. (2001). USLE erosion model evaluation on six locations between IV and IX Region of Chile. *Ciencia Investigaciones Agriculturas*, (28), 7–14.
Huang, Z., Ouyang, Z., Li, F., Zheng, H., & Wang, X. (2010). Response of runoff and soil loss to reforestation and rainfall type in red soil region of southern China. *Journal of Environmental Sciences*, *22*(11), 1765–1773. http://doi.org/10.1016/S1001-0742(09)60317-X
Hudson, B. D. (1994). Soil organic matter and available water capacity. *Journal of Soil and Water Conservation*, *2*(49), 189–194.
Institute of Water Research. (2002). *Technical Guide to RUSLE Use in Michigan*. Michigan State University.
Instituto Nacional de Estadística y Censos. (2015, February 16). Retrieved from http://www.ecuadorencifras.gob.ec
InVEST Sediment Retention Model User Guide. (2014). The Natural Capital Project. Retrieved from http://data.naturalcapitalandresilienceplatform.org/invest-releases/documentation/current_release/sediment_retention.html
Irvem, A., Topaloglu, F., & Uygur, V. (2007). Estimating spatial distribution of soil loss over Seyhan River Basin in Turkey. *Journal of Hydrology*, (336), 30–38.
Jimenez, J. A. (1984). A hypothesis to explain the reduced distribution of the mangrove Peliciera rhizophorae. *Biotropica*, *16*(4), 304–308.
Kansas Water Science Center (USGS). (2013). *River Sediment Studies in Kansas*. Retrieved from

http://ks.water.usgs.gov/reservoir-sediment
Kathiresan, K., & Bingham, B. L. (2001). Biology of mangroves and mangrove ecosystems. *Advances in Marine Biology*, *40*, 81–251.
Kitoh, A., Kusunoki, S., & Nakaegawa, T. (n.d.). Climate change projections over South America in the late 21st century with the 20 and 60 km mesh Meteorological Research Institute atmospheric general circulation model (MRI-AGCM). *Journal of Geophysical Research*, *116*(D6), 2011.
Kraus, K. W., Lovelock, C. E., McKee, K. L., Lopez-Hoffman, L., Ewe, S. M. L., & Sousa, W. P. (2008). Environmental drivers in mangrove establishment and early development: A review. *Aquatic Botany*, *89*, 105–127.
Lal, R. (2001). Soil degradation by erosion. *Land Degradation & Development*, *12*(6), 519–539. http://doi.org/10.1002/ldr.472
Lawler, D. M. (1993). The measurement of river bank erosion and lateral channel change: A review. *Earth Surface Processes and Landforms*, *18*(9), 777–821.
Le Bissonnais, Y., Monteir, C., Jamagne, M., Daroussin, J., & King, D. (2002). Mapping erosion risk for cultivated soil in France. *Catena*, *46*(2-3), 207–220.
Lee, J.-H., & Heo, J.-H. (2011). Evaluation of estimation methods for rainfall erosivity based on annual precipitation in Korea. *Journal of Hydrology*, *409*(1-2), 30–48.
Lefohn, A. S., Knudsen, H. P., & Shadwick, D. S. (2005). *Using Ordinary Kriging to Estimate the Seasonal W126, and N100 24-h Concentrations for the Year 2000 and 2003.* (pp. 1–10). United States. A.S.L. & Associates. Retrieved from http://webcam.srs.fs.fed.us/pollutants/ozone/spatial/2000/contractor_2000_2003.pdf
Le, H. D., Smith, C., Herbohn, J., & Harrison, S. (2012). More than just trees: Assessing reforestation success in tropical developing countries. *Journal of Rural Studies*, *28*(1), 5–19. http://doi.org/10.1016/j.jrurstud.2011.07.006
Lewis, R. (2005). Ecological engineering for successful management and restoration of mangrove forests. *Ecological Engineering*, (24), 403–418.
Lim, K. J., Sagong, M., Engel, B. A., Tang, Z., Choi, J., & Kim, K.-S. (2005). GIS-based sediment assessment tool. *CATENA*, *64*(1), 61–80. http://doi.org/10.1016/j.catena.2005.06.013
Liu, Y.-J., Wang, T.-W., Cai, C.-F., Li, Z.-X., & Cheng, D.-B. (2014). Effects of vegetation on runoff generation, sediment yield and soil shear strength on road-side slopes under a simulation rainfall test in the Three Gorges Reservoir Area, China. *Science of The Total Environment*, *485-486*, 93–102. http://doi.org/10.1016/j.scitotenv.2014.03.053
Lo, A., El-Swaify, S. A., Dangler, E. W., & Shinshiro, L. (1985). Effectiveness of EI30 as an erosivity index in Hawaii. In *Soil Erosion and Conservation* (pp. 384–392). Soil Conservation Society of America.
Marden, M. (2012). Effectiveness of reforestation in erosion mitigation and implications for future sediment yields, East Coast catchments, New Zealand: A review. *New Zealand Geographer*, *68*(1), 24–35.
Marden, M., Herzig, A., & Basher, L. (2014). Erosion process contribution to sediment yield before and after the establishment of exotic forest: Waipaoa catchment, New Zealand. *Geomorphology*, *226*, 162–174. http://doi.org/10.1016/j.geomorph.2014.08.007
Martin, A., Gunter, J. T., & Regens, J. L. (2003). Estimating erosion in a riverine watershed. *Environmental Science and Pollution Research*, (10), 245–250.
McCool, D. K., Foster, G. R., Renard, K. G., Yoder, D. C., & Weesies, G. A. (1995). Proceedings from DoD Interagency Workshop on Technologies to Address Soil Erosion on DoD Lands.
Menz, M. H., Dixon, K. W., & Hobbs, R. J. (2013). Hurdles and opportunities for landscape-scale restoration. *Science*, *339*(6119), 526–527.
Merritt, W. S., Letcher, R. A., & Jakeman, A. J. (2003). A review of erosion and sediment transport models. *Environmental Modelling & Software*, *18*(8-9), 761–799.

http://doi.org/10.1016/S1364-8152(03)00078-1
Moldenhauer, W. C., & Hudson, N. W. (1988). *Conservation Farming on Steep Lands*. Ankeny, Iowa: The Soil and Water Conservation Society.
Nair, P. (1991). State-of-the-art of agroforestry systems. *Forest Ecology and Management*, *45*, 5–29.
Nearing, M. A., Pruski, F. F., & O'neal, M. R. (2004). Expected climate change impacts on soil erosion rates: A review. *Journal of Soil and Water Conservation*, *59*(1), 43–50.
Newton, A. C., del Castillo, R. F., Echeverría, C., Geneletti, D., González-Espinosa, M., Malizia, L. R., … Williams-Linera, G. (2012). Forest Landscape Restoration in the Drylands of Latin America. *Ecology and Society*, *17*(1). http://doi.org/10.5751/ES-04572-170121
Ngwira, A. R., Aune, J. B., & Mkwinda, S. (2012). On-farm evaluation of yield and economic benefit of short term maize legume intercropping systmes under conservation agriculture in Malawi. *Field Crops Research*, *132*, 149–157.
Ozcan, A. U., Erpul, G., Basaran, M., & Erdogan, H. E. (2008). Use of USLE/GIS technology integrated with geostatistics to assess soil erosion risk in different land uses of Indagi Mountain Pass-Cankiri, Turkey. *Environmental Geology*, (53), 1731–1741.
Pannell, D. J., Llewellyn, R. S., & Corbeels, M. (2014). The farm-level economics of conservation agriculture for resource-poor farmers. *Agriculture, Ecosystems & Environment*, *187*, 52–64. http://doi.org/10.1016/j.agee.2013.10.014
Perillo, G. M. E. (1995). *Geomorphology and Sedimentology of Estuaries*. Elsevier.
Perillo, G. M. E., & Lavelle, J. W. (1989). Sediment transport processes in estuaries: An introduction. *JGRC Journal of Geophysical Research: Oceans*, *94*(C10), 14287–14288.
Pimentel D, Harvey C, Resosudarmo P, Sinclair K, Kurz D, McNair M, … Blair R. (1995). Environmental and economic costs of soil erosion and conservation benefits. *Science (New York, N.Y.)*, *267*(5201), 1117–23.
Pimentel, D., & Kounang, N. (1998). Ecology of Soil Erosion in Ecosystems. *Ecosystems Ecosystems*, *1*(5), 416–426.
Pollen, N. (2007). Temporal and spatial variability in root reinforcement of streambanks: Accounting for soil shear strength and moisture. *CATENA*, *69*(3), 197–205. http://doi.org/10.1016/j.catena.2006.05.004
Power, S., Delage, F., Chung, C., Kociuba, G., & Keay, K. (2013). Robust twenty-first-century projections of El Nino and related precipitation variability. *Nature*, *502*(7472), 541–545.
Prado, J. P. B., & Nobrega, M. T. (2005). Estimates of siol losses in the Ipiranga river basin in Cidade Baucha, State of Parana, with application of the Universal Soil Loss Equation. *Acta Scientiarum Technology*, *27*, 33–42.
Ramos Scharrón, C. E. (2010). Sediment production from unpaved roads in a sub-tropical dry setting — Southwestern Puerto Rico. *CATENA*, *82*(3), 146–158. http://doi.org/10.1016/j.catena.2010.06.001
Ramos-Scharrón, C. E., & MacDonald, L. H. (2007a). Development and application of a GIS-based sediment budget model. *Journal of Environmental Management*, *84*(2), 157–172. http://doi.org/10.1016/j.jenvman.2006.05.019
Ramos-Scharrón, C. E., & MacDonald, L. H. (2007b). Measurement and prediction of natural and anthropogenic sediment sources, St. John, U.S. Virgin Islands. *CATENA*, *71*(2), 250–266. http://doi.org/10.1016/j.catena.2007.03.009
Reid, L., & Dunne, T. (1984). Sediment Production from Forest Road Surfaces. *Water Resources Research*, *20*(11), 1753–1761.
Relf, D. (2009). Mulching for a healthy landscape. Retrieved from https://vtechworks.lib.vt.edu/handle/10919/48323
Revised Universal Soil Loss Equation (RUSLE) EPA Pesticide Project. (2000). [US EPA, U.S. Department of Agriculture, National Resources Conservation Service and Agriculture]. Retrieved from http://www.epa.gov/oppefed1/models/water/met_ca_citrus.htm

Robichaud, P. R., Jordan, P., Lewis, S. A., Ashmun, L. E., Covert, S. A., & Brown, R. E. (2013). Evaluating the effectiveness of wood shred and agricultural straw mulches as a treatment to reduce post-wildfire hillslope erosion in southern British Columbia, Canada. *Geomorphology*, *197*, 21–33. http://doi.org/10.1016/j.geomorph.2013.04.024

Robichaud, P. R., Lewis, S. A., Wagenbrenner, J. W., Ashmun, L. E., & Brown, R. E. (2013). Post-fire mulching for runoff and erosion mitigation. *CATENA*, *105*, 75–92. http://doi.org/10.1016/j.catena.2012.11.015

Roose, E. (1996). *Land Husbandry-Components and Strategy: Erosion Control Practices* (70 FAO Soils Bulletin No. ISBN 92-5-103451-6). Rome: FAO Corporate Document Repository.

Roose, E. J. (1973). Dix-sept annees de mesures experimentales de l'erosion et du ruissellement sur un sol ferrallitique sableux de.

Sapountzis, M. A., Efthimiou, G. S., & Stefanidis, P. S. (2007). The contribution of agrotechnical works following a fire to the protection of forest soils and the regeneration of natural forest. In *Eco-and Ground Bio-Engineering: The Use of Vegetation to Improve Slope Stability* (pp. 353–359). Springer. Retrieved from http://link.springer.com/chapter/10.1007/978-1-4020-5593-5_35

Sass, C. K., & Keane, T. D. (2012). *Application of Rosgen's BANCS Model for NE Kansas and the Development of Predictive Streambank Erosion Curves1*. Wiley Online Library. Retrieved from http://onlinelibrary.wiley.com/doi/10.1111/j.1752-1688.2012.00644.x/full

Shi, Z. H., Huang, X. D., Ai, L., Fang, N. F., & Wu, G. L. (2014). Quantitative analysis of factors controlling sediment yield in mountainous watersheds. *Geomorphology*, *226*, 193–201. http://doi.org/10.1016/j.geomorph.2014.08.012

Silva, R., Martínez, M. L., Hesp, P. A., Catalan, P., Osorio, A. F., Martell, R., … Govaere, G. (2014). Present and Future Challenges of Coastal Erosion in Latin America. *Coas Journal of Coastal Research*, *71*(sp1), 1–16.

Souris, D. M. (2014). Ecuador [Computer Sciences Researcher and GIS Developer, IRD]. Retrieved from http://www.savgis.org/ecuador.htm#DEM30

Southgate, D., & Whitaker, M. (1992). Promoting resource degradation in Latin America: tropical deforestation, soil erosion, and coastal ecosystem disturbance in Ecuador. *Economic Development and Cultural Change*, 787–807.

Special Area Management Planning in Ecuador's Rio Chone Estuary. (2015, February 16). Retrieved February 16, 2015, from http://www.academia.edu/3777694/Special_Area_Management_Planning_in_Ecuadors_Rio_Chone_Estuary

Stahl, P. W., & Pearsall, D. M. (2012). Late pre-Columbian agroforestry in the tropical lowlands of western Ecuador. *Quaternary International*, *249*, 43–52. http://doi.org/10.1016/j.quaint.2011.04.034

Stram, D. L., Kincaid, C. R., & Campbell, D. E. (2005). Water quality modeling in the Rio Chone Estuary. *Journal of Coastal Research*, 797–810.

Tang, Q., He, C., He, X., Bao, Y., Zhong, R., & Wen, A. (2014). Farmers' Sustainable Strategies for Soil Conservation on Sloping Arable Lands in the Upper Yangtze River Basin, China. *Sustainability*, *6*(8), 4795–4806. http://doi.org/10.3390/su6084795

Troeh, F., Hobbs, J., & Donahue, R. (1999). Soil and Water Conservation: Productivity and Environmental Protection. *New Jersey: Prentice-Hall*.

Twilley, R. R., Montano Armijos, M., Valdivieso, J. M., & Bodero, A. (1999). The Environmental Quality of Coastal Ecosystems in Ecuador: Implications for the Development of Integrated Mangrove and Shrimp Pond Management. In *Ecosistemas de Manglar en America Tropical* (pp. 199–230). Instituto de Ecologia A.C. Mexico.

United States Department of Agriculture. (2015, March 11). Reforestation. Retrieved from http://www.fs.fed.us/restoration/reforestation/

Wang, F., & Chapman, P. M. (2001). Assessing sediment contamination in estuaries. *Environmental Toxicology & Chemistry*, *20*(1).

Weill, M. D. M., & Sparovek, G. (2008). Erosion study in the ceveiro watershed (Piracicaba, sp.). I-Estimation of soil loss rates and sensitivity factor analysis of the USLE model. *Revista Brasileira de Ciencia Do Solo*, *32*(2), 801–814.

Wenner, E., Sanger, D., Upchurch, S, & Thompson, M. (n.d.). *Characterization of the Ashepoo-Combahee-Edisto (ACE) Basin, South Carolina*. SCNDR Marine Research Insitute. Retrieved from http://nerrs.noaa.gov/doc/siteprofile/acebasin/html/intro/execsum.htm

Wilber, D. H., & Clarke, D. G. (2001). Biological Effects of Suspended Sediments: A Review of Suspended Sediment Impacts on Fish and Shellfish with Relation to Dredging Activities in Estuaries. *North American Journal of Fisheries Management*, *21*(4), 855–875.

Wischmeier, W., & Smith, D. (1965). Predicting Rainfall Erosion Losses from Cropland East of the Rocky Mountains: Guide for Selection of Practices for Soil and Water Conservation. *U.S. Department of Agriculture Handbook No. 537*.

Wischmeier, W., & Smith, D. (1978). Predicting Rainfall Erosion Losses-A Guide to Conservation Planning. *U.S. Department of Agriculture Handbook No. 537*.

Wolanski, E., Moore, K., Spagnol, S., D'Adamo, N., & Pattiaratchi, C. (2001). Rapid, Human-Induced Siltation of the Macro-Tidal Ord River Estuary, Western Australia. *Estuarine, Coastal and Shelf Science*, *53*(5), 717–732.

Wolman, M. G., & Schick, A. P. (1967). Effects of Construction on Fluvial Sediment, Urban and Suburban Areas of Maryland. *Water Resources Research*, *3*(2), 451–464.

Woznicki, S., & Nejadhashemi, A. P. (2013). Spatial and Temporal Variabilities of Sediment Delivery Ratio. *Water Resources Management*, *27*(7), 2483–2499.

Wunder, S. (1996). Deforestation and the uses of wood in the Ecuadorian Andes. *International Mountain Society: Mountain Research and Development*, *16*(4).

Zheng, H., Chen, F., Ouyang, Z., Tu, N., Xu, W., Wang, X., ... Tian, Y. (2008). Impacts of reforestation approaches on runoff control in the hilly red soil region of Southern China. *Journal of Hydrology*, *356*(1-2), 174–184. http://doi.org/10.1016/j.jhydrol.2008.04.007

Zhou, P., Luukkanen, O., Tokola, T., & Nieminen, J. (2008). Effect of vegetation cover on soil erosion in a mountainous watershed. *CATENA*, *75*(3), 319–325. http://doi.org/10.1016/j.catena.2008.07.010

8.0 Appendix

8.1 Selection of High Priority Management Areas

To substantiate the InVEST Sediment Retention, we produced a map to showcase areas of the Rio Chone watershed that have the potential to generate the greatest amount of sediment according to fundamental erosion principles. The answers provided by this analysis corroborate the InVEST model, so conceptual framework used in the creation of the prioritization map is of particular value to management.

The physical erosional parameters included are: hillslope, distance to streams, soil erodibility, and magnitude of annual precipitation. Each parameter is assigned a color gradient depicting the severity of its potential erosion risk. Rather than reclassifying and aggregating raster representations of the different parameters, we chose to retain the high level of clarity in the vector representation. We expect the map to be more useful when it fully depicts the interaction of the erosional parameters, rather than identifying grid cells that have high potential erosion risk. We anticipate that a more complete understanding of the interaction of parameters will provides important insight to localized decision making for erosion management.

Decisions on bin size for parameter classifications were made keeping in mind the relative importance of each parameter, and an effort was made to limit the effect of selection bias by avoiding the use of too many bins.

8.1.1 Stream Buffer

Buffers were made from the stream network created by the InVEST model, extending 100m and 500m from each stream.

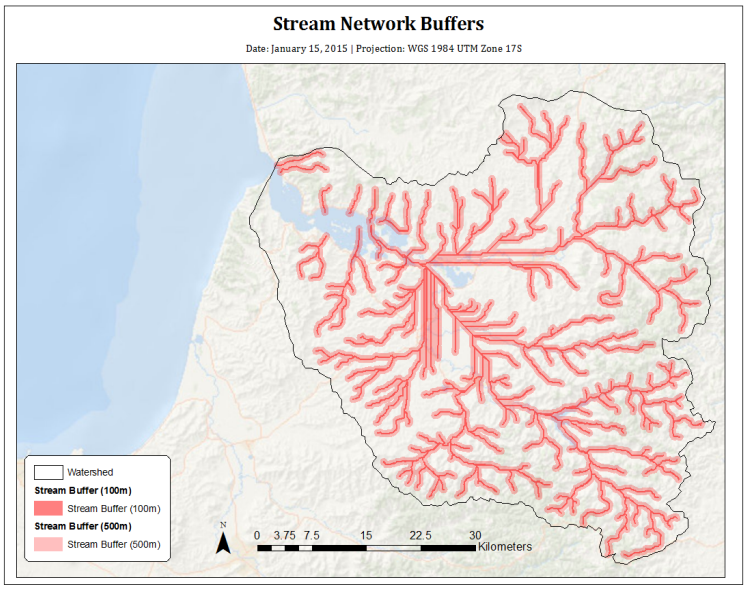

Figure 8.1 Stream network buffers within the Rio Chone watershed

8.1.2 Hillslope

Hillslope was calculated from our watershed digital elevation model (Appendix 8.2). Risk was assigned based on the relative distribution of slopes within the watershed.

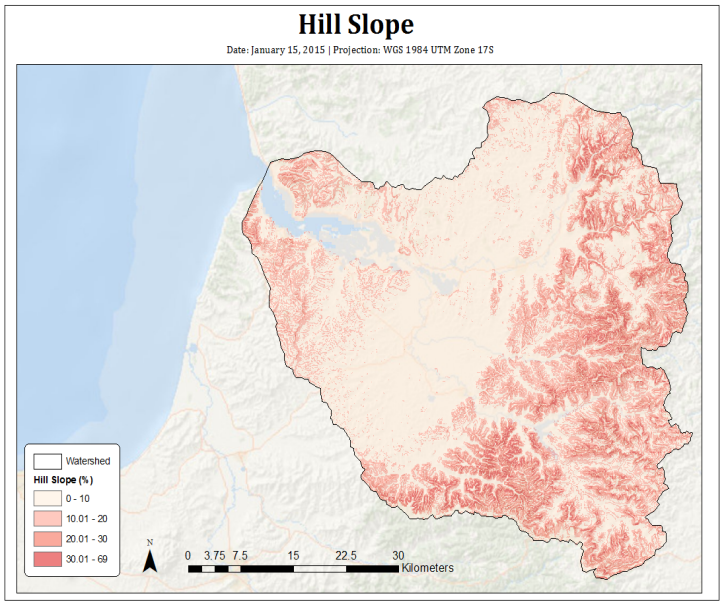

Figure 8.2 Hillslopes in the Rio Chone watershed

8.1.3 Annual Precipitation

Precipitation data was downloaded from the 30 arc-second WoldClim global dataset (Hijmans et al., 2005). Intuitively, greater precipitation entails greater erosion risk.

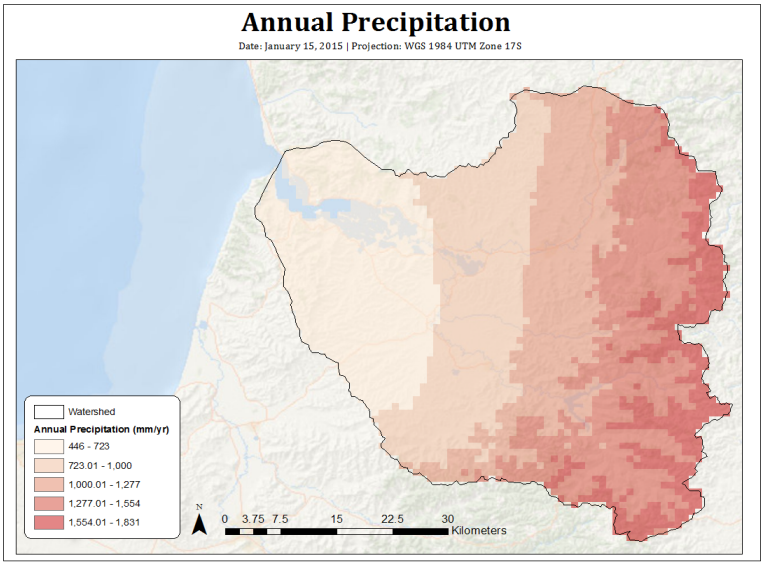

Figure 8.3 Annual precipitation within the Rio Chone watershed

4.3.4 Soil Erodibility

Erodibility is a measure of the susceptibility of a soil particle to detachment and transport by rainfall and runoff. Refer to appendix section 8.2 for a full description of the data layer.

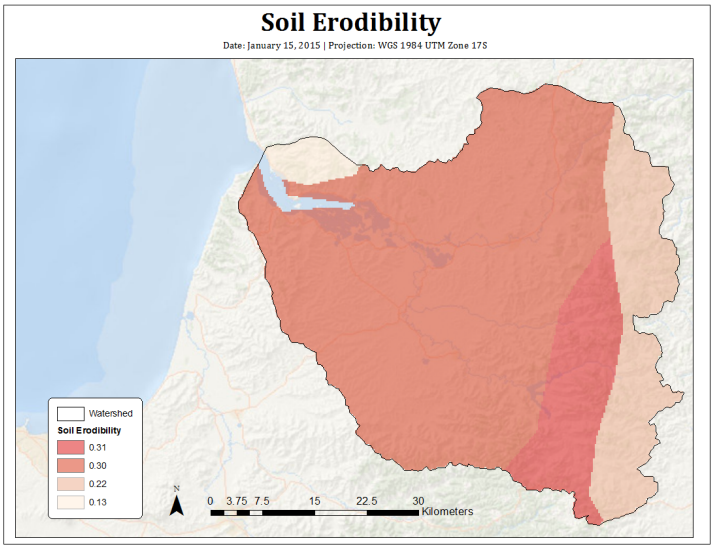

Figure 8.4 Soil erodibility in the Rio Chone watershed

The combination of these data layers gives a more complete idea of the physical potential that exists for erosion within the watershed. This map does not include land use, but should be used when deciding between areas that have the potential for reforestation or soil conservation. The intuition gained from studying this map should also drive locational

decisions within the spatial management of soil conservation techniques, as well as reforestation, in the Rio Chone watershed.

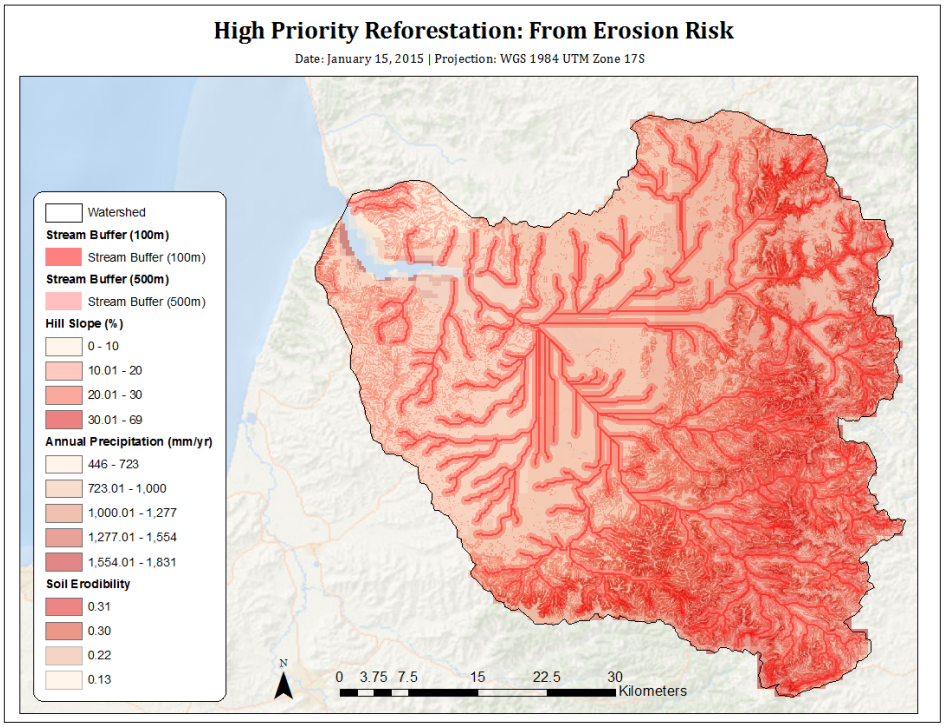

Figure 8.5 High priority reforestation sites to address erosion risk in the Rio Chone watershed

8.2 Data Inputs

The InVEST model requires several different datasets. Data was largely collected from open-access sources, as discussed below. Pre- and post-processing of datasets was performed in ArcGIS 10.2 and MATLAB.

1. **Digital Elevation Model (DEM):**

The DEM automated calculation of the Slope and Slope-Length components of the RUSLE equation for our ROI. This 30m resolution raster was created by Dr. Marc Souris, a computer sciences researcher and GIS developer; it was compiled and constructed by IRD/MS with SavGIS, generated by manually digitizing contour lines. With a resolution of 30mx30m, this allowed for a fairly accurate portrayal of the local topography. The DEM is a GIS raster dataset with an elevation value for each cell. Pre-processing of the raster included clipping the raster to the appropriate size (performed automatically during the model run) and multiple iterations of sink fills using tools in the ArcGIS ArcHydro toolbox. Filling a sink raises any point in the topography of the DEM that would make water pool inappropriately instead of allowing it to flow downstream.

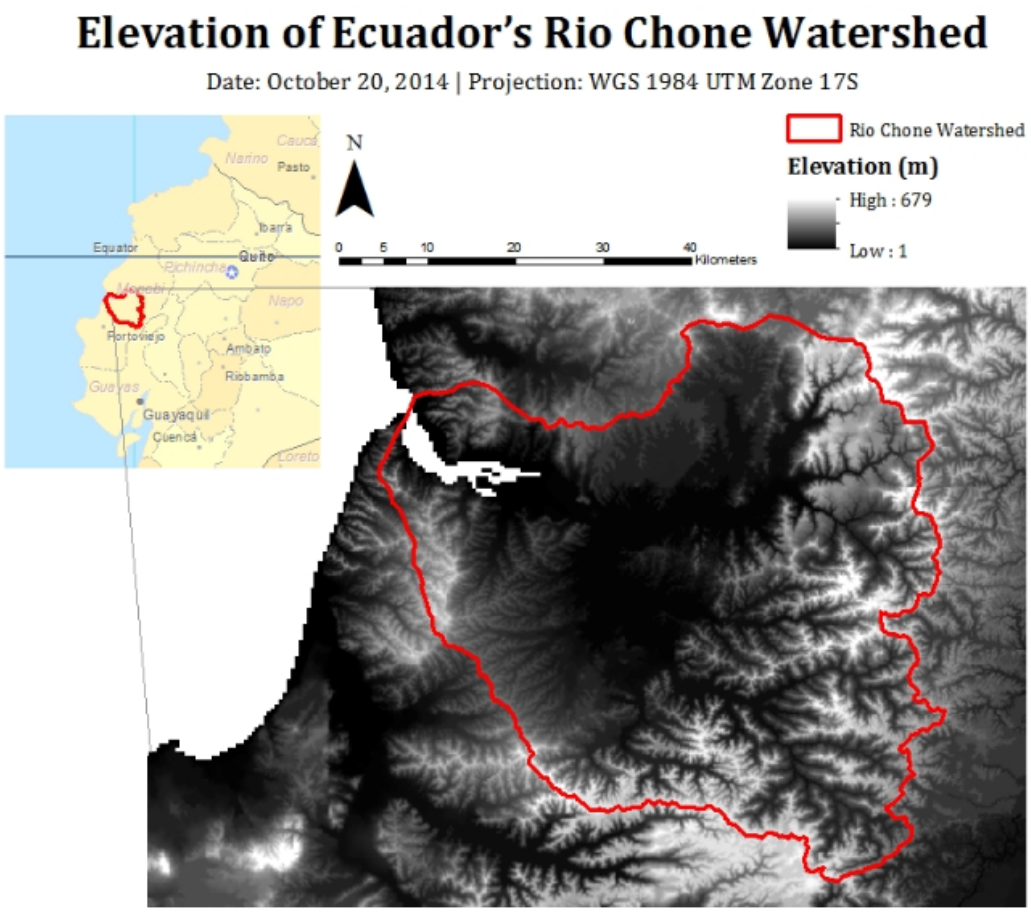

Figure 8.6 Elevation of Ecuador's Rio Chone watershed created in ArcGIS 10.2

Because the InVEST model automates calculation of the LS factor byway of the DEM, our research group did not have to perform this task manually.

2. Rainfall Erosivity Index (raster):

The rainfall erosivity index was a GIS raster dataset with an erosivity index value for each grid cell expressed in units MJ*mm*(ha*h*yr)^-1. Determined by Smith (Wischmeier and Smith, 1965), it was purported that the energy available to move sediment grains during precipitation events is the product of the total amount of kinetic energy (E) contained in the weather event, and the maximum 30-minute intensity (I_{30})of the event. Known as the *EI* parameter, the R-factor hinges upon this value: *R* is the average annual sum of the *EI* parameters for all storms in a year (Cooper, 2011). In effect, the R-factor represents the potential for a drop of water to detach individual soil particles from soil clods, based on the energy and intensity of the drop of water as it hits each grain.

Calculation of the R-factor requires an extensive dataset, and is difficult in data limited regions. Numerous methods have therefore been devised to estimate the R-factor from annual precipitation data. Lo et. al (1985) examined rainfall erosivity data for 99 sites in Hawaii (Lee & Heo, 2011). Their research produced the following linear equation that uses

mean annual precipitation to estimate rainfall erosivity with a coefficient of determination (r^2) of 0.897. The equation is expressed as the following:

$$\mathbf{R = 38.5 + 0.35\ P}$$

Where,

R = annual mean rainfall erosivity (10 MJ mm ha^{-1} h^{-1} yr^{-1})
P = annual mean precipitation (mm yr^{-1})

This equation is considered an appropriate estimator of rainfall erosivity in subtropical regions, and was thus applicable to the Rio Chone estuary watershed (Lee and Heo, 2011).

Mean monthly precipitation data (1950-2000) was downloaded from the 30 arc-second WorldClim global climate dataset (Hijmans et al., 2005). Using the method developed by Lo et al. (1985) we calculated R factors ranging from 194 to 679 (Figure 3.X).

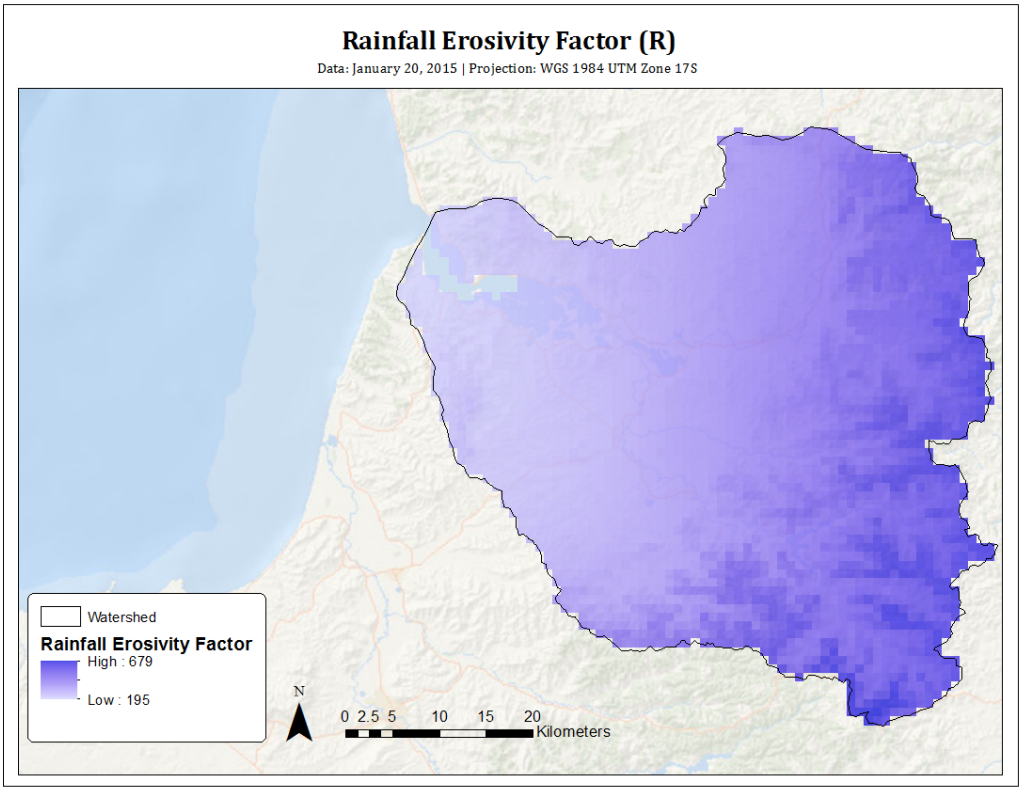

Figure 8.7 Rainfall erosivity values for the Rio Chone watershed

3. Soil Erodibility Index (raster):

The soil erodibility index was a GIS raster dataset with an erodibility index value for each grid cell expressed in tonne/hectare. Soil erodibility is a measure of the susceptibility of a soil particle to detachment and transport by rainfall and runoff. This is the principle reason behind the limitation of the USLE in the types of erosion it predicts. The largest factor

affecting *K* is the texture of the soil grain, however structure, organic matter content, and permeability also contribute to susceptibility. The geomorphology of an environment is solely represented in this factor during USLE modeling; the structure of a soil affects both the susceptibility to detachment and infiltration, or conversely runoff. Soils high in clay have lower K values (0.05 - 0.15) as they resist detachment. Soils with coarser textures (e.g. sandy soils) have low K values as well (0.05 - 0.2), despite the ease of detachment; this is due to low runoff from increased rates of infiltration as pore sizes increase with texture. Soils with medium textures, including the silt loam soils, have moderate K values (0.25 - 0.4) as they are susceptible to both detachment and runoff production. Of all the soil types, those high in silt content, or fine grained, are the most erodible. Due to ease of detachment, they tend to crust and produce high runoff rates. K values for soils range up from 0.4 (Institute, 2002).

Another consideration when assigning K values to soil types: the organic matter content. Organic matter reduces the susceptibility of soil to detachment, reducing erodibility in turn. In addition, higher organic content concentrations increases the infiltration capacity of a soil, diminishing the amount of water that runs off of the surface to transport sediment with it (Institute, 2002). Hudson (1994) showed that for percent a soil increases in organic matter, it's available water holding capacity increased by 3.7%. Adding organic matter to soil will increase the water holding capacity and in turn infiltration for three reasons: first, increasing the amount of carbon in an environment can stimulate biologic activity; soil organisms favor carbon-rich compositions. The increased soil activity of micro- and macrofauna, such as earthworms, will generate physical pathways in soil beds for water conveyance by indirectly increasing the soil's porosity via bioturbation. Worms build burrows lined with glue-like secretion from their bodies. Second, organic material on topsoil can prevent the soil from sealing and crusting by raindrop impact. As raindrops hit bare soil, the energy of the raindrop velocity detaches individual soil particles from aggregates. Detached particles can clog surface pores, producing relatively impermeable surface layers of sediment. Lastly, organic matter in soils can cause particles to aggregate, again increasing porosity as pore spaces become larger. The stability of soil aggregates depends on the bonding or adhesion properties of organic materials, such as worm casts and secretions, organic gels, fungal hyphae and bacterial waste products (Benites and Bot, 2005).

Table 8.1 Estimating soil erodibility (*K* factor) based on soil texture and organic material content. From InVEST (2014)

Textural Class	Spanish Texture Class	Soil composition			Mean K (based on % organic material)		
		Sand	Silt	Clay	unknown	< 2%	≥ 2 %
Clay	*Arcilloso*	0-45	0-40	40-100	0.22	0.24	0.21
Sandy Clay	*Arcilloso arenoso*	45-65	0-20	35-55	0.2	0.2	0.2
Silty Clay	*Arcilloso limoso*	0-20	40-60	40-60	0.26	0.27	0.26
Sand	*Arenoso*	86-100	0-14	0-10	0.02	0.03	0.01
Sandy Loam	*Franco arenoso*	50-70	0-50	0-20	0.13	0.14	0.12
Clay Loam	*Franco - arcilloso*	20-45	15-52	27-40	0.3	0.33	0.28
Loam	*Franco*	23-52	28-50	7-27	0.3	0.34	0.26
Loamy Sand	*Franco arenoso*	70-86	0-30	0-15	0.04	0.05	0.04
Sandy Clay Loam	*Franco arenso arcilloso*	45-80	0-28	20-35	0.2	0.2	0.2
Silty Clay Loam	*Franco limoso arcilloso*	0-20	40-73	27-40	0.32	0.35	0.3
Silt	*Limoso*	0-20	88-100	0-12	0.38	0.41	0.37
Silty Loam	*Franco limoso*	20-50	74-88	0-27	0.38	0.41	0.37

Soil data for the Rio Chone estuary was collected from the open-access Harmonized World Soil Dataset (HWSD). A consortium of soils information, this raster layer was a product of efforts between the Food and Agriculture Organization of the United Nations (FAO) and the International Institute for Applied Systems Analyses. Large volumes of regional and national updates of soil information was married with information already available within the 1:5,000,000 scale FAO-UNESCO Digital Soil Map of the World (Harmonized, 2009).

Pre-processing of the soil raster included downloading the dataset and clipping it to the ROI. Four different soil types were assigned to the Rio Chone watershed according to the HWSD: arenosols, cambisols, phaeozems, and luvisols. Using Table 8.1 above, *K* values were assigned to each grid cell within the soil erodibility raster.

4. Land use/land cover (raster):

The land use/land cover data layer was a GIS raster dataset with an integer LULC code for each cell. The code corresponded to a biophysical table, a .CSV table containing model information corresponding to each of the land use classes found in the LULC raster (discussed below). A key component for terrestrial and water models, this spatially continuous raster grid is a representation of how land is being used. Delineation by land

cover can be done manually, however the size of our ROI prompted search for an outside, open-access data source. Our LULC raster was collected from the European Space Agency, who provides land cover maps for 2005 and 2009. For our analyses, the Global Land Cover Map "GlobCover 2009" was used to represent baseline (current) conditions. ESA released their GlobCover 2009 product on December 21, 2010, after the GlobCover chain was run by ESA and the Universite catholique de Louvian in order to produce bi-monthly and annual mosaics for the year 2009 and to derive a new global land cover map from these time series mosaics. GlobCover 2009 is based on Envisat Medium Resolution Imaging Spectrometer Instrument (MERIS) Fine Resolution (300m) mode data, using geographic coordinates in a Plate-Carree projection (WGS84 ellipsoid). Automated classifications are produced using 20 Terabytes of MERIS FRS level 1B data that have been processed to create the land surface reflectance mosaics for each of the two calendar years assessed. The surface reflectance mosaics were obtained using a series of pre-processing steps , after which a classification chain process transforms cloud-free reflectance mosaics into a land cover map. Its thematic legend of land classifications is compatible with the UN Land Cover Classification System (LCCS). Validation of the GlobCover 2005 and 2009 products has been performed by an international group of land cover experts who provided commentary and feedback as end-users, in addition to the performance of an internal assessment by ESA (Data User, 2010). A manual validation was performed by our research group to validate its applicability to our study location.

The following is a description of GlobCover 2009's land cover classes, based upon the LCCS classification system (Arino et al., 2011):

Table 8.2 Land cover classification system and the GlobCover 2009 product legend. From Arino et al. (2011)

Value	GlobCover legend	LCCS Label	LCCS Entry	
11	Post-flooding or irrigated croplands (or aquatic)	Irrigated tree crops // Irrigated shrub crops // Irrigated herbaceous crops // Post-flooding cultivation of herbaceous crops	A11 Cultivated Terrestrial Areas and Managed Lands	
14	Rainfed croplands	Rainfed shrub crops // Rainfed tree crops // Rainfed herbaceous crops		
20	Mosaic cropland (50-70%) / vegetation (20-50%)	Cultivated and managed terrestrial areas / Natural and semi-natural primarily terrestrial vegetation		
30	Mosaic vegetation (50-70%) / cropland (20-50%)	Natural and semi-natural primarily terrestrial vegetation / Cultivated and managed terrestrial areas		
40	Closed to open (>15%) broadleaved evergreen or semi-deciduous forest (> 5m)	Broadleaved evergreen closed to open trees // Semi-deciduous closed to open trees	Woody - Trees	A12 Natural and Semi-natural Terrestrial Vegetation
50	Closed (>40%) broadleaved deciduous forest (>5m)	Broadleaved deciduous closed to open (100-40%) trees		
60	Open (15-40%) broadleaved deciduous forest/woodland (>5m)	Broadleaved deciduous (40-(20-10)%) woodland		
70	Closed (>40%) needleleaved evergreen forest (>5m)	Needleleaved evergreen closed to open (100-40%) trees		
90	Open (15-40%) needleleaved deciduous or evergreen forest (>5m)	Needleleaved evergreen (40-(20-10)%) woodland // Needleleaved deciduous (40-(20-10)%) woodland		
100	Closed to open (>15%) mixed broadleaved and needleleaved forest (>5m)	Broadleaved closed to open trees / Needleleaved closed to open trees		
110	Mosaic forest or shrubland (50-70%) / grassland (20-50%)	Closed to open trees / Closed to open shrubland (thicket) // Herbaceous closed to open vegetation		
120	Mosaic grassland (50-70%) / forest or shrubland (20-50%)	Closed to open shrubland (thicket) // Herbaceous closed to open vegetation / Closed to open trees		
130	Closed to open (>15%) (broadleaved or needleleaved, evergreen or deciduous) shrubland (<5m)	Broadleaved closed to open shrubland (thicket)	Shrub	
140	Closed to open (>15%) herbaceous vegetation (grassland, savannas or lichens/mosses)	Herbaceous closed to very open vegetation // Closed to open lichens/mosses	Herbaceous	
150	Sparse (<15%) vegetation	Sparse trees // Herbaceous sparse vegetation // Sparse shrubs		

Table 8.2 (Cont'd)

160	Closed to open (>15%) broadleaved forest regularly flooded (semi-permanently or temporarily) - Fresh or brackish water	Closed to open (100-40%) broadleaved trees on temporarily flooded land, water quality: fresh water // Closed to open (100-40%) broadleaved trees on permanently flooded land, water quality: fresh water	A24 Natural and Seminatural Aquatic Vegetation
170	Closed (>40%) broadleaved forest or shrubland permanently flooded - Saline or brackish water	Closed to open (100-40%) broadleaved trees on permanently flooded land (with daily variations), water quality: saline water // Closed to open (100-40%) broadleaved trees on permanently flooded land (with daily variations), water quality: brackish water // Closed to open (100-40%) semi-deciduous shrubland on permanently flooded land (with daily variations), water quality: saline water // Closed to open (100-40%) semi-deciduous shrubland on permanently flooded land (with daily variations), water quality: brackish water	
180	Closed to open (>15%) grassland or woody vegetation on regularly flooded or waterlogged soil - Fresh, brackish or saline water	Closed to open shrubs // Closed to open herbaceous vegetation	
190	Artificial surfaces and associated areas (Urban areas >50%)	Artificial surfaces and associated areas	**B15 Artificial Surfaces**
200	Bare areas	Bare areas	**B16 Bare Areas**
210	Water bodies	Natural water bodies // Artificial water bodies	**B28 Inland Waterbodies, snow and ice**
220	Permanent snow and ice	Artificial perennial snow // Artificial perennial ice // Perennial snow // Perennial ice	

Once downloaded, the LULC raster was clipped to the borders of the study region, the Rio Chone watershed.

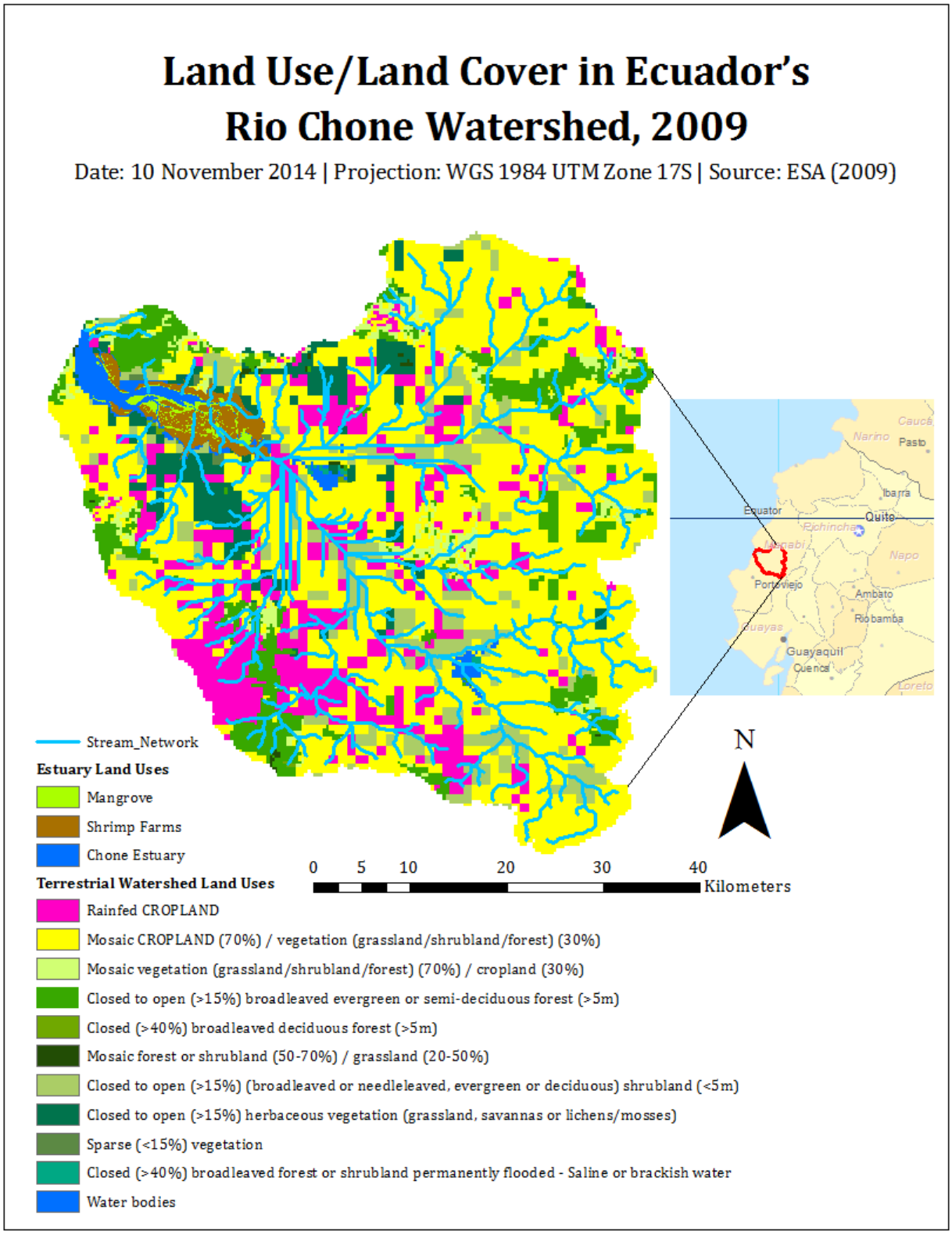

Figure 8.8 Map portrayal of the land use/land cover raster used in InVEST's Sediment Retention Model. Data from ESA's product GlobCover 2009

A manual validation was performed to test the accuracy of the LULC raster against the study region. Manual classification of cropland/mosaic cropland was performed for a subset of the study area and the entirety of the visible water bodies in Google Earth, then compared to the KMZ (file extension for a placemark holder used by Google Earth) imported version of the GlobCover 2009's rendition of croplands/mosaic croplands (to include the pixels with LULC classes containing ≥ 70% croplands, to include class values 14 and 20; see Table 8.2 above) and water bodies. As recommendations for reducing soil erosion would be based upon managing lands that had been converted away from their naturally vegetated stated, namely agricultural plots, the relevancy of validating other LULC classifications was negligible.

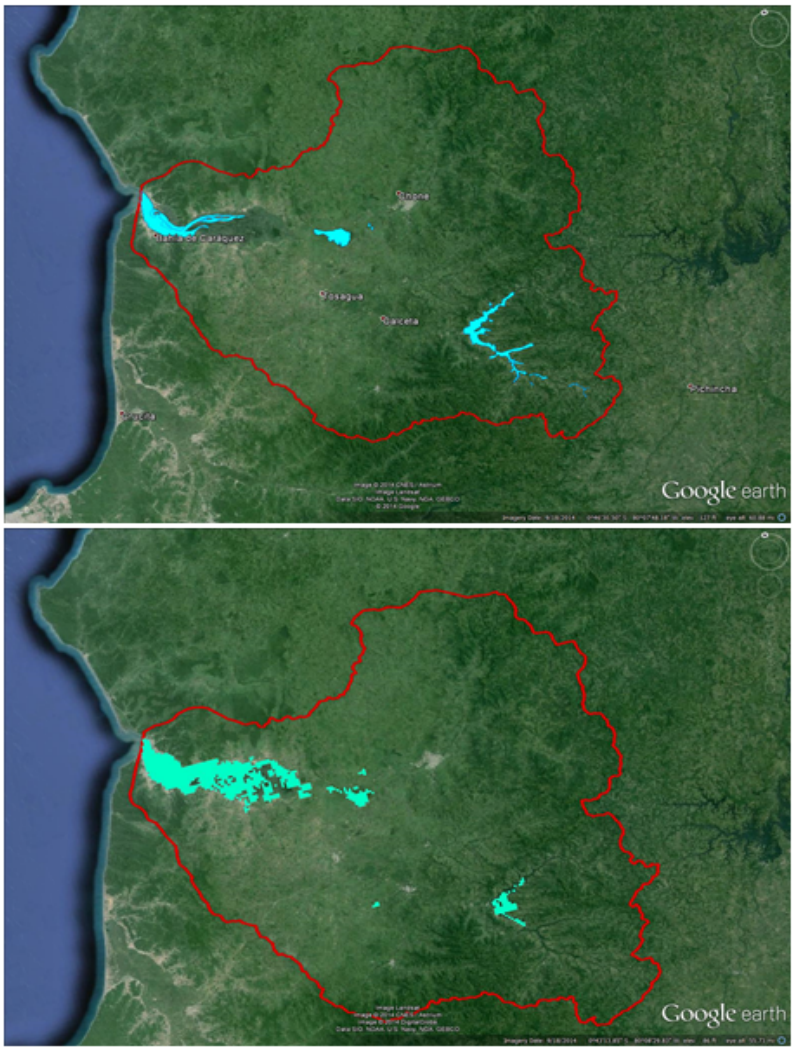

Figure 8.9 Comparison of manually delineated water bodies (top) to automated classification of water bodies in ESA's GlobCover 2009 product (bottom). Manual delineation performed in Google Earth

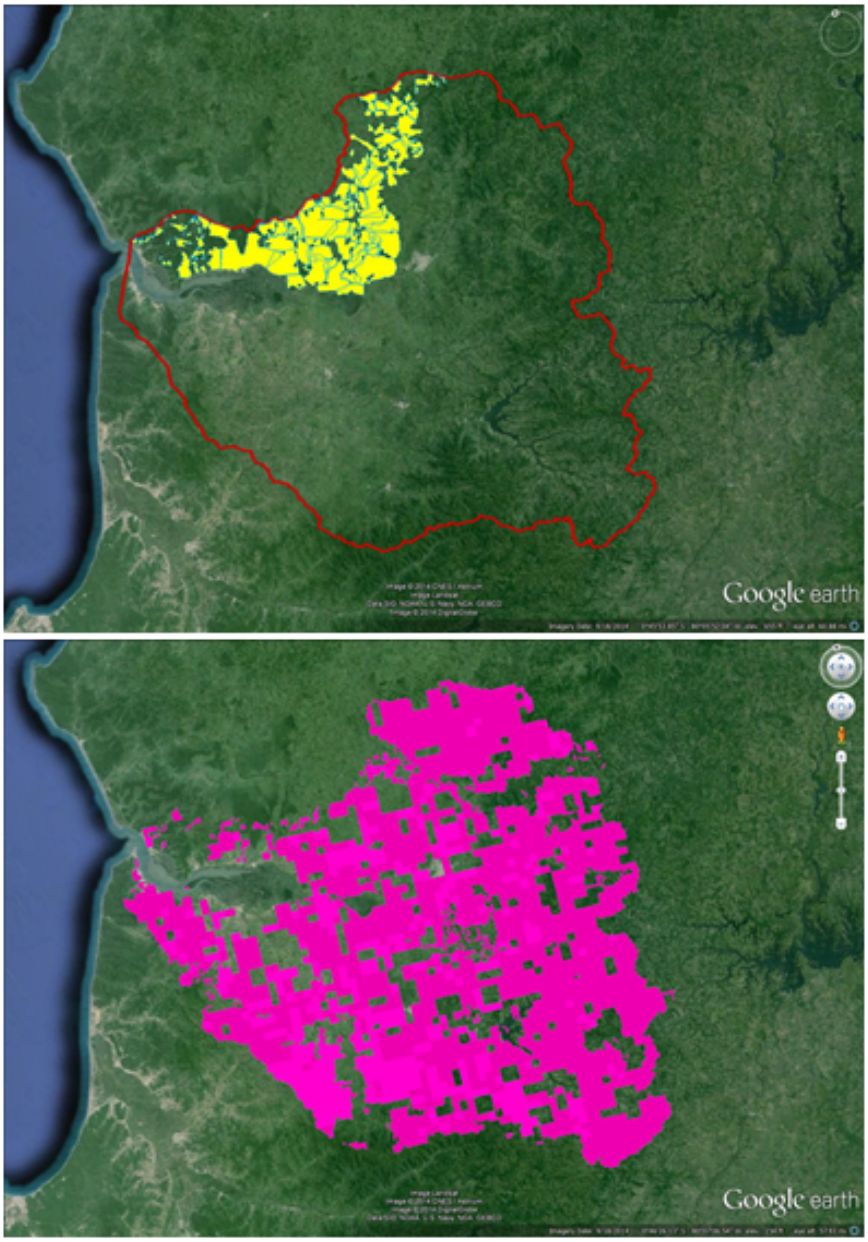

Figure 8.10 Comparison of manually delineated crop lands for a subset of the RIO (top) to automated classification of croplands in ESA's GlobCover 2009 product (bottom). Manual delineation performed in Google Earth

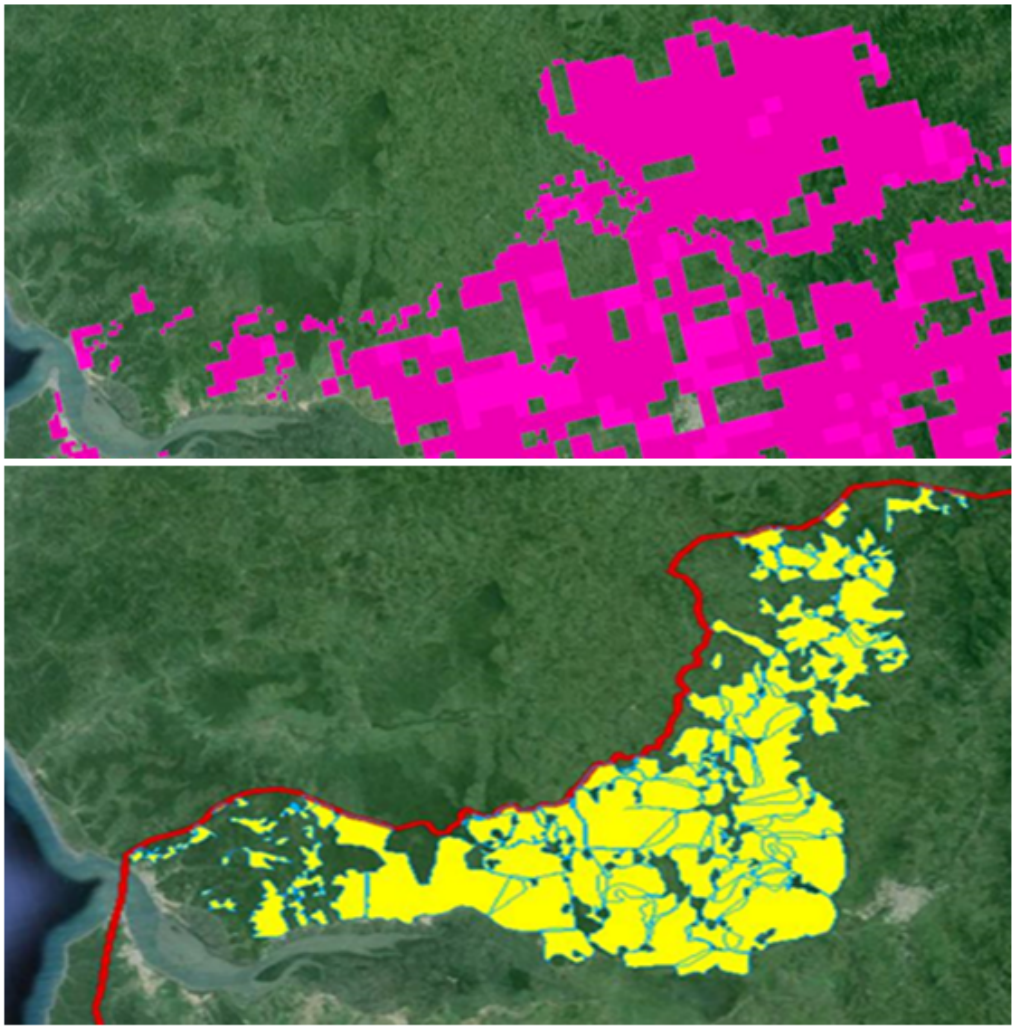

Figure 8.11 Zoomed in perspective of the comparison of manually delineated croplands for a subset of the ROI (top) to automated classification of croplands in ESA's GlobCover 2009 product. Manual delineation performed in Google Earth

5. Delineated watershed (shapefile):

A polygon shapefile representing the outline of the watershed was required. The DEM was used to delineate a watershed manually using tools in ArcGIS's ArcHydro toolbox. Terrain pre-processing included filling sinks in the DEM, obtaining the flow accumulation and flow direction, followed by a delineation according to a manually placed pour point.

6. Biophysical Table:

To accompany the LULC raster, a .CSV biophysical table was required. The biophysical table included model information corresponding to each of the land use classes, including:

1. Land use code: a unique integer for each LULC class
2. Class description: descriptive name of land use/land cover class
3. C factor: the cover-management factor for the RUSLE, as a floating point value between 0 and 1
4. P factor: the support practice factor for the RUSLE, as a floating point value between 0 and 1
5. Sediment retention efficiency: the sediment retention value for each LULC class, as a floating point value between 0 and 1 (percent per pixel area)

8.2.1 Cover Management Factor (*C*)

The cover management factor in RUSLE reflects the effect of cropping and management practices on erosion rates. The *C* variable is an expression of the effects vegetative cover, soil cover, soil biomass, and soil disturbance activities have on the dislodging and transport of soil grains. An indicator of how the land management will influence sediment production, it is the factor most often used to compare the relative impacts of management options on conservation plans. The cover management factor is based on the concept of deviation from a standard, where the most erosive scenario (standard) is an area under clean-tilled continuous-fallow conditions with a 100% soil loss expectation. The *C* factor reduces the amount erosion as a percentage multiplier, where *C* would be less than 1 if the vegetative cover, or canopy cover, on a soil surface would confer a reduction in soil loss during a rain event. A *C* factor of 0.25 would reduce the amount of erosion by 75% of the amount that would have occurred under continuous fallow conditions; erosion would be 25% of the original rate.. Rain dropping on an abstracting surface atop the soil surface can dissipate the kinetic energy of the water droplet or abstract the water altogether. In effect, *C* represent surface roughness, as roughness ponds water in depression to reduce the erosivity of a raindrop's impact. Additionally, roughness indicated the degree of clodiness and the likelihood that the surface will form sedimentous crusts to increase surface runoff RUSLE applies the *C* factor variable as an average soil loss ratio weighted according to the distribution of rainfall erosivity during the year; soil loss ratios vary with time as canopy, ground cover, roughness, soil biomass, and consolidation change (Institution, 2002).

C factors were assigned to each of the LULC classifications in the LULC raster for the Rio Chone estuary. Assignments were based upon a review of literature values, and can be seen in Table 8.3 below. According to Hanratty (1989), the major crops farmed on Ecuador's dry tropical coast are sugarcane, soybeans and corn. As such, *C* values for cropland/mosaic cropland were calculated assuming agricultural lands were dedicated to the growth of these specific crop types in equal parts (Hanratty, 1989).

8.2.2 Support Practice Factor (*P*)

Similar to the *C* factor, the support practice factor (*P*) represents the amount of erosion reduction one can expect according to the conservation practices being utilized on a parcel of land. Again, this variable is based on the concept of deviation from a standard, where the most erosive scenario (standard) is straight row farming up-and-down slope. When

considering how to go about reducing the amount of soil lost from a farmed plot of land, alterations in how the land is farmed to reduce erosion rates would be represented by this value. A *P* factor of 0.3, associated with a less erosive agricultural practice such as no-till or strip-contouring, would reduce the amount of expected erosion by 70% (30% of the original rate) (Institute, 2002).

P factors were assigned to each of the LULC classifications in the LULC raster for the Rio Chone estuary. Assignments were based upon a review of literature values, and can be seen in Table 8.3 below. The conservation values explored were based upon considerations discussed by Roose (1996), whose concepts were extrapolated to the dry mountainous coastal environment of the Rio Chone watershed to determine likely conservation practice candidates for the ROI.

Table 8.3 *C* and *P* factor assignments and justifications

C Factor

Land Use Code	Land Use Description	Crop type	C Factor	Region	Source	C Factor for Chone (Weighted Average)
14	Rainfed croplands					0.36
		Sugarcane	0.306	Brazil	Wellard Sparovek (2008)	
		Soybeans	0.23	Brazil	Amaral et. al (2008)	
		Corn	0.55	Brazil	Wellard Sparovek (2008)	
20	Mosaic cropland (70%) / vegetation (grassland/shrubland/forest) (30%)	**Cover Type**				0.26
		Cropland	0.36			
		Grassland	0.01		Invem et. al (2007)	
		Shrubland	0.06	United States	Drake (2005)	
		Forest	0.04	Turkey	Ozcan et. al (2008)	
30	Mosaic vegetation (grassland/shrubland/forest) 70%) / cropland (30%)			United States	Martin et. al (2003)	0.13
40	Closed to open (> 15%) broadleaved evergreen or semi-deciduous forest (>5m)			Turkey	Benzer (2010)	0.003
50	Closed (>40%) broadleaved deciduous forest (>5m)					0.004
110	Mosaic forest or shrubland (50%) / grassland (50%)					0.035
130	Closed to open (> 15%) (broadleaved or needleleaved, evergreen or deciduous) shrubland (<5m)					0.06
140	Closed to open (> 15%) herbaceous vegetation (grassland, savannas or lichens/mosses)					0.01
150	Sparse (< 15%) vegetation					0.85
170	Closed (>40%) broadleaved forest or shrubland permanently flooded - Saline or brackish water			Slovakia	Cebecauer and Hofierka (2008)	0.003
210	Water bodies			United States	Drake (2005)	0

P Factor

Land Use Code	Land Use Description	Conservation Method	P Factor	Region	Source	P Factor for Chone
14	Croplands	***Diversified Crops***	0.45	Malaysia	Troeh et. al (1999)	0.45
		Up and Down Slope	1	Greece	Gitas et. al (2009)	
		Strip Cropping, Cross-Slope	0.75	Greece	Gitas et. al (2009)	
		Terracing	0.5	Brazil	Wellard Sparovek (2008)	
		Buffer Strip-Cropping	0.3	West Africa	Roose (1996)	
		Contour Ridging				
		Slopes of 1-8%	0.5	West Africa	Roose (1996)	
		Slopes of 8-12%	0.6	West Africa	Roose (1996)	
		Slopes of 12-20%	0.8	West Africa	Roose (1996)	
		Slopes of >20%	1	West Africa	Roose (1996)	
		Strip Cropping, Contoured	0.25	Greece	Gitas et. al (2009)	
		Contour Tied Ridging	0.1			
		No-Till Mulching	0.01	West Africa	Dewaulle (1973)	
20	Mosaic cropland (70%) / vegetation (grassland/shrubland/forest) (30%)					0.38
30	Mosaic vegetation (grassland/shrubland/forest) 70%) / cropland (30%)					0.28
40	Closed to open (> 15%) broadleaved evergreen or semi-deciduous forest (>5m)	**Permanent Vegetation**		Brazil	Prado et. al (2005)	0.2
50	Closed (>40%) broadleaved deciduous forest (>5m)					0.2
110	Mosaic forest or shrubland (50%) / grassland (50%)					0.2
130	Closed to open (> 15%) (broadleaved or needleleaved, evergreen or deciduous) shrubland (<5m)					0.2
140	Closed to open (> 15%) herbaceous vegetation (grassland, savannas or lichens/mosses)					0.2
150	Sparse (< 15%) vegetation			Chile	Honorato et. al (2001)	0.85
170	Closed (>40%) broadleaved forest or shrubland permanently flooded - Saline or brackish water					0.2
210	Water bodies			Malaysia	Troeh et. al (1999)	0.5

8.2.3 Sediment Retention Efficiency

The sediment retention efficiency was a value for each LULC class as a floating point value between 0 and 1. A percent per pixel area, this value represented the percentage of soil that would be retained per year according to the type of land use/land cover regime occurring on that particular plot of land. Because there is no gold standard for sediment retention efficiencies according to land use, this value's importance is largely the relative effectiveness of each land type included in the assessment to retain sediment in relation to all of the other land types in consideration. We assigned sediment retention efficiencies to each LULC class in the Rio Chone watershed by utilizing the literature reviewed values proposed by the NatCap InVEST team as proxies. When possible, we took sediment retention efficiency values from the literature that were calculated for regions that matched the climate and vegetation regimes of Ecuador's Manabi coastline. Sediment retention efficiency values for each model scenario can be seen in their biophysical tables (see section 3.4.3).

7. **Threshold Flow Accumulation:**

The threshold flow accumulation is the number of upstream cells that must flow into a cell before it is considered part of a stream. This is used to classify streams in the DEM, and validates that the model has a spatial component. This threshold determines where hydraulic routing is either discontinued or remains continuous to transport a sediment grain downgradient to a delivery channel. A threshold of 100 cells was chosen, meaning any cells with a flow accumulation of 100 cells or more would become incorporated into the stream network.

8. **Sediment Threshold Table:**

The sediment threshold table was a .CSV file containing annual sediment load threshold information for the entire watershed, lumping all cells of the watershed together (ignores spatial distribution). While required, this table is in place to allow valuation assessments to be performed, which our study group opted not to pursue. As such, certain variables were arbitrarily chosen and will therefore be omitted.

8.3 Model Outputs

The Sediment Retention model provides the following outputs: 1) parameter log, a text file listing parameter values for each run, 2) the total potential soil loss per pixel in the original land cover calculated from the RUSLE equation (tonnes/pixel), 3) the total potential soil loss per pixel in the original land cover without the *C* or *P* factors applied (tonnes/pixel), 4) the total sediment retained due to the direct effect of landcover (tonnes/pixel), 5) the total sediment retained on the landscape due to sediment filtration through land cover (tonnes/pixel), 6) the total amount of sediment exported from each pixel that reaches the stream (tonnes/pixel), 7) a pixel-level mask of the calculated stream network, useful for interpreting and debugging pixel-level output, and 8) a table containing biophysical values

for each watershed, including the total amount of potential soil loss in the watershed as calculated by the RUSLE equation.

8.4 Photographs from Ecuador

Note: Figures not included in List of Figures.

Figure I. Measuring flow rates and gathering channel geometry measurements on the Carrizal river, Rio Chone watershed. Photograph by Natalie Phares

Figure II. Carrizal river, Rio Chone watershed. Photograph by Natalie Phares

Figure III. Touring the Rio Chone estuary. Photograph by Natalie Phares

Figure IV. Hillslopes surrounding the Rio Chone estuary. Photograph by Steven Johnson

Figure V. Hillslopes and cutbanks surrounding the Rio Chone estuary. Photograph by Steven Johnson

Figure VI. Shrimp ponds in the upper Rio Chone estuary. Photograph by Steven Johnson

Figure VII. Mangrove roots, Rio Chone estuary. Photograph by Steven Johnson

Figure VIII. Mangrove roots, Rio Chone estuary. Photograph by Steven Johnson

Figure IX. Shrimp pond effluent point, Rio Chone estuary. Photograph by Steven Johnson

Figure X. Shrimp pond owner requesting visitors to leave, Rio Chone estuary. Photograph by Natalie Phares

Figure XI. Collecting water quality data in a shrimp pond, Rio Chone estuary. Photograph by Francesca de Leon

Figure XII. Collecting water quality data in a shrimp pond, Rio Chone estuary. Photograph by Francesca de Leon

Figure XIII. Working with the Universidad Católica de Bahía de Caráquez, Ecuador. Photograph by Natalie Phares

Figure XIV Mangroves at the Isla de Corazon Refugio de Vida Silvestre, Rio Chone estuary. Photograph by Steven Johnson

Figure XV. On the Rio Chone estuary. Photograph by Natalie Phares

Figure XVI. On the Rio Chone estuary. Photograph by Steven Johnson